April 2012

Gold Nanoparticle Cytotoxicity

Andrew Thomas Carey
Worcester Polytechnic Institute

Houssam Lazkani
Worcester Polytechnic Institute

A Major Qualifying Project Submitted to Faculty of Worcester Polytechnic Institute In Partial Fulfillment of the Requirements for the Degree of Bachelor of Science

Submitted by:

Houssam Lazkani

Andrew Carey

Submitted to:

Project Advisor:

Professor Terri Camesano

April 26, 2012

Abstract

The industry of nanotechnology is growing faster than the understanding of nanoparticle's long term health and environmental effects, which has brought about research regarding nanoparticle cytotoxicity. Our research focused on studying interactions between supported lipid bilayers with varying sized bare unconjugated gold nanoparticles. The interactions were monitored on an instrument, known as a Quartz crystal microbalance. From the results, size wasn't a variable that governed how the bare gold nanoparticles affected the membrane. A major factor in the results was the lack of reproducibility. The existence of defects during the formation of the SLB is in itself a variable in the experiment and will need to be treated thusly in future nanoparticle-lipid bilayer research.

Table of Contents

Table of Figures

Table of Tables

Executive Summary

The significance of nanoparticles is growing every day due to incredible discoveries in a variety of fields ranging from bioengineering to consumer goods. With this rise of uses, the concentration of nanoparticles that finds its way into the body and the environment will increase likewise. Though the toxicity of bulk gold is known, not much is known regarding long term health and environmental effects of its nanosize equivalent. This has brought about the emergence of nanotoxicology, research centered on risk related research and development. The physical and biological properties that make gold nanoparticles advantageous can also pose a potential risk to consumers and the environment. Our research focuses on modeling a probable natural interaction that will occur as the applications of gold nanoparticles increase. This interaction is between varying sized (2,5,10, and 40 nm) bare spherical gold nanoparticles and lipid bilayer prepared of Phosphotidylcholine (PC). This research intended on observing the mechanisms of interaction of gold nanoparticles and possible cytotoxicity.

Methodology

A Q-SENSE E4 system and silicon dioxide crystal sensors were used as the site for these interactions to take place. The gold nanoparticles of interest were developed through a reducing process and delivered as spherical colloid solutions ranging in concentrations from $\sim 10^{10} - 10^{14}$ Nanoparticles/ mL.

The experiment procedure consisted of three main sections: forming the PC egg bilayer, establishing water-polymer baseline, and introduction of the gold nanoparticles. Early experiments did not include the water-polymer baseline and was instead just a water baseline. The polymer, polymethacrylic acid, was used to mimic naturally synthesized polymers in humic

material.[1] These interactions are constantly monitored and recorded with the Q-soft software that accompanies the QCM-D. The data was then studied in a plotting software, SigmaPlot, and then analyzed further by performing an overtone analysis on each of the graphs. The overtone analysis provides an understanding of the interactions at different distances into the bilayer.

Results and Discussion

Concluded from previous research, it was found that nanoparticles interact with lipid bilayers by three different mechanisms: membrane thinning, adhesion, and expanding of pre-existing defects. In respect to our research, membrane thinning would be equivalent to an increase in frequency and therefore a decrease in mass of the bilayer. Expanding of pre-existing defects or adhesion would correlate to addition of mass and therefore a decrease in frequency on the data plots. Examples of mass loss and mass gain are shown in Figure-ES 1 and Figure-ES 2. These graphs are further described in our results section.

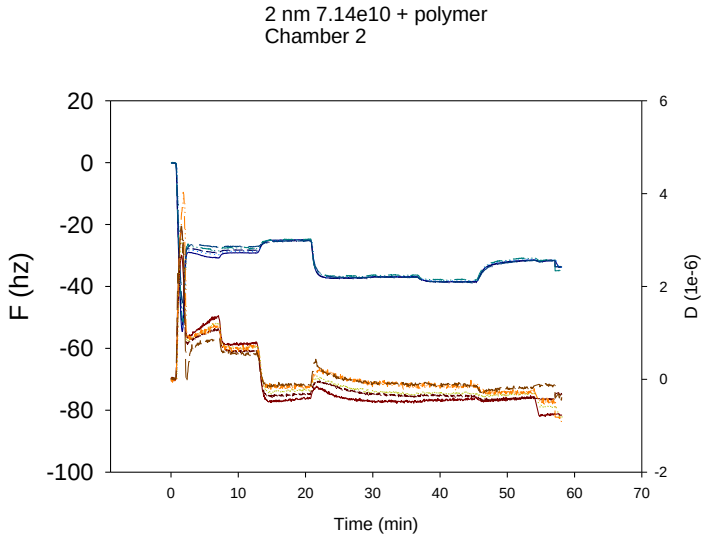

Figure-ES 1: 2nm QCM-D Results for 2 nm gold nanoparticles;

Blue lines represent frequency and red lines represent dissipation

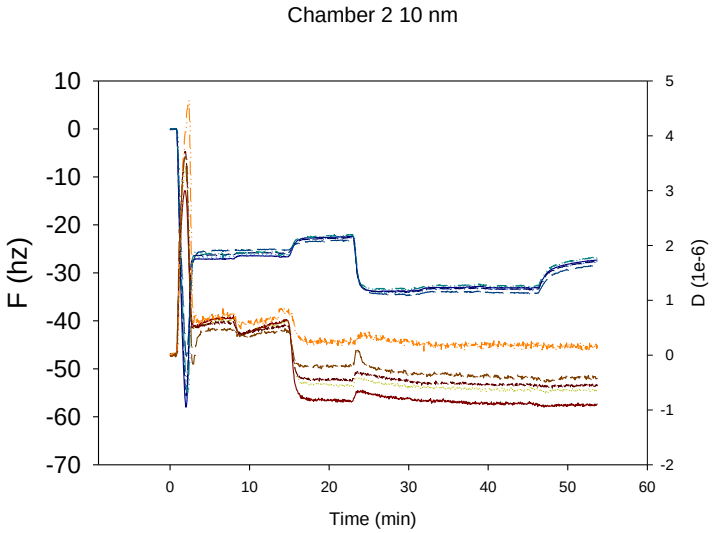

Figure-ES 2:2nm QCM-D Results for 10 nm gold nanoparticles;

Blue Lines represent frequency and red lines represent dissipation

Change in rigidity can be determined with the use of the overtone analysis. Mass loss was observed in three of the four gold nanoparticle sizes. The 2,10, and 40 nm gold nanoparticles also showed increased rigidity along with the loss of mass. The 5nm gold nanoparticle showed opposite results for both categories with a mass gain accompanied by a decrease in rigidity. Examples of the graphs are shown below by Figure-ES 3 and Figure-ES 4. These are explained in discussion.

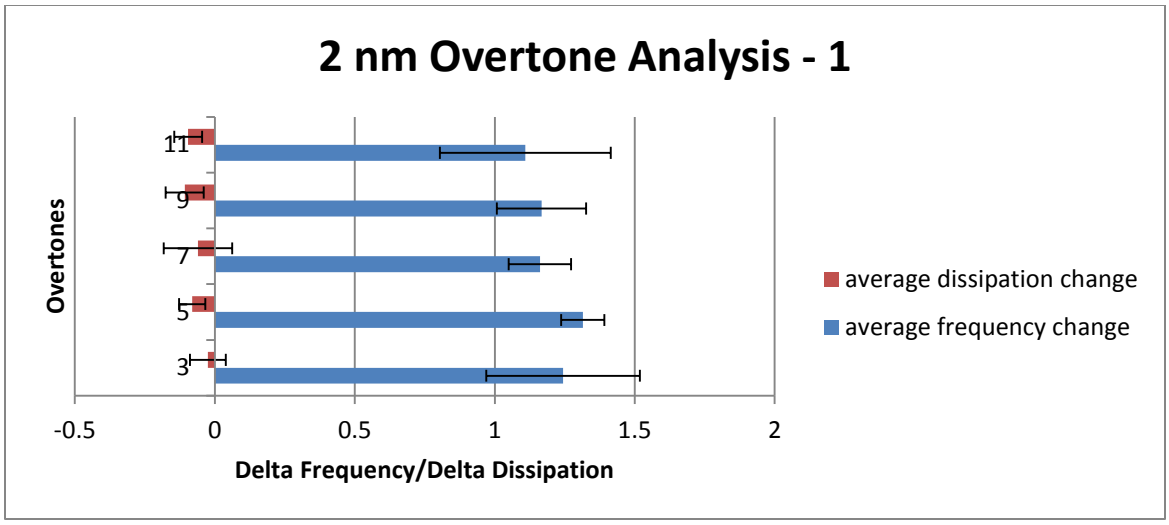

Figure-ES 3: Overtone Analysis of 2nm nanoparticles showing an increase in frequency equivalent to a loss of mass

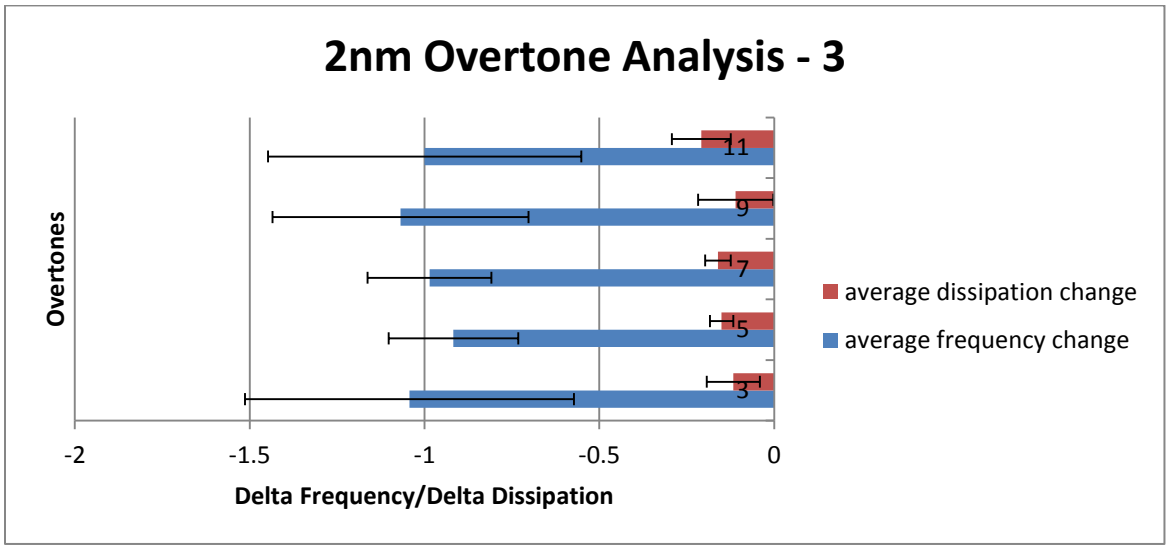

Figure-ES 4: Overtone Analysis of 2 nm nanoparticles showing a decrease in frequency representing an addition of mass

Conclusion

This research set out to observe possible cytotoxicity of gold nanoparticles and has demonstrated destructive effect on the membrane for all sizes of bare gold nanoparticles. An association between mass change and rigidity change was also observed. These results had very low reproducibility due to different defects that can be created during membrane formation. The

defects, however, can be analogous to ones found in membranes of live cells; therefore the same interactions can occur. This means that the more nanoparticles waste finds its way into the environment, the more toxic it can potentially be to vital bacteria.

To further understand the mechanism of interactions between the gold nanoparticles and the membrane, research should possibly concentrate on specific surface features in the hopes of identifying defects and using them or eliminating them.

Introduction

According to the ASTM standard, a nanoparticle is defined as any particle with at least two dimensions between approximately 1 and 100 nanometers (nm).[2] Although some authors have recognized anything outside of that range as a nanoparticle as well, the formal definition excludes particles below 1 nm to avoid confusion with small clusters of atoms and larger aggregated particles. The importance of nanoparticles has been increasing significantly due to recent technological advances in a wide variety of fields, ranging from electronics to medicine. The number of applications will only increase as it is projected that the production of nanoparticles will increase from estimated 2,300 tons produced today to 58,000 tons by 2020.[3] The industry of nanotechnology is growing faster than the understanding of nanoparticle's long term health and environmental effects. The U.S. National Nanotechnology Initiative reports only 4% ($40 million) of funding in nanotechnology research is dedicated to R&D of nanoparticle risk.[4] The number of nanoparticle applications will continue to rise and the need for a complete understanding of their cytotoxicity will do the same. This project will take a look at one interaction between gold nanoparticles and a supported lipid bilayer (SLB), in order to understand mechanisms of possible cytotoxicity.

As a relatively new technology, nanotechnology seems to have an endless number of applications in such fields as biomedical engineering, medicines, electronics, energy, and food. The advantages of nanoparticles range just as widely as their applications. Generally, advantages of nanoparticles are due to the property changes that occur as the size is brought to the nanoscale. These properties can include, but are not limited to, color, thermal and electrical conductivity, and strength. The surface area to volume ratio of nanoparticles allows for increased chemical reactivity, when compared to its regular sized equivalent.[5] All these advantages can then be

introduced within the body because of the nanoparticles ability to move easily throughout the body's natural membranes and barriers.

These general advantages have lead researchers to study applications of gold nanoparticles. Some consumer products currently on the market that use gold nanoparticles include, Nanorama – Gold Toothpaste, Nano Engine Oil, and Nano Gold Energizing Cream. [6] More commonly, gold nanoparticle research is focused on biomedical applications and drug delivery. This includes a wide range of investigations in cancer nanotechnology[7] and gene transfer.[8] A chart describing some research topics in gold nanoparticle cancer technology can be found in Appendix A. An interesting example includes that of gold nanoparticles as an imaging sensor to highlight brain tumor during surgery where the treated nanoparticle preferentially attaches to a target cell.[9] With all these advantages and current applications, long term health and environmental effects can easily be overlooked. The same biological and physical properties of nanoparticles that make them effective also pose a potential risk to both consumers and the environment.[10]

It is not just the physical and biological properties that differ from the nanoscale material to its bulk form. For this reason, a new branch of toxicology known as nanotoxicology is taking place to better understand risks associated with nanoparticles. The material studied in this report is one of the key examples as bulk gold is typically inert but gold nanoparticles are not; thereby making them so useful in imaging and drug delivery.[11] The nanoparticles ability to move easily throughout the body raises concerns of the possibility of nanoparticles crossing non-targeted biological barriers. Research is currently taking place to understand any possible environmental or health and safety risks of nanoparticles but this is after the implementation of thousands of engineered nanoparticles in the fields mentioned above. [12] Rather than research cytotoxicity

through classic methods like direct exposure or injection, both in vivo and in vitro, it was our intention to understand the interactions that occur between the membranes and nanoparticles.

Our research focused on studying interactions between supported lipid bilayers (SLBs) with varying sizes of bare unconjugated gold nanoparticles. The use of SLB's was essential to these experiments because it accurately modeled a biological system in terms of fluidity and impermeability to ions.[13] A range of 2-40 nanometer gold particles was used, with interactions being monitored on an instrument, known as a Quartz crystal microbalance with dissipation monitoring (QCM-D). This would allow us to further explore any change in membrane properties, whether it is an increase in mass due to nanoparticle adsorption or mass loss caused by a breakdown of the membrane.[14] To provide a more accurate model, it was also suggested by Dr. Camesano to use polymethacrylic acid (PMAA) in solution with water and nanoparticles.[15] This synthetic polymer closely resembles natural compounds found in humic material such as soil and water environments.[16] To further understand these interactions, analysis of individual overtones was done to build a mechanism that could describe how membranes and nanoparticles interact with one another.[17] Knowledge of these interactions of the bilayer-bare gold nanoparticle interactions will allow for an understanding of cytotoxicity and provide a baseline for future research with gold nanoparticles.

Background

What is a Nanoparticle?

According to the ASTM standard, a nanoparticle is defined as any particle with at least two dimensions between approximately 1 and 100 nanometers (nm).[18] Although some authors have recognized anything outside of that range as a nanoparticle as well, the formal definition excludes particles below 1 nm to avoid confusion with small clusters of atoms and larger aggregated particles. In the past, the word has been used to describe a variety of materials from particulates in the air to ultrafine particles. But when referring to the relatively recent technology, nanoparticles are not just about size, but particles that have a "novel" trait that gives the researcher the ability to fabricate, characterize, and manipulate properties at the nanometer level, properties including strength, electrical and thermal conductivity, optical response, elasticity or wear-resistance. [19] These traits are considered "novel" because they are specific to the nanoparticle and cannot be displayed on the atomic level or the bulk material.

Gold Nanoparticles

Gold Nanoparticles Synthesis

Gold nanoparticle colloid solution, the nanoparticles of interest in this paper, are made by placing gold in a reducing agent, allowing particles to form atom by atom over a period of twelve days. The accuracy of this patented process is highlighted in Table 2 in the appendix. The exact process of the gold nanoparticles used in this experiment is a proprietary method, but there are some well-known methods dating back to the 1950s. The oldest and simplest method is the

Turkevich method which involves chloauric acid and sodium citrate as the reducing agent.[20] There are many methods that can produce a wide variety of shapes and sizes but all of which require a reducing agent to begin the process and a capping agent to stop the reaction at the respective physical dimensions.

Use of Gold Nanoparticle as Model

Bulk gold is believed to be relatively inert and non-toxic. They are also considered to be one of the most stable metal nanoparticles.[21] These traits have led to the use of gold nanoparticles in many bioengineering functions ranging from imaging to drug delivery.[22] It is essential to understand every aspect of this developing, especially molecular interactions and possible cytotoxicity. To understand the effects of gold nanoparticles will also give insight into other rigid inorganic materials considered to be non-toxic at the nanoparticle level. [23]

Gold Nanoparticle Cytotoxicity

Due to the use of gold colloids as far back as the 1920s, research in gold nanoparticle interactions has covered a wide range of gold particles to cell interactions[24]. The majority concentrating on medical applications by nuclear transfection and targeting, due to the ease at which a small nanoparticle enters a cell. The size of nanoparticles is similar to that of cellular components and proteins, allowing for bypass of natural mechanical barriers.[25] Studies of interactions have included both that of in vivo and in vitro, with the majority in the latter.

A particularly relevant research, done by Hillyer and Albrecht, studied the gastrointestinal uptake and distribution of metallic colloidal gold particles following oral administration to mice. Resulting in a confirmation of nanoparticle uptake in the Peyer's patch

regions and breaks in the tips of villi. Through the use of multiple sized nanoparticles, the research concluded that the gold nanoparticles, depending on size, could be persorbed through gaps created by extruding enterocytes.[26] Size dependency will be a key variable in the future understanding of engineered nanoparticles interactions with biological cells. Other studies have tried to understand possible cytotoxicity of gold nanoparticles. A group of researchers, Connor et al., examined the uptake and toxicity in human leukemia cells of three different sized nanoparticles with an assortment of surface modifiers. The in vitro continuous exposure assay determined that though rapid absorption of the particles takes place, the nanoparticles are not toxic to that specific human cell.[27] Similar studies of functionalized gold nanoparticles and toxicity are summarized in Table 1, in Appendix A. These experiments can only give insight into the end result of the interactions and not the mechanism itself.

Gold Nanoparticle-Supported Lipid Bilayers (SLBs) Interactions

Egg Phosphotidylcholine (PC) Lipid Bilayer

Phosphotidylcholine (PC) was used to make the vesicle solution needed for these experiments. PC is a phospholipid widely used in experimentation to mimic the physical properties of natural biological membranes in order to complete studies without the need of live systems.[28] This model membrane helped in establishing accurate information about the mechanics of metabolic transportation through membranes and led to various advancements in medicine. Phospholipids are normally extracted from byproducts of the manufacturing of organic oils.[29] PC can be isolated and separated from chicken egg yolk then purified for pharmaceutical uses using several difference processes such as preparative high-performance liquid chromatography (HPLC) or gram-scale fractionation. These methods are further described in an article that can be found in the bibliography written by Tae ho Yoon and In Ho Kim.[30] Previous

research has been conducted to model and observe the interactions between gold nanoparticles and supported lipid bilayers.

Previous Gold Nanoparticle- SLBs Research

Researchers set out to develop a molecular dynamics simulation of gold nanoparticle and lipid bilayer interactions based off experimental data. They were able to observe penetration, both in a model and backed up experimentally, which increases the greater the charge density.[31] A molecular dynamic model can be seen in… in the appendix. Another group concluded that instead of the nanoparticle penetrating the surface, but instead diffuses into existing defects and consequently expands them. This research team from the University of Michigan concluded that though many nanoparticles induce defects, both membrane thinning and pore formation, gold nanoparticles aggregate in the lipid at the site of an existing defect.[32] With the use of quartz crystal microbalance with dissipation monitoring technology (QCM-D), specific mechanisms of interaction between gold nanoparticles and supported lipid bilayer can be detected.

Quartz Crystal Microbalance with Dissipation

The QCM-D has been an effective way of measuring changes in mass and properties of viscoelasticity of the medium being tested. The use of the QCM technology extends through several fields of study, including radioactivity, ultrasound and biomolecular interactions.

QCM technology is based on the piezoelectric effect that describes the oscillations formed when pressure is applied to quartz crystals.[33] These effects were first introduced by Pierre and Jacques Curie in the 1880's when studying the relationship between mechanical stresses and electricity. Later pioneered research ranging from radioactivity to acoustics.[34]

Specifically with the use of quartz crystals, the piezoelectric effect creates a dipole moment that vibrates the crystal at its resonance frequency. The addition of mass slows the vibrations, therefore decreasing the frequency reading. The direct relationship between frequency and mass is governed by the following equation:

$$\Delta m = \frac{C}{n}\Delta f$$

where n is the harmonic number given by the wavelength and C is defined by properties of the quartz crystal itself.[35]

The realization of QCM's ability to also monitor energy dissipation came well after 1980, when Shinshu University in Japan first used the machine for liquid applications rather than the usual gas phase or vacuum applications. When liquids are used, the crystals vibrations are dampened. This interferes with the equation above because the resonance frequency is changing. This along with frequency measurements allows the QCM-D to detect loss of mass along with changes in the properties such as viscoelasticity of the medium being tested.[36]

Dissipation measurements opened up opportunities for countless biological studies. QCM-D technology helped provide real-time results of biomaterial interactions which allowed for the advancement in biomedical devices. For example, QCM-D can be used to see how well a material used for contact lenses is avoiding interactions with tear fluid hence keeping the lens free of buildup caused by the lipids, proteins, and salts found in tears. Another example is optimizing the interaction of implants with their surroundings while avoiding formation of scar tissue around the implant.[9] Chalmers University of Technology and Göteborg University looked at how different macromolecules such as mono and multilayered protein and lipid films can be absorbed and detected by a QCM-D. This work played an important role in understanding the

kinetics behind the interaction of these molecules with different surfaces such as titanium dioxide and oxidized gold. It was found that water being trapped in these structures greatly affected dissipation readings by decreasing the rigidity of the bilayer.[37] Since then, much of the research has been using different lipids, proteins, and even DNA to further explore cellular membrane interactions.[8]

Our research involved the formation of a stabilized lipid bilayer (SLB) as a model membrane on a quartz crystal. Rather than using metal sheets as described above, non-functionalized gold nanoparticles of varying sizes were introduced in order to observe membrane-nanoparticle interaction and possible membrane destabilization or adsorption.

Methodology

Materials

Gold nanoparticles were purchased from Nanocs. 2, 5, 10, and 40 nanometer particle sizes were used. These are bare and non-functionalized nanoparticles, which will allow a control for future experiments with other gold nanoparticles.

Polymethacrylic acid (PMAA) was purchased from Polymer Source Inc. With a polydispersity index of 1.06, it is used to mimic naturally synthesized polymers in humic material. Humic material helps in stabilization and prevents aggregation of gold nanoparticles.[38]

All chemicals mentioned in methodology, unless otherwise noted, were purchased from Sigma Aldrich.

Setup

The QCM-D used in these experiments was a Q-SENSE E4 with silicon dioxide sensors purchased from Q-SENSE. The sensors were placed inside the chambers, making sure a seal is formed. The chambers were then locked into place and the appropriate tubes were attached.

Pre-experiment Cleaning Procedure

With the pump set at 0.3 mL/min, ethanol was first used to clean the tubes, sensors, and chambers of any impurities. Water was then used to wash the ethanol away and prepare for 2% sodium dodecyl sulfate (SDS) to be introduced. This is a compound often used in detergents, and served to further clean the QCM-D. Water was then again used to remove any remaining SDS, and air was pumped to dry the chambers. A general rule of 2 mL per chamber was used to determine the amount of liquid needed. After the chambers were partially dried, the crystals were

removed and properly rinsed with milli-q water. The crystals and the chambers were all completely dried using nitrogen gas. The crystals will then move to the Plasma-Prep for the final stage of cleaning.

Plasma Cleaning

A SPI Plasma-Prep™ II Plasma Etcher was used to clean the silicon dioxide crystals prior to running the experiment. This process is used to remove a very thin layer of atoms from the surface of samples with the purpose of removing loosely held contaminants.

First, AC power was turned on and allowed to warm up for about 2 minutes. About 10 watts are used for this procedure, as higher power removes more layers from the surface. During warm-up, the dial on the oxygen tank to flow the gas through the machine, and the glass chamber was removed and the crystals were placed inside. The pump was turned on and the "VACUUM" switch was flipped up. The glass chamber was gently pushed in to allow for a perfect seal and a complete vacuum to form. The mesh door was then closed and the "ON" switch was flipped. The "LEVEL" dial was turned to about 50 %, then using the "TUNNING" dial, the instrument was tuned until there was a purple glow in the chamber. The level was then turned up all the way until a stronger glow. At this point, the crystals were being etched and a timer was set for 45 seconds. To stop the etching, the level was turned all the way down and the "ON" and "VACUUM" switches were flipped down. This process was repeated again to ensure purity on the surface of the crystals. To remove the crystals, the pump was turned off. The mesh door was opened and the chamber was removed after pressure was returned to normal. The crystals were then reinstalled inside the chambers which were locked into place once again as previously described in the setup procedure.

Making the Buffer

The buffer was made by mixing 100mM of sodium chloride and 10mM of tris base (2-Amino-2-hydroxymethyl-propane-1,3-diol). pH was adjusted to 7.8 using hydrochloric acid.

Making the Vesicle Solution

Concentrated PC solution was first made by dissolving 100mg per 1 mL of ethanol. This can be stored in a freezer for later use. To make the stock, 15 mL of the concentrate was placed in a vial where the ethanol was evaporated using nitrogen. Ethanol was further evaporated by placing the vial in a vacuum chamber over night. 6 mL of buffer was then added to the vial and a freeze thaw cycle was performed. This cycle involved placing the solution in a dry ice bath until thoroughly frozen, then thawed with warm water and vortexed for 15 seconds. This was repeated 5 times and time at freezing and thawing were recorded.

A Fisher Scientific sonicator was used to sonicate the vial on pulse mode on 30% duty cycle (on for 3 seconds, off for 7 seconds) for 30 minutes. The solution was then centrifuged for 10 minutes at 15,000 rpm and 4 C. This left a concentrated solid mass at the bottom of the vial and the supernatant was removed using a pipette. 6mL of buffer was then added and the solution was stored in nitrogen gas at 7 C. [39]

Making the Polymer Solution

PMAA was used in a concentration of 100 milligrams per 1 liter of milli-q water. This was done in batches of about 30-40 mL in order to get more accurate readings on the scale.

Making the Nanoparticle Solution

The nanoparticle consists of 6.9 mL of the polymer solution and 0.1 mL of nanoparticle stock resulting in a concentration of $7.14 * 10^{10}$ nanoparticles/mL. This was done with 2, 5, 10, and 40 nm stock solutions.

Experimental Procedure

With the instrument on, Q-soft software was used to set the temperature. In the "Acquisition" drop down menu, "Setup Acquisition" was selected. Then in the "Temperature" tab, the number was changed to 23 C. In the "Sensors" tab, "quick-check found resonances" and "auto-start measurement" were checked off. "Find and Run" was then selected. This was used to tune the crystals and make sure there were no defects or impurities.

With the instruments ready, buffer was first run through the QCM-D in order to normalize the sensors and set the baseline frequency. Then the vesicle solution was introduced at a flow rate of .15 mL/min. After about 8 minutes, when the membrane had successfully formed and stabilized, buffer was reintroduced for 8 minutes at the same flow rate. This was followed by water for 8 min. The water polymer solution was then run for 8 min, this is the baseline where changes are monitored. The nanoparticle, polymer, and water solution was then ran for 10 minutes followed by a second water and polymer for 8 min. Having these two water and polymer sections, with nanoparticles introduced in between, will allow for analysis of only one variable after the experiment. A water rinse was then added for 8 min to end the experiments.

Cleaning Procedure – after the experiment

This procedure was the same as the steps taken prior to the running the experiment; however, the ethanol was excluded along with the plasma etching.

Plotting Frequency and Dissipation

The images produced in Q-Soft by the QCM-D show two sets of overtones graphed over the duration of the experiment. Frequency was shown in blue lines and dissipation was graphed in red and orange lines. To allow for more accurate analysis, these graphs were transposed into SigmaPlot. Only the overtones of interest (3,5,7,9, and 11) were plotted. First, the data was transferred to Microsoft Excel to ease organization. Time was changed from seconds to minutes, and then the data was transferred to SigmaPlot using colors similar to those used in Q-Soft to avoid confusion.

Overtone analysis

In order to further understand interactions between nanoparticles and the bilayer, an analysis was done using each individual overtone. To do this, a point was taken just after nanoparticle introduction, at a time that the reading looked stable. Data from each overtone was transferred to excel and subtracted by data from a point just before nanoparticle introduction. This was done for all four chambers as long as the data was clean enough. The average frequency and dissipation changes were then calculated and plotted on a bar graph with error bars showing the standard deviation.[40]

Results

For clarification purposes, each stage in the experiment has been assigned a number.

- Stage 1: vesicle formation
- Stage 2: buffer
- Stage 3: water
- Stage 4: water + polymer
- Stage 5: water + polymer + nanoparticles
- Stage 6: water + polymer
- Stage 7: water

Formation of the Bilayer

Successful formation of the bilayer was characterized by Figure 1. In most cases, a rapid decrease of around 70 hz in frequency (in blue) was first witnessed roughly 2 minutes after the introduction of the vesicle solution. This was then followed by an increase of about 45 hz, ending with a constant value of the newly supported lipid bilayer -25 hz. The dissipation curve (in red) was close to the inverse of the frequency curve. The graph went up to 5e-6 then back down to 1e-6 where it remained flat until the next step of the procedure.

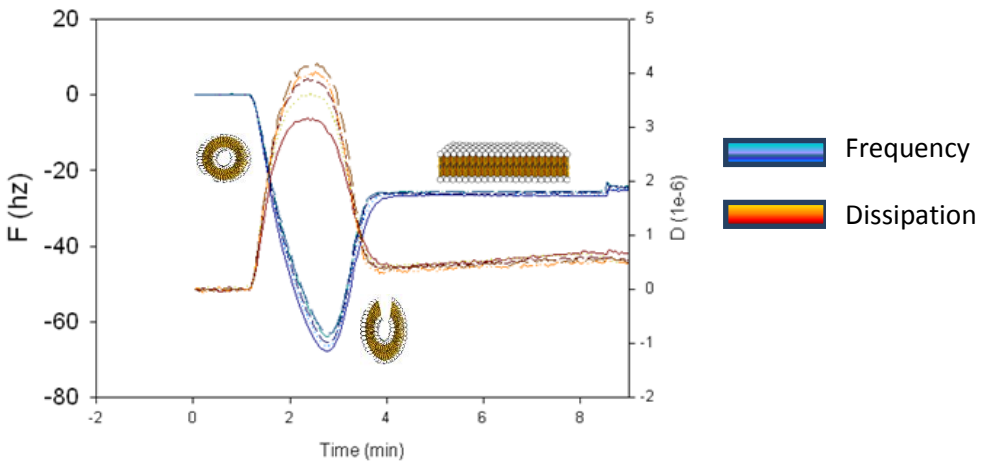

Figure 1: QCM-D graph showing successful vesicle formation and an illustration of an SLB

2 nm Gold NanoparticlesQCM-D Results

Within the multiple experiments performed with 2 nm gold nanoparticles, three different interaction trends were witnessed. The first, shown in Figure 2 showed an increase in frequency as the nanoparticles were being introduced in stage 5. The frequency then remained the same in stage 6.

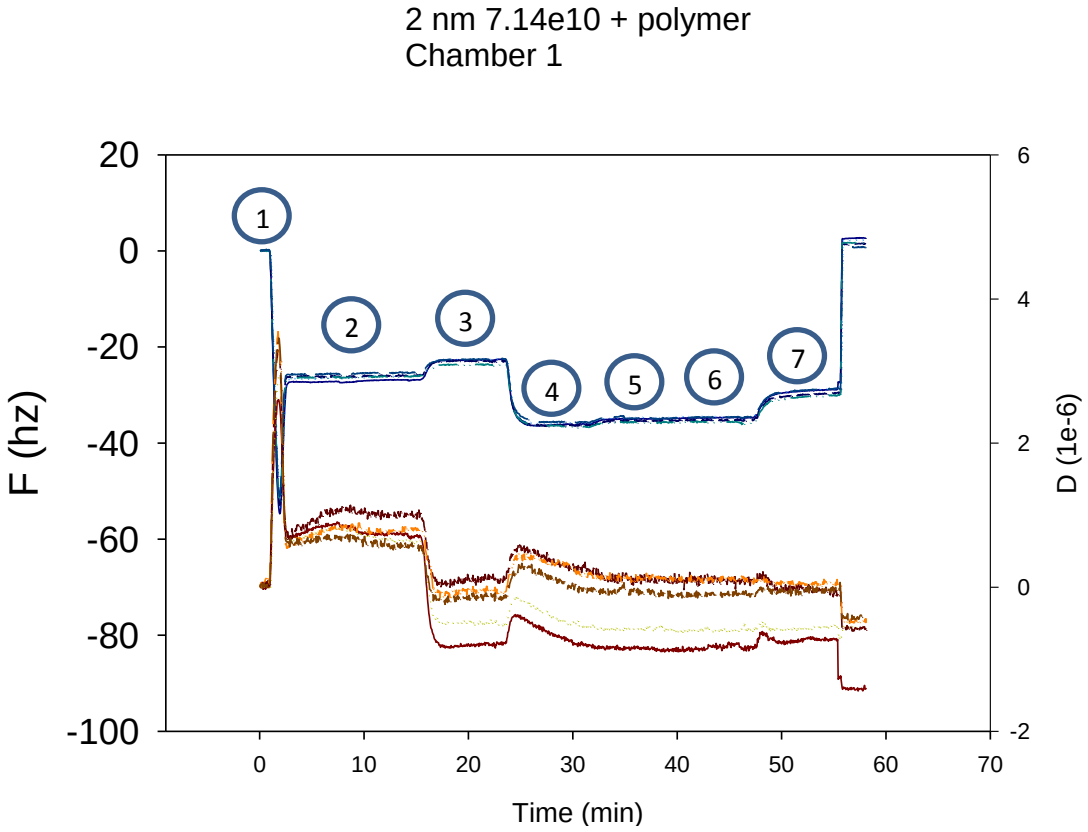

Figure 2: chamber 1 results of a trial using 2nm particles

Figure 3 showed a decrease in frequency at stage 5, followed by a slight increase at stage 6.

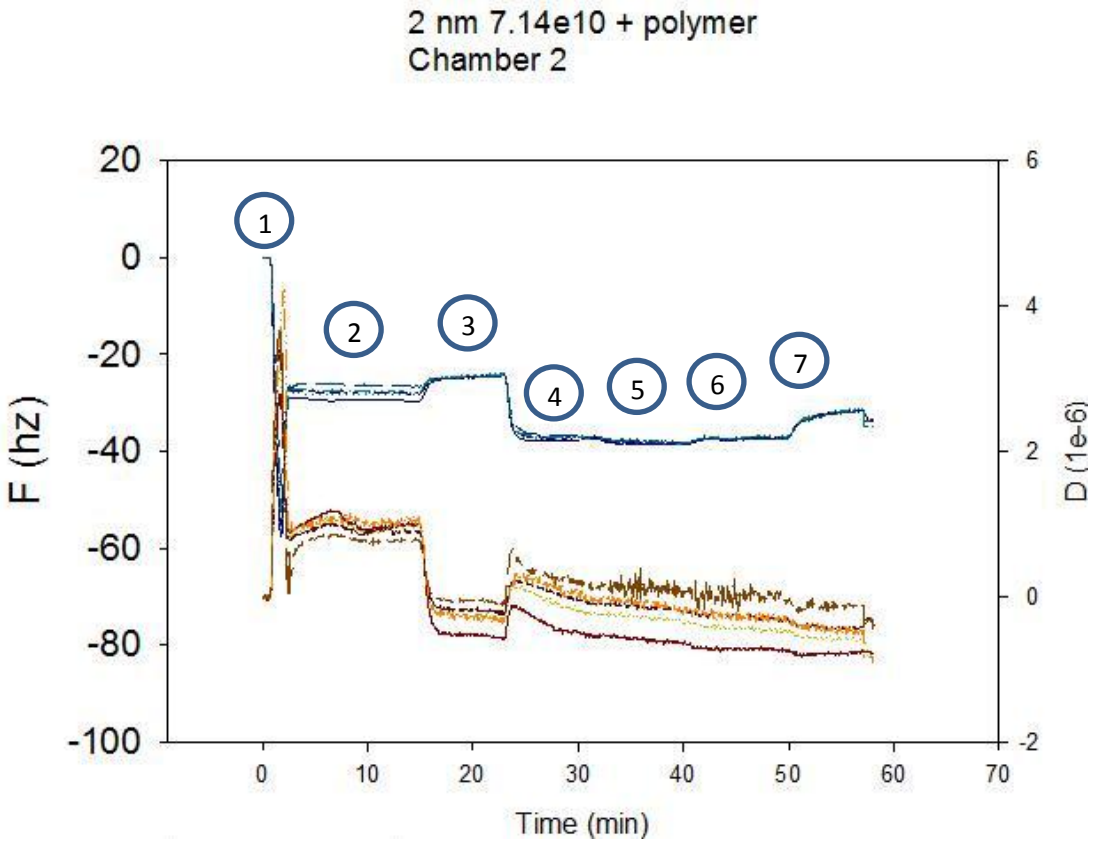

Figure 3: chamber 2 results of a trial using 2nm particles

The third result showed an increase similar to that in Figure 2, however there was a negative change in frequency between stage 4 and stage 6. This is shown in Figure 4. Additionally, all three results a decrease in rigidity that was constant from stage 4 to stage 6. These experiments should theoretical show the same results for interaction but were different due to an inconsistency from one experiment to another.

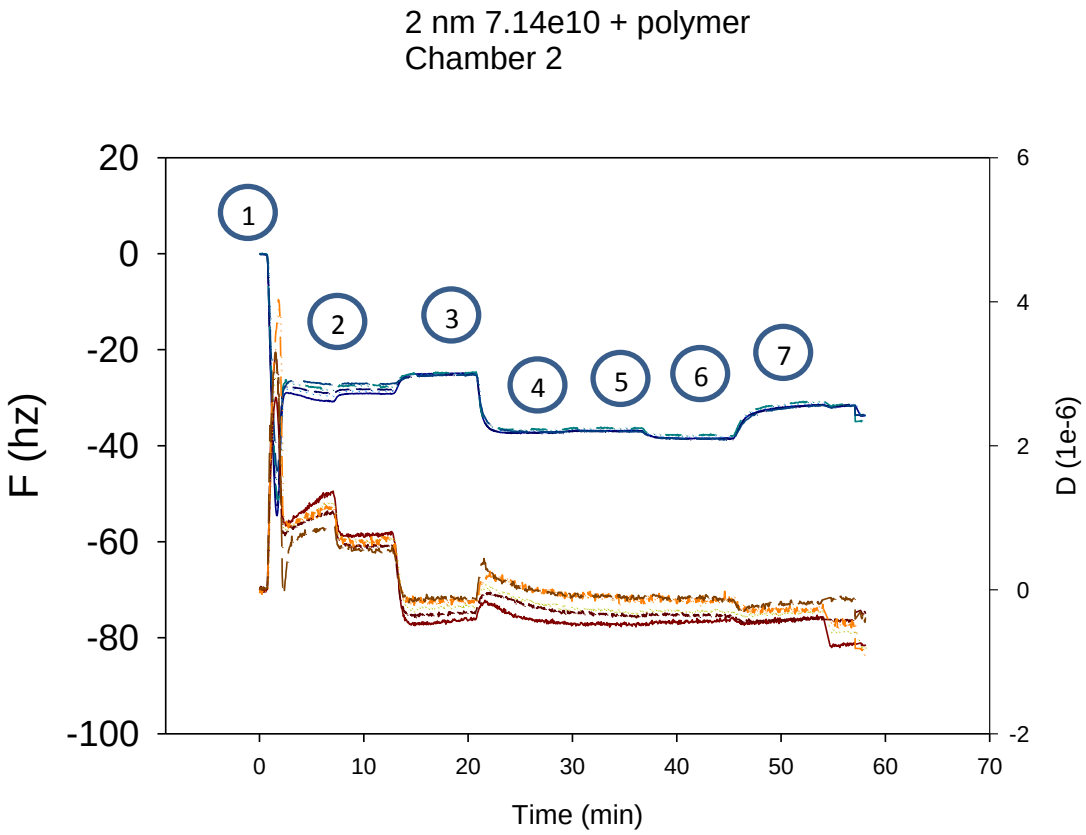

Figure 4: chamber 2 results of a trial using 2nm particles

5 nm Gold Nanoparticles QCM-D Results

The nanoparticles that will be discussed in this section are 5nm spherical gold nanoparticles. QCM-D results generally showed a decrease of about 2 hz when the nanoparticles were introduced in stage 5. The frequency after nanoparticle interaction, however, varied with different trials. Figure 5 showed a higher frequency (-25 hz) during stage 6 than in stage 4 (-30 hz). There was also an increase in dissipation from an average of -0.5 to 1e-6 simultaneous with the decrease in frequency caused by the nanoparticles. Figure 6 showed a frequency of -31 hz, a change from -28 hz seen at stage 4. Dissipation remained somewhat constant at -0.5 throughout these changes.

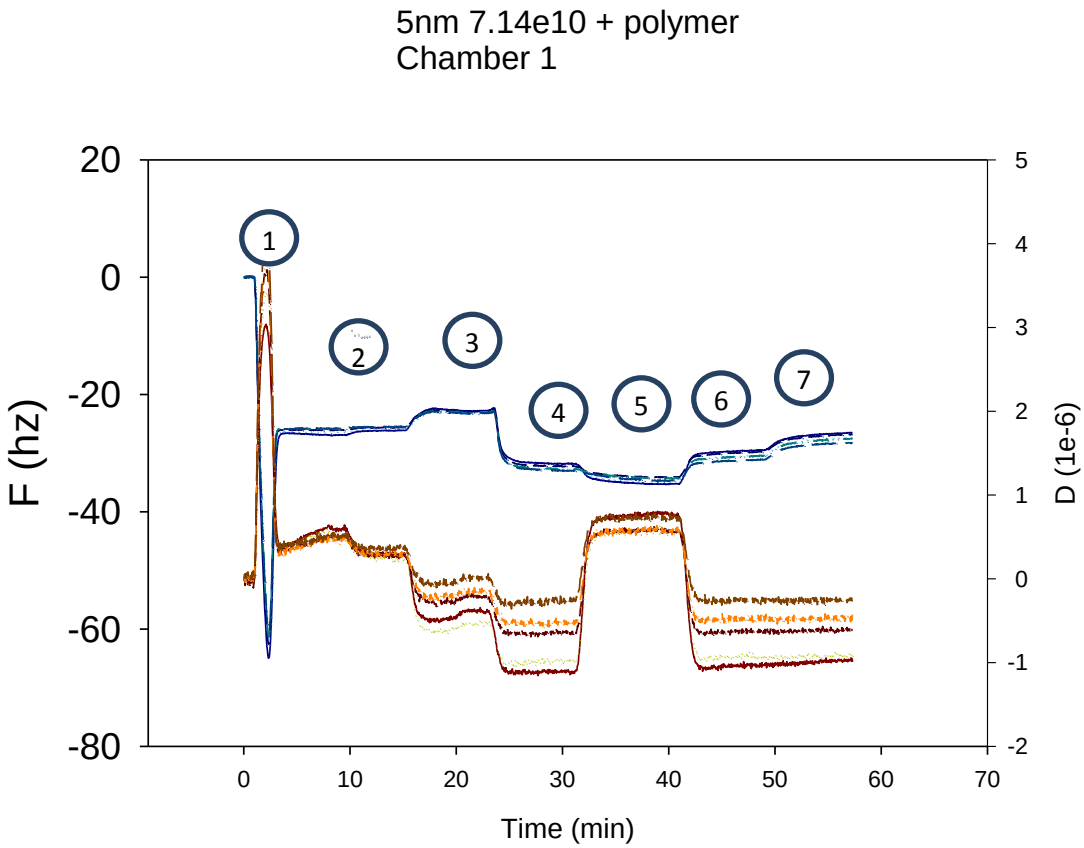

Figure 5: chamber 1 results of a trial using 5nm particles

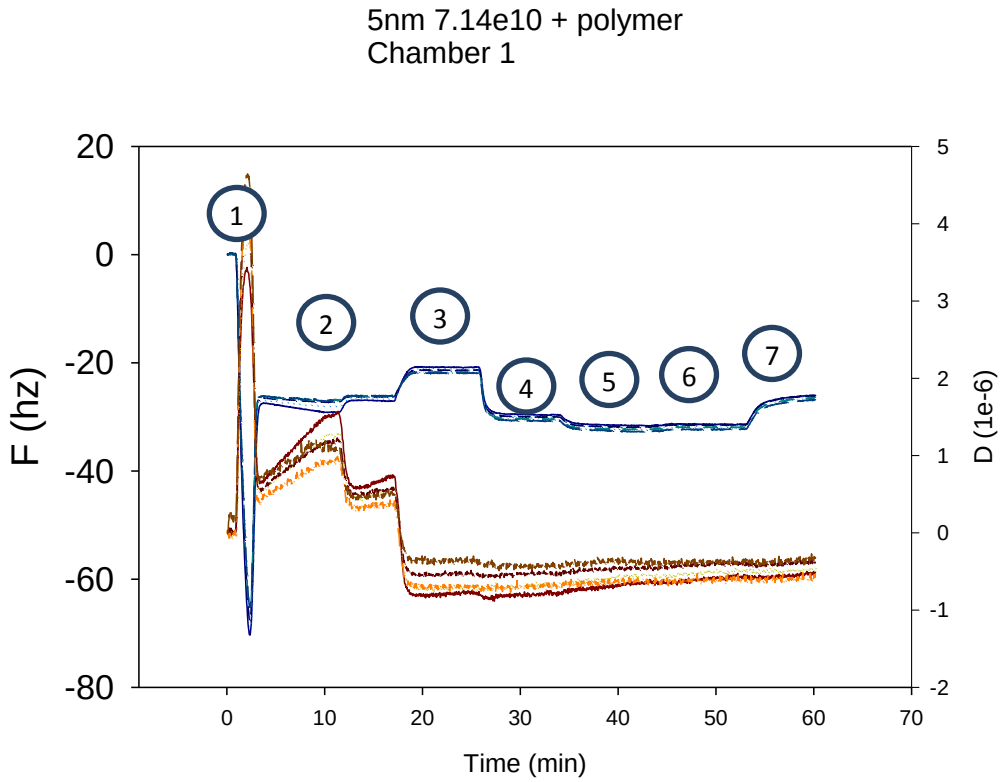

Figure 6: chamber 1 results of a trial using 5nm particles

10 nm Gold Nanoparticles QCM-D Results

The nanoparticles that will be discussed in this section are 10nm spherical gold nanoparticles. We generally saw an increase of about 3 hz from stage 4 to stage 5. The frequency then slightly dropped (about 1 hz) when only water and polymer were flowing again during stage 6. This is illustrated in Figure 7. Dissipation seemed to have slightly decreased from stage 4 to stage 6.

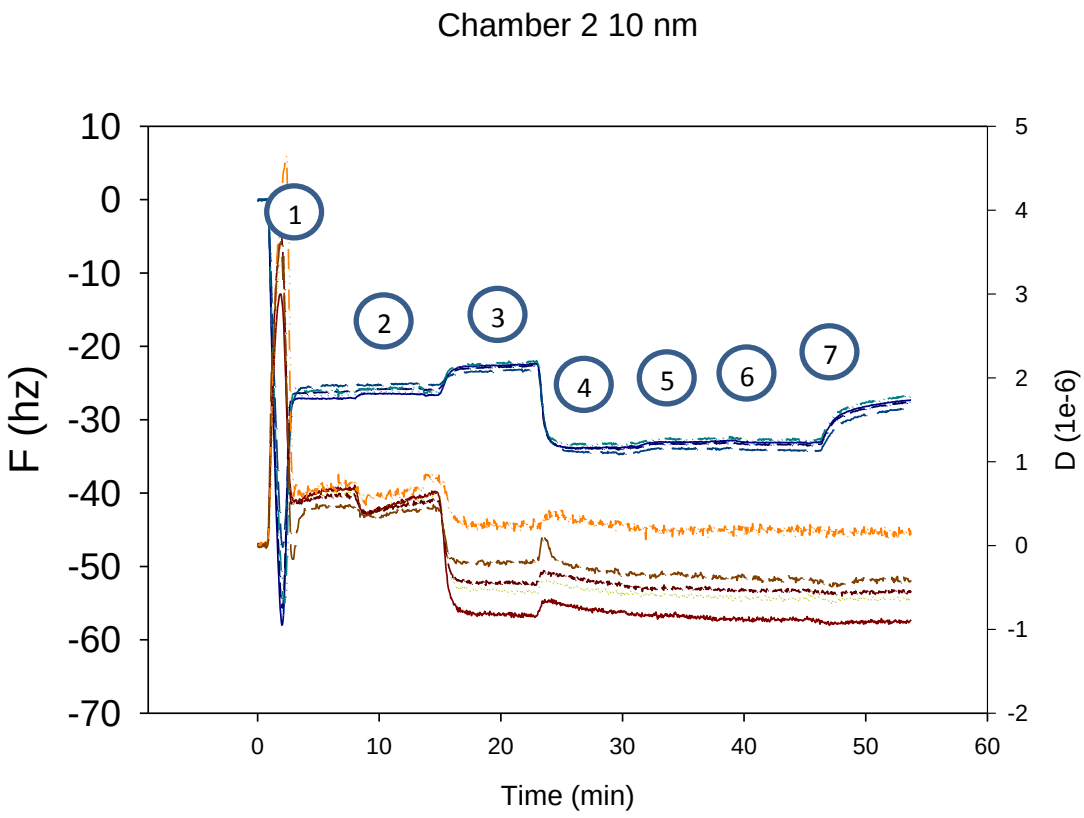

Figure 7: chamber 2 results of a trial using 10nm particles

40 nm Nanoparticles QCM-D Results

The nanoparticles that will be discussed in this section are 40nm spherical gold nanoparticles. As in the 10 nm results, 40 nm nanoparticle interactions generally resulted in an increase of about 3 hz from stage 4 to stage 5 although the frequency slightly increased (about 1 hz) when only water and polymer were flowing again during stage 6. This is illustrated in Figure 8. Dissipation seemed to have slightly decreased from stage 4 to stage 6.

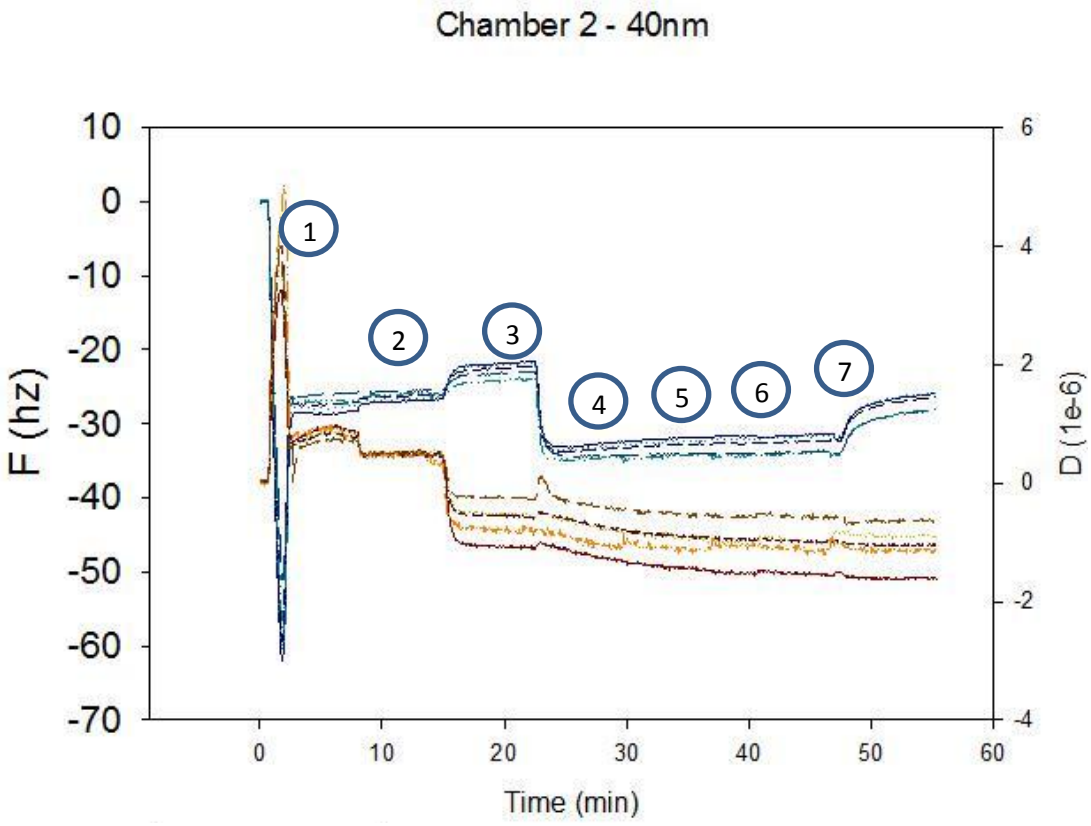

Figure 8: chamber 2 results of a trial using 40nm particles

Discussion

Formation of the Bilayer

The first decrease in frequency, at step 1, shown in Figure 1 relates to an increase in mass due to the vesicles trapping fluid and expanding on the sensors. The dissipation increase, at step 1, represents a low rigidity caused by the fluid. Consequently, the following increase in frequency, at step 2, is caused by the vesicles bursting and releasing the fluid (losing mass) to return to their lowest energy state and form a single, stabilized layer on the sensor. The stabilized frequency at step 3, with a negative frequency roughly ~-25 htz shows that the layer has remained on the crystal. The simultaneous decrease in dissipation is due to the increased rigidity of the bilayer as the molecules line up and form a single, fluid-free layer.

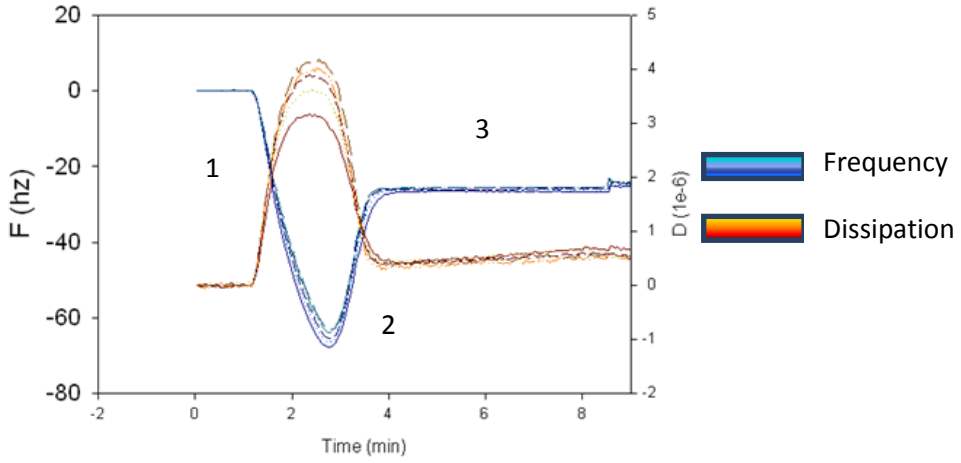

Figure 9: QCM-D graph showing successful vesicle formation and an illustration of an SLB

Repeatability of Experiments

Throughout the research, there was an underlying problem with reproducing data from experiment to experiment. Reproducibility problems ranged from failed experiments, inconsistent data sets between experiments, and even contradictory data sets during the same experiment. The latter of three can occur do to the fact the Q-Sense E4 QCM-D has four chambers running four trials per experiment. All four chambers feed from the same vials, so the variable has to come from the formation of the lipid bilayer from the shared vesicle solution. Research has been done to better understand the vesicle formation into a bilayer and results show that a single uniform bilayer is not always the end result of this transformation. Bilayer defects are common and caused by improper assembly of the vesicle solution, especially during the freeze-thaw method.[41] This could account for the problem between experiments which were performed with different vesicle solutions. Another study, completed with the use a QCM-D, showed that the dissipation at the end of bilayer formation can be correlated to possible defects in the system. Intact vesicles produce a higher change in dissipation than bilayer patches. [42] Our results show varying vesicle formations dissipations ranging from 2-0. These defects can exhibit results that are not consistent with the actual mechanism of the nanoparticle size.

2 nm Results

Figure 10 shows the overtone analysis done for 2nm interactions with an increase in frequency, as shown in Figure 2. The increase in frequency here shows a mass loss occurring instantaneously at nanoparticle introduction. This could have been caused by the formation of holes throughout the bilayer as the nanoparticles pass the bilayer. Hole formation is a common mechanism of nanoparticle interactions[43] and as the particles are uncharged is consistent with

Figure 17 located in the appendix. Rigidity also seemed to slightly increase throughout the bilayer; however it was more prominent in the bottom layers than at the surface. As holes were being created, some polymer could have filled in the gaps. This would have accounted for the small increase in rigidity.

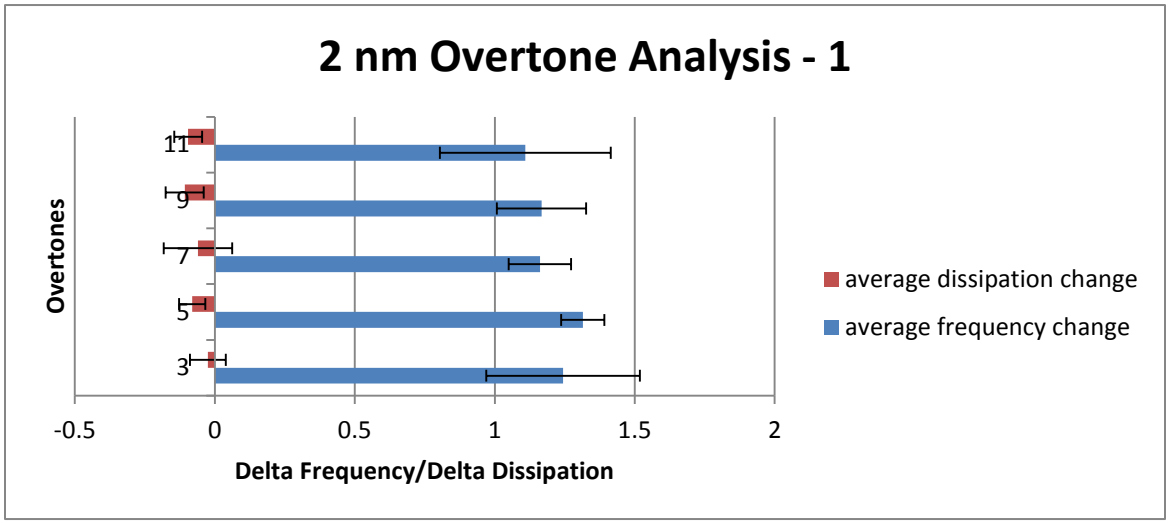

Figure 10: Overtone analysis for 4 chambers using 2nm particles

Figure 11 analyzes the results of 2nm decrease in frequency as illustrated by Figure 3 . This again showed mass loss but for a different reason. The mass loss occurred suddenly at the introduction of the water and polymer rinse. At the introduction of nanoparticles there was actually an increase in mass. This interaction is consistent with reports that nanoparticles will expand pre-existing defects. This research was done in vitro and a rinse did not occur to see if the nanoparticles adhered to the bilayer.[44] The polymer again enters the bilayer adding some rigidity to the structure where the defects were expanded.

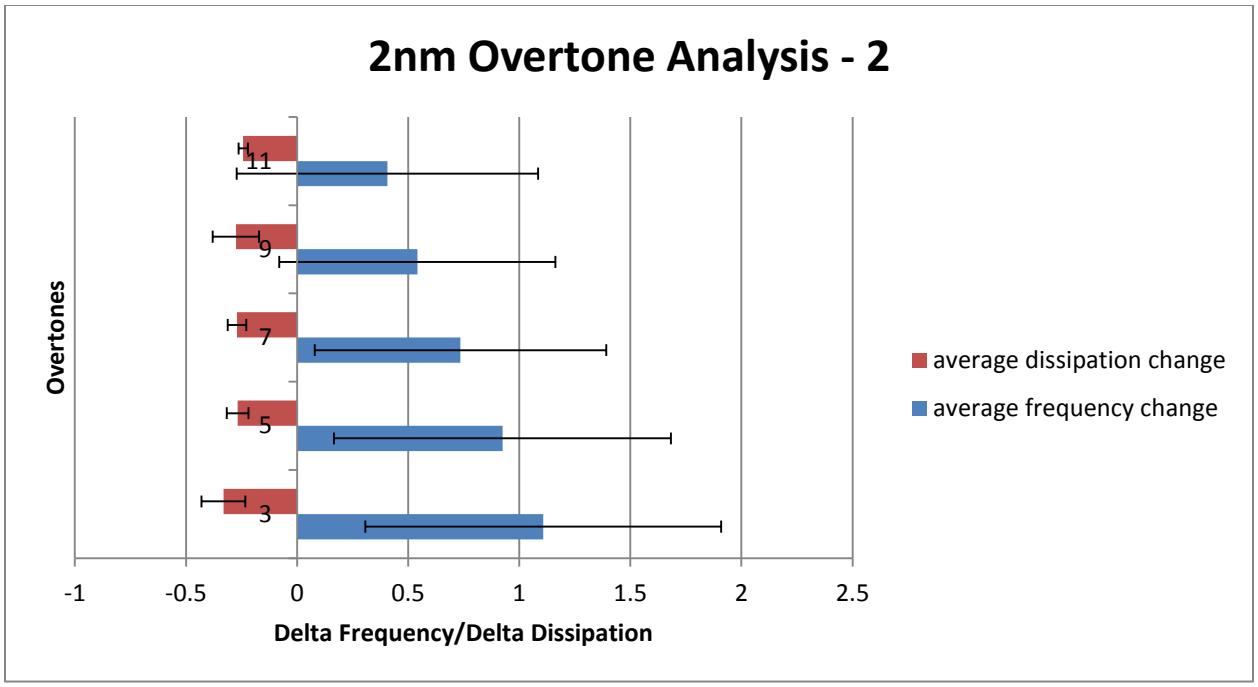

Figure 11: Overtone analysis for 4 chambers using 2nm particles

Figure 12 clearly shows an increase in mass accompanied by higher rigidity throughout the membrane. This represents nanoparticle adsorption as shown by Figure 4, where particles adhered to the membrane and were too resilient to be washed away by the water and polymer solution. In addition, the particles are naturally more rigid than the membrane. This adds to the overall stiffness of the material, more so than the polymer. This interaction only occurred in two chambers during one experiment. The QCM-D chart in Figure 4 shows that the dissipation was highest in this experiment then any of the other 2nm results. As previously stated, this correlates to possible non-ruptured vesicles and therefore defects in the membrane.

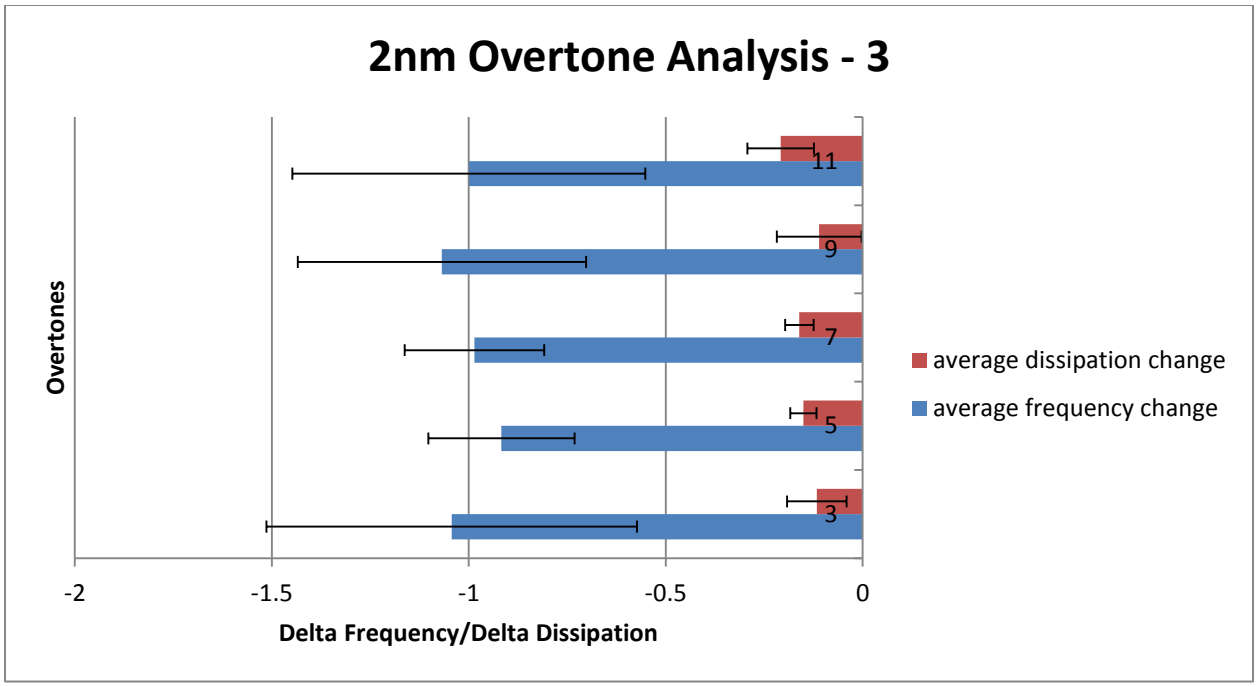

Figure 12:Overtone analysis for 3 chambers using 2nm particles

5 nm Results

Just as with the first two 2 nm overtone bar graphs, 5nm nanoparticles show a definite mass loss when comparing the sample before and after nanoparticle introduction. This time we saw a very small decrease in rigidity at the surface, and an increase on the bottom layers as seenin Figure 13. This could be cause by water filling in the holes and destabilizing the membrane.

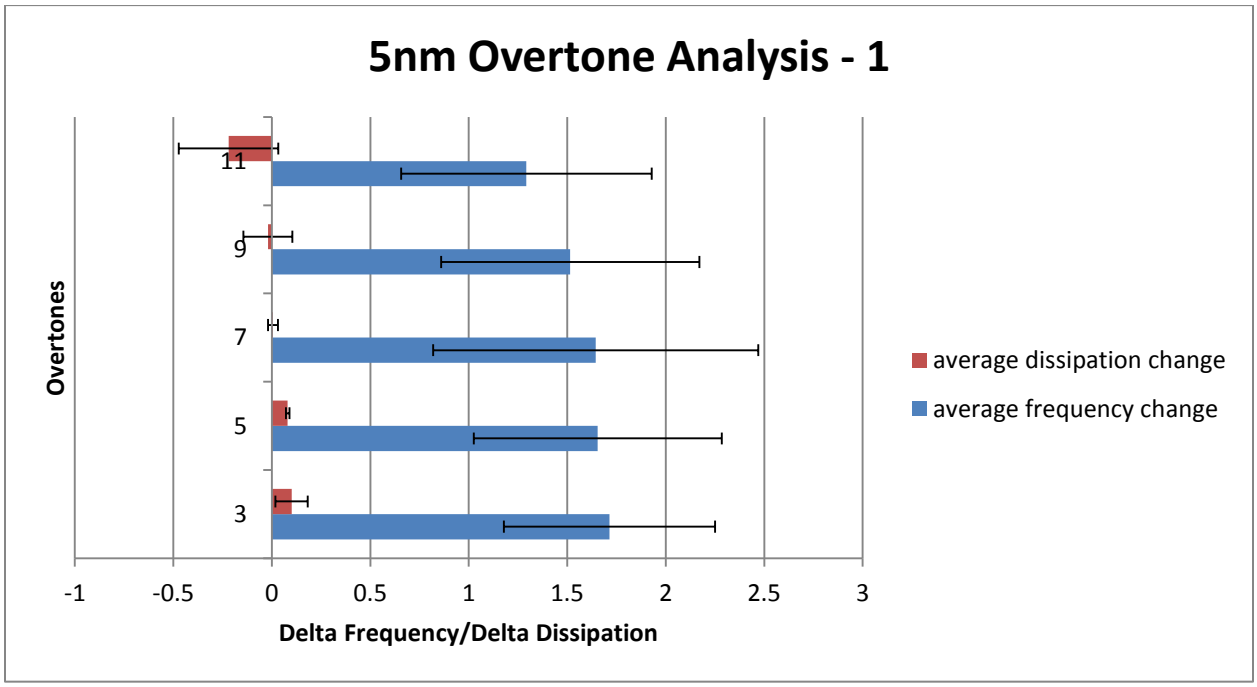

Figure 13: Overtone analysis for 4 chambers using 5nm particles

10 nm/40 nm Results

Once again, mass loss and an increase in rigidity were witnessed in a similar interaction of 2nm in Figure 2. The large molecules form holes that produce mass loss that is greatest at the surface as shown by Figure 14 and Figure 15.

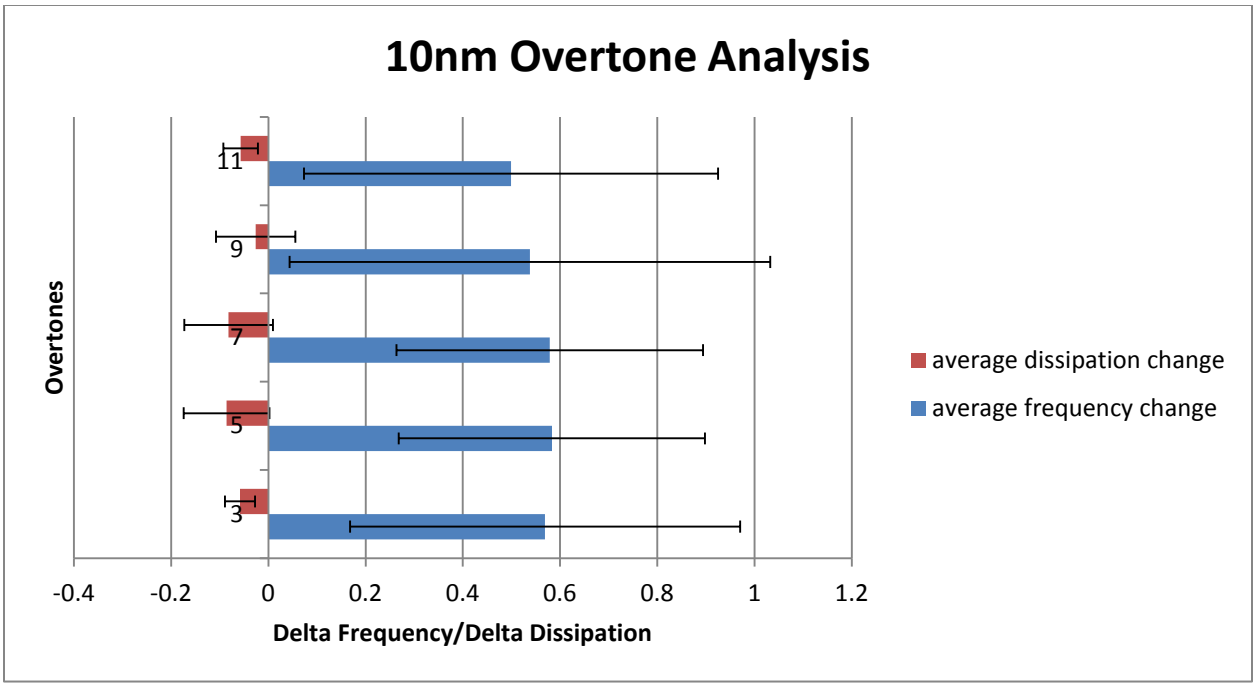

Figure 14: Overtone analysis for 4 chambers using 10nm particles

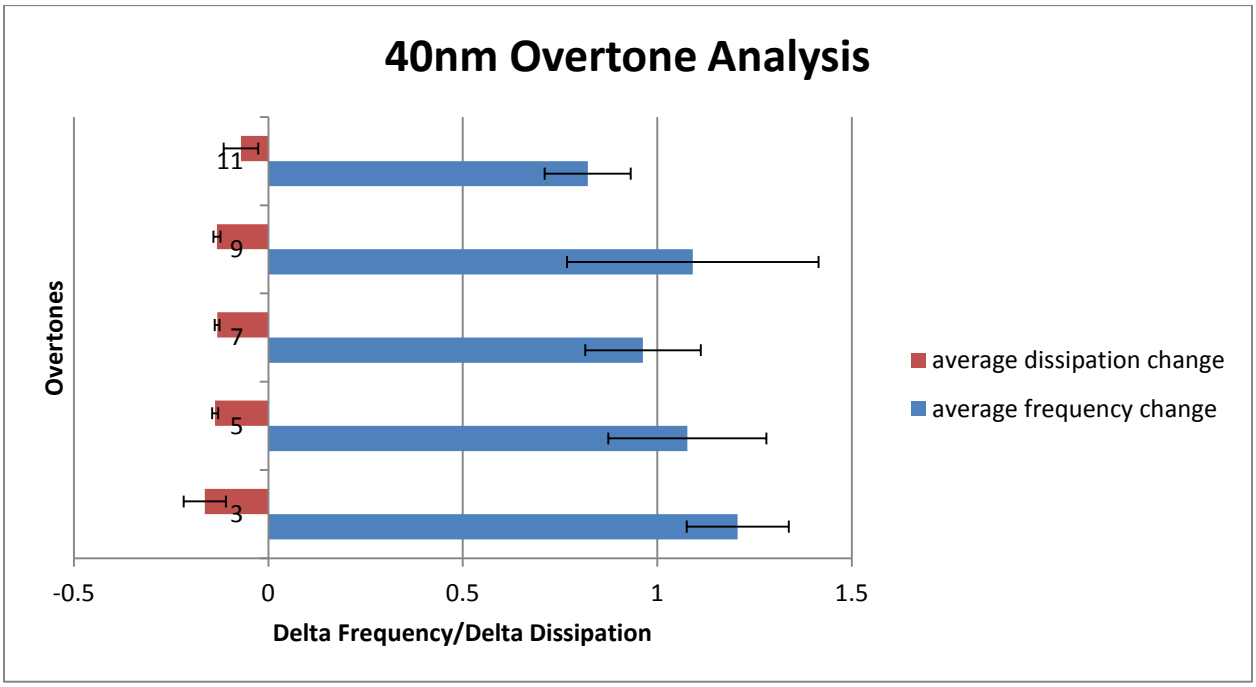

Figure 15: Overtone analysis for 4 chambers using 40nm particles

Effect of Nanoparticle Size on Membrane Interaction

Table 1 below shows the number of results that occurred for either mass loss or mass gained, at each size of the nanoparticle. Raw data can be found in the appendix. It is clear that the favored interaction caused a mass loss in the membrane along with an increase in rigidity. This shows that the uncharged bare gold nanoparticles interacted at the surface, damaged the membrane, and then left the system.[45] This allows the polymer to fill in and possibly increase the rigidity. Results for the 5nm particles were different, however we believe that if given more trials and overcoming any problem with reproducibility, the results would eventually favor mass loss and rigidity increase.

Table 1: cumulative results of all runs done in this experiment. All raw data can be found in the appendix

SIZE (nm)	**MASS LOSS # of results**	**MASS GAIN # of results**	**Rigidity**
2	9	5	Increased Rigidity
5	2	4	Decreased Rigidity
10	11	2	Increased Rigidity
40	6	2	Increased Rigidity

The results do show that there is no effect due to size of these bare nanoparticles. Mass loss is occurring independently of size and no adherence is taking place with the bilayer and the bare nanoparticles.

Conclusion and Recommendations

From the results above, size wasn't a variable that governed how the bare gold nanoparticles affected the membrane. All four sizes relatively acted the same way. Although results favored mass loss and an increase in rigidity, all interactions seem to have changed the structure of the SLB in some way, whether it was a degradation of the membrane or adsorption of nanoparticles to the membrane. We did not witness any cases of the bilayer not being affected by the introduction of nanoparticles.

An important thing to consider is the lack of reproducibility in these experiments. The existence of defects during the formation of the SLB is in itself, a variable in the experiment. Future research should take these defects into consideration and inevitably strive to control them, either by completing removing them from the system to model a healthy lipid bilayer or to control the existence of them and represent a flawed bilayer.

The defects in the model membrane are analogous to those that can be found in living cells. If nanoparticles are to be used more in industrial processes and bioengineering application, they will ultimately end up in either waste streams or within the body and interact with both healthy and damaged cells.

Appendix

APPENDIX A: Supplementary Background Information

Table 2: Cytotoxicity of gold nanoparticles[3]

Table 4. Cytotoxicity of gold nanoparticles.

Cell line	Surface coating	Exposure conditions	NP concentration (average size)	Test	Exposure duration	Toxicity	Author	Year
COS-7 cells	PEI2	$3x10^5$ cells/ well	N/A	MTT	6 h + 42 h	70-80% viability after transfection	Thomas [76]	2003
Human liver carcinoma, HepG2	BSA, 4 targeting peptides	85% confluency	N/A (d=20-25 nm)	LDH	12 h	Viability slightly compromised (<5%)	Tkachenko [77]	2003
COS-1, Red blood cells, E.coli	NH3, COOH	80% confluency, 96-well plate	0.38, 0.75, 1.5, or 3 μM	MTT, Trypan blue	1, 2.5, 6, 24 h	LD50 (Cos-1): anionic ~1 μM and cationic >7.37 μM; similar for other cell types	Goodman [12]	2004
HeLa, 3T3/NIH, HepG2	BSA, 4 targeting peptides	75% confluency	150 pM (d=22 nm)	LDH	3 h	Cell viability reduced by 20% in HeLa cells, but only 5% in 3T3/NIH	Tkachenko [78]	2004
Leukemia cell line, K562	citrate, biotin, L-cysteine, glucose, CTAB	10^4 cells/ well	0-250 μM Au atoms (d=4, 12, 18 nm)	MTT	3 days	No apparent toxicity at 250 μM, glucose and cysteine modified not toxic up to 25 μM	Connor [24]	2005
Human breast carcinoma xenograft cells, MDA-MB-231	coumarin-PEG-thiol, mPEG-thiol (neg. control)	10^5 cells/ well in 96-well plates	50-200 μg mL^{-1} (d=10 nm)	Cell Titer 96	24 h	Nanoparticles are internalized but essentially non-toxic up to 200 μg mL^{-1}	Fu/Shenoy [28/29]	2005
RAW264.7 macrophage cells	lysine, PLL, FITC	10^5 cells/ well in 96-well plates	10, 25, 50, and 100 μM (d=3-8 nm)	MTT	24, 48, 72 h	100 μM - after 72 hr cell viability to decreased to 85%	Shukla [25]	2005
Human dermal fibroblasts	citrate	N/A	0-0.8 mg mL^{-1} (d=13+/-1 nm)	microscopy	2-6 days	Dose-dependent decrease in cell area & density; many vacuoles	Pernodet [79]	2006

Table 3: Nanopartz technology comparison

	Nanopartz™Accurate™ Spherical Gold Nanoparticles	**Other Technologies**
Monodispersity	High (<2%)	Low (>15%)
Size Accuracy	High (+/-2nm)	Low
Linewidths	Narrow	Broad
Storage lifetime	Years	6 months at 4C
Ability to ligand exchange	Easy	More difficult

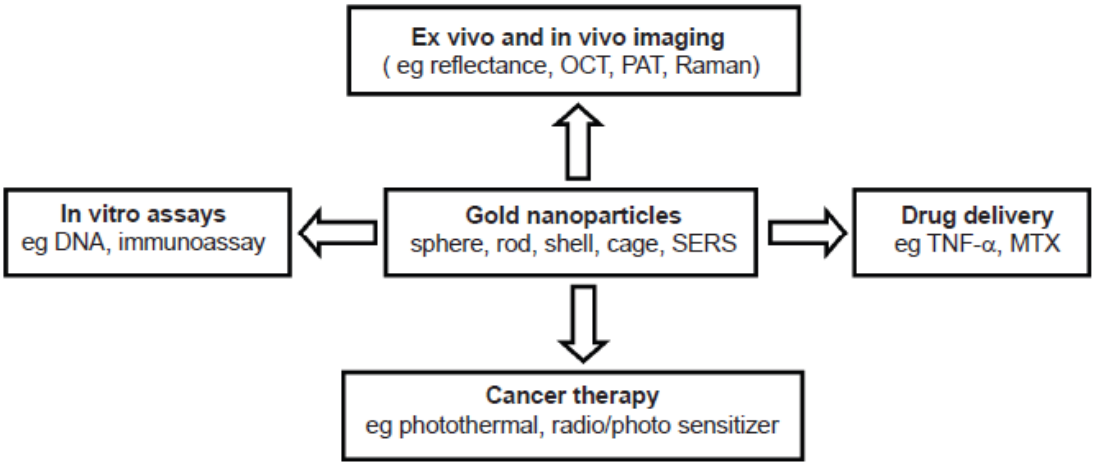

Figure 16: Some Applications of Gold Nanoparticles in Cancer Nanotechnology

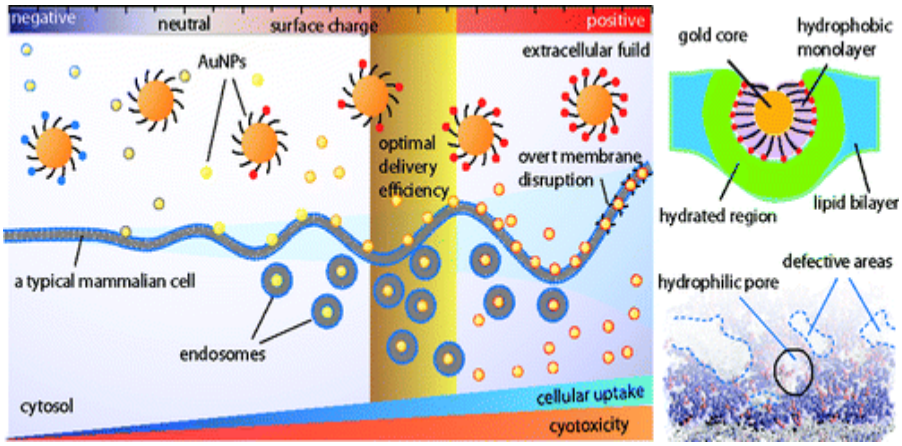

Figure 17: Penetration of Varied Charged Gold Nanoparticles

APPENDIX B: ALL QCM-D Data Graphs

2 nm 2-17-2012 QCM-D Results

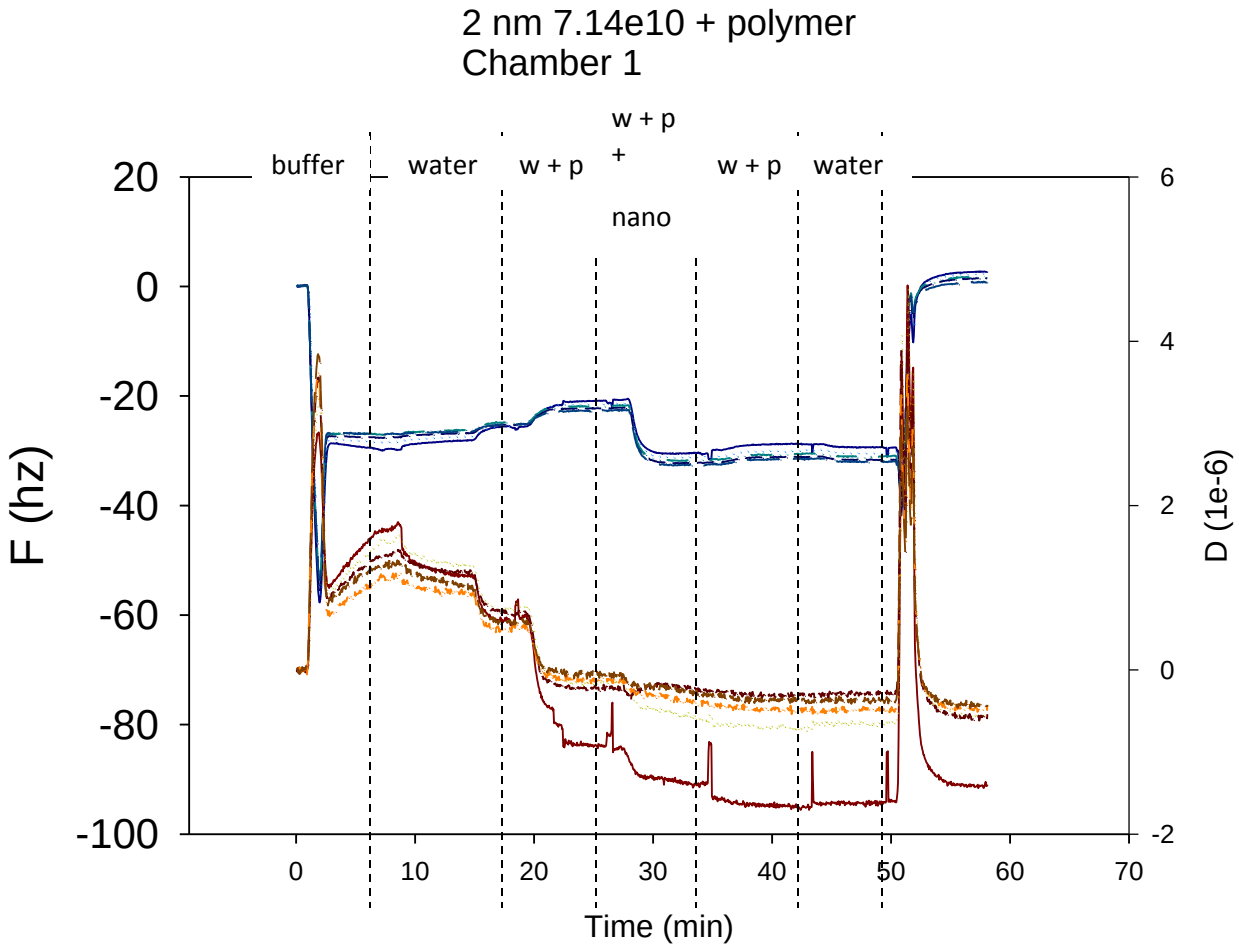

7:58
buffer

18:04
water

26:00
water+polymer

34:48
water polymer au

44:00
water + polymer 2

50:00
water

58:00
end

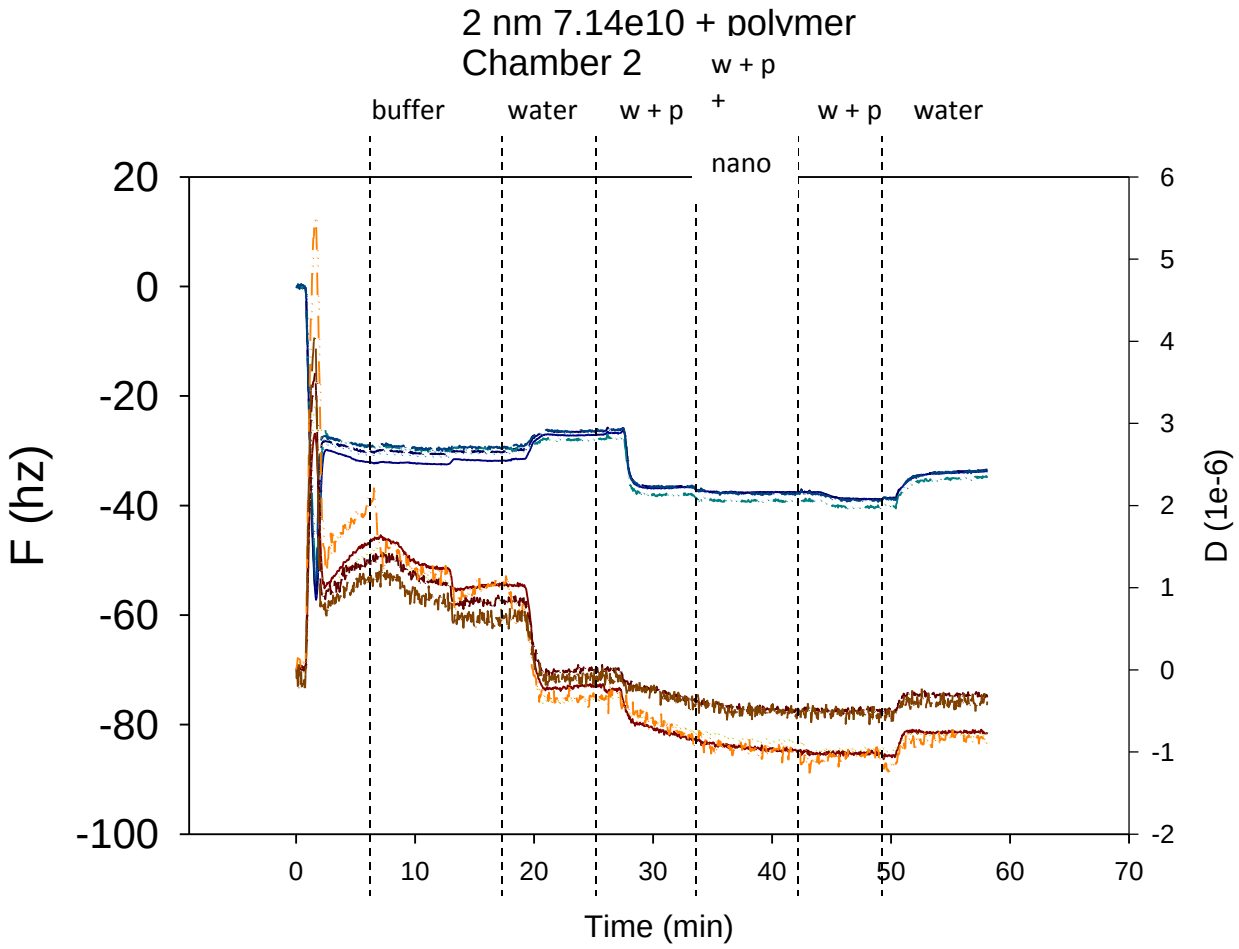

F3
F5
F7
F9
F11
D3
D5
D7
D9
D11

7:58
buffer

18:04
water

26:00
water+polymer

34:48
water polymer au

44:00
water + polymer 2

50:00
water

58:00
end

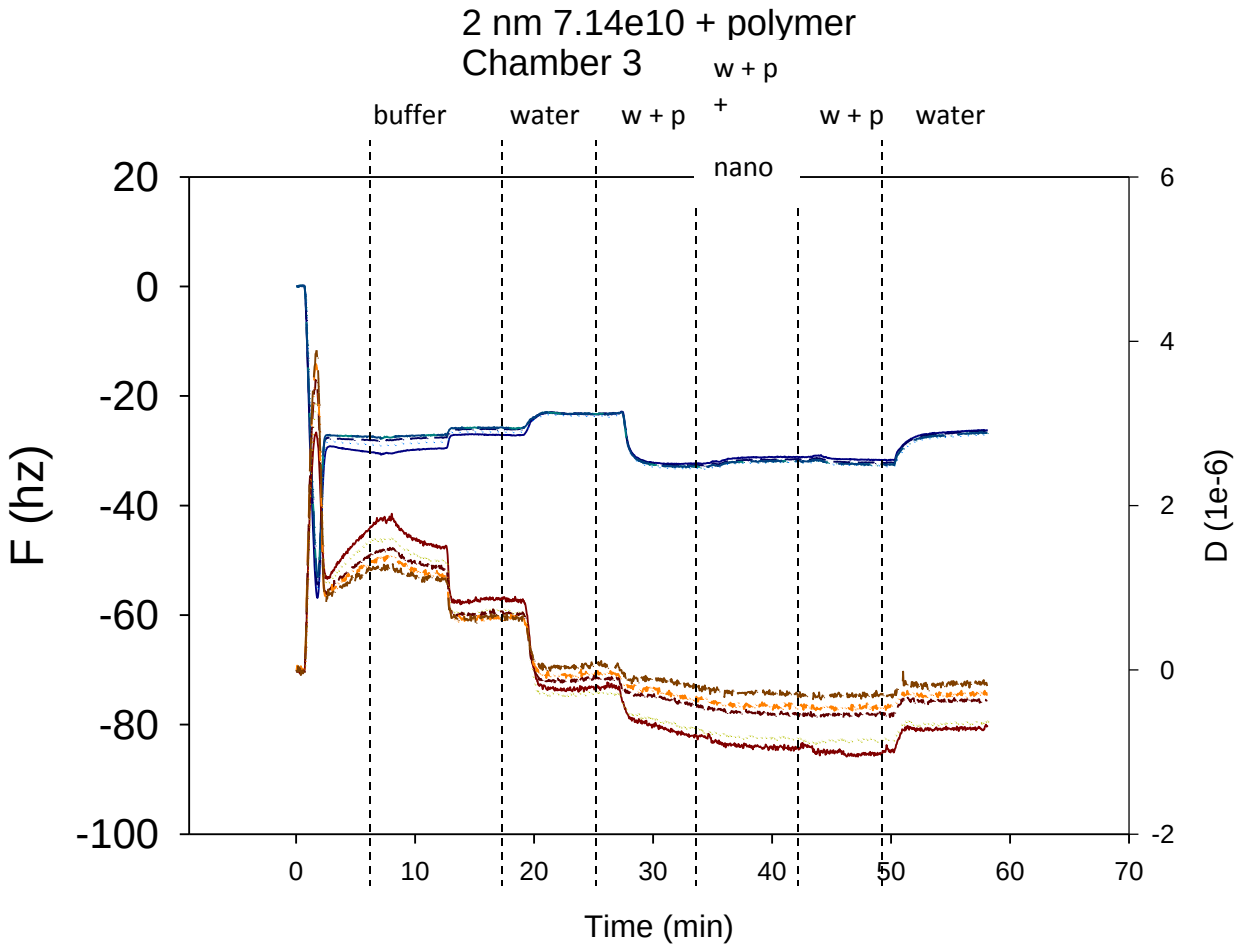

F3
F5
F7
F9
F11
D3
D5
D7
D9
D11

7:58
buffer

18:04
water

26:00
water+polymer

34:48
water polymer au

44:00
water + polymer 2

50:00
water

58:00
end

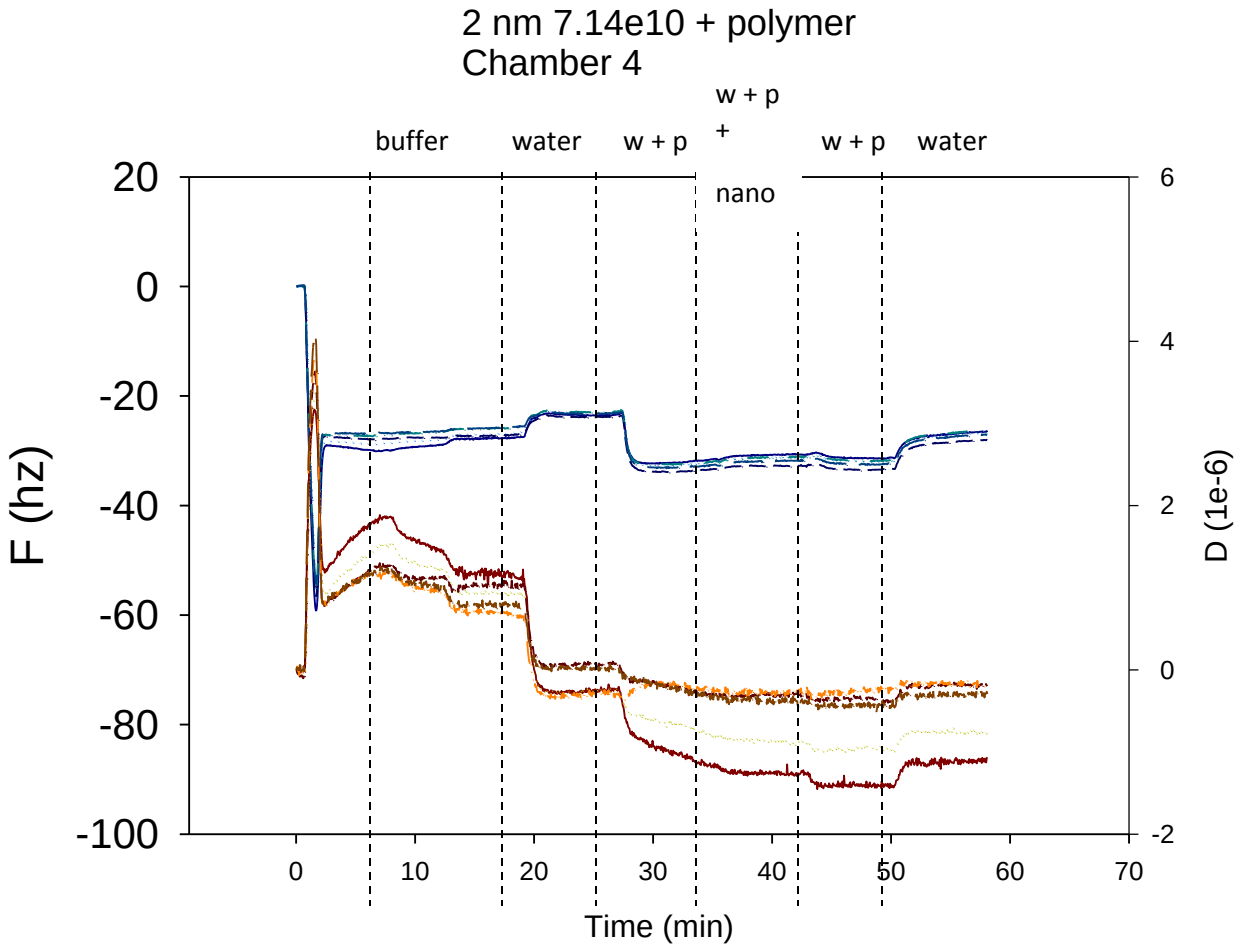

F3
F5
F7
F9
F11
D3
D5
D7
D9
D11

7:58
buffer

18:04
water

26:00
water+polymer

34:48
water polymer au

44:00
water + polymer 2

50:00
water

58:00
end

2 nm 2-21-2012 QCM-D Results

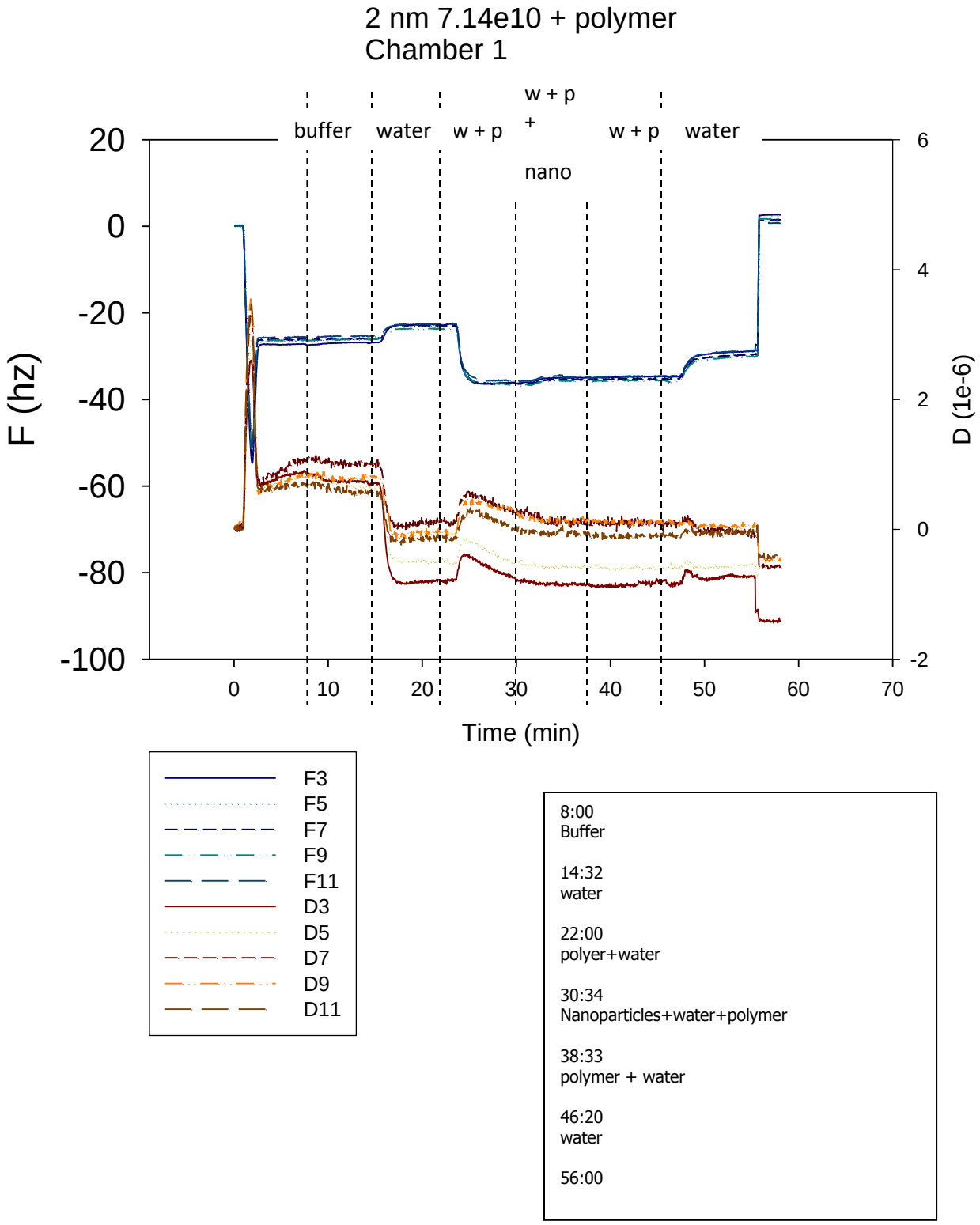
2 nm 7.14e10 + polymer
Chamber 1
buffer
water
w + p
w + p
+
nano
water
F (hz)
D (1e-6)
Time (min)
20
0
-20
-40
-60
-80
-100
6
4
2
0
-2
0
10
20
30
40
50
60
70
F3
F5
F7
F9
F11
D3
D5
D7
D9
D11
8:00
Buffer
14:32
water
22:00
polyer+water
30:34
Nanoparticles+water+polymer
38:33
polymer + water
46:20
water
56:00

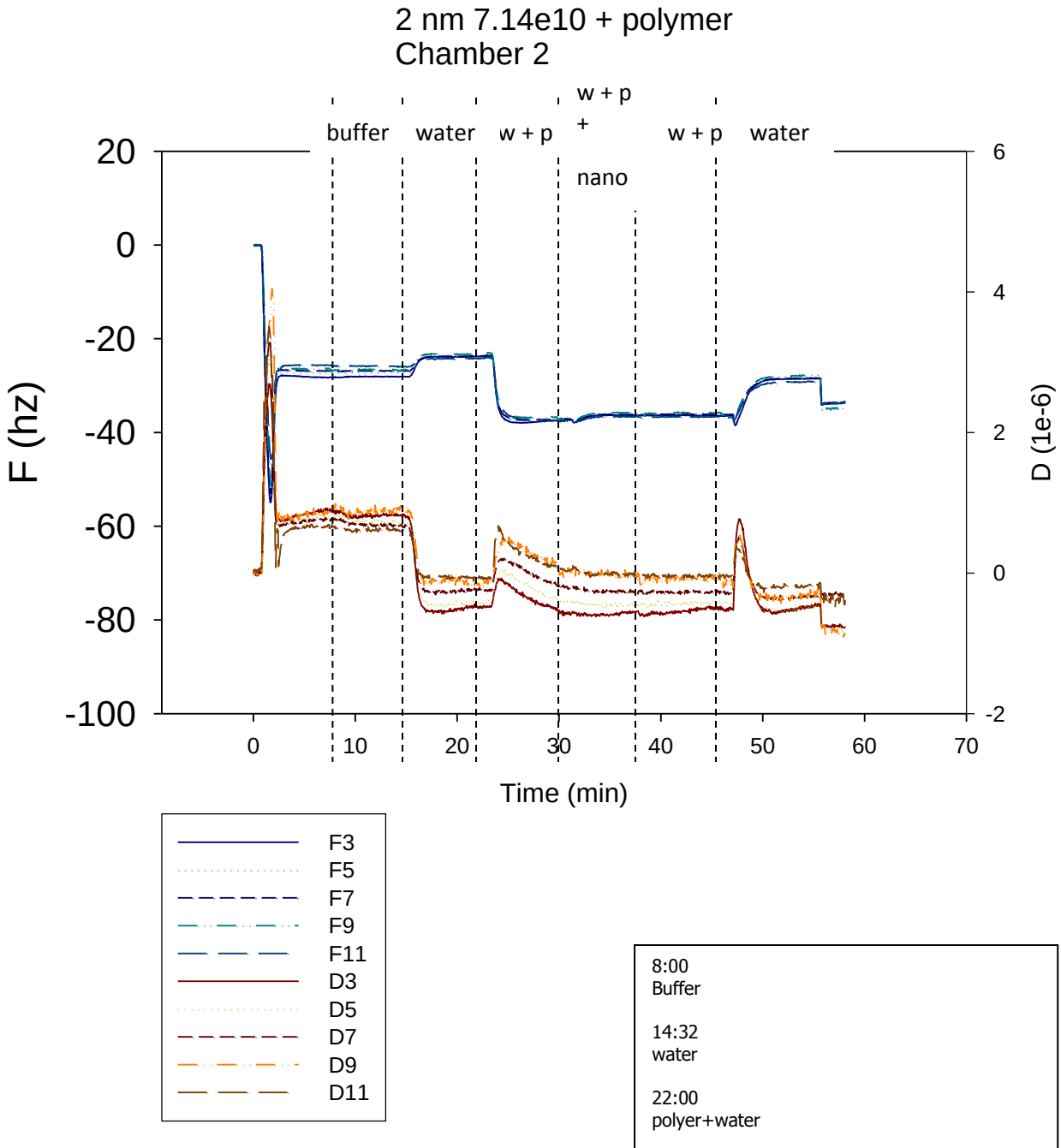

8:00
Buffer

14:32
water

22:00
polyer+water

30:34
Nanoparticles+water+polymer

38:33
polymer + water

46:20
water

56:00

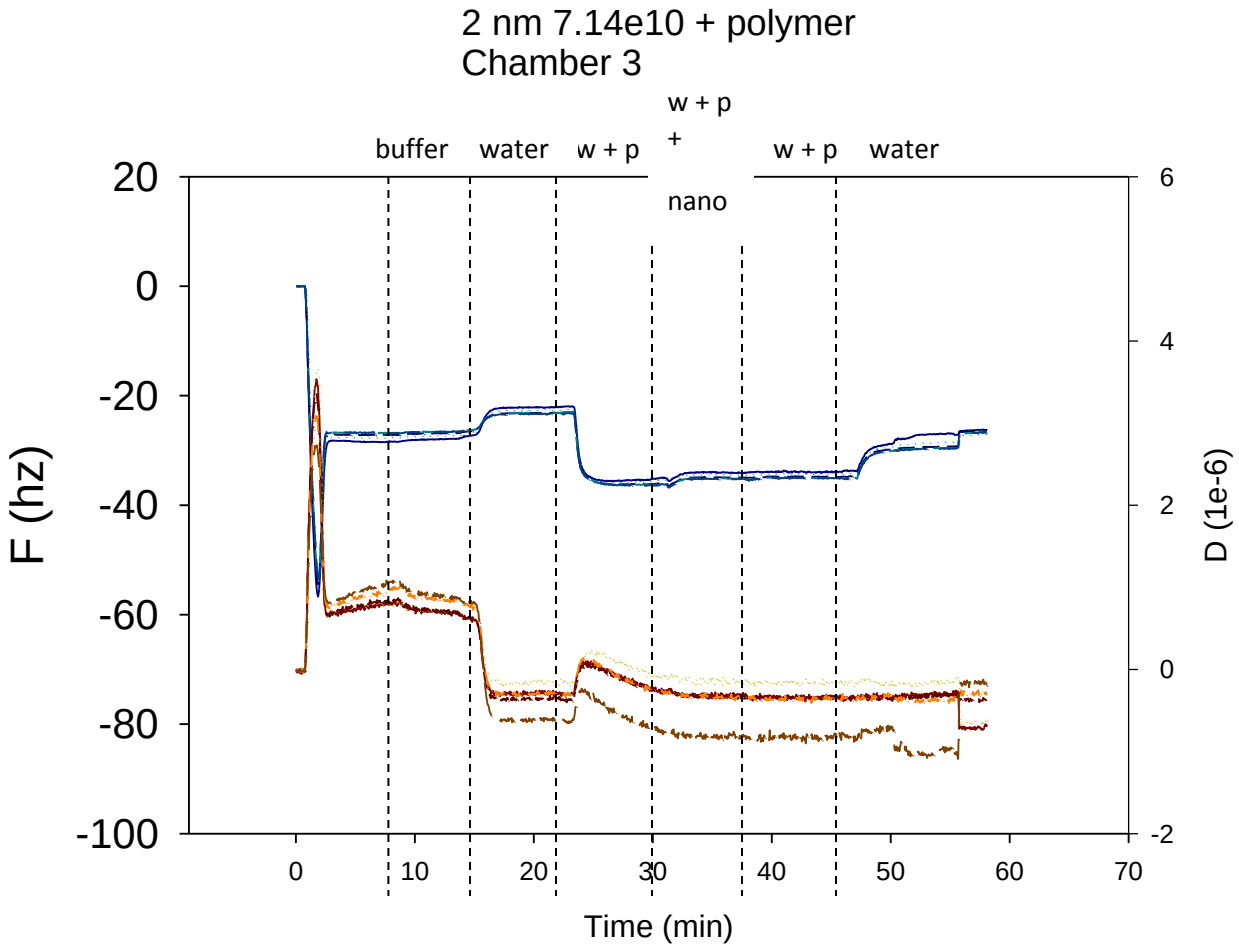

8:00
Buffer

14:32
water

22:00
polyer+water

30:34
Nanoparticles+water+polymer

38:33
polymer + water

46:20
water

56:00

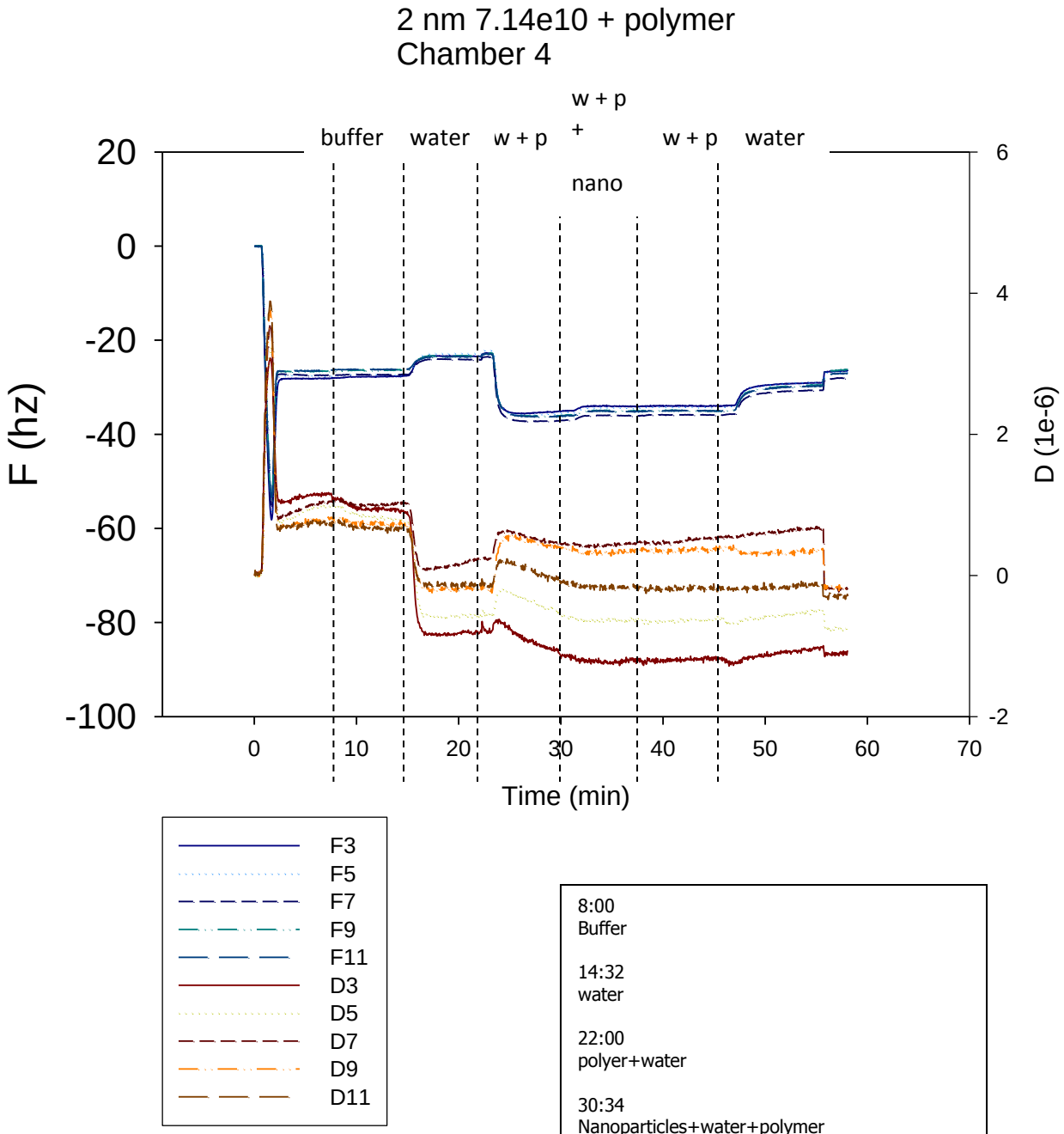
2 nm 7.14e10 + polymer
Chamber 4
buffer
water
w + p
w + p
+
nano
water
F (hz)
D (1e-6)
Time (min)
F3
F5
F7
F9
F11
D3
D5
D7
D9
D11
8:00
Buffer
14:32
water
22:00
polyer+water
30:34
Nanoparticles+water+polymer
38:33
polymer + water
46:20
water
56:00

a

2 nm 2-23-2012 QCM-D Results

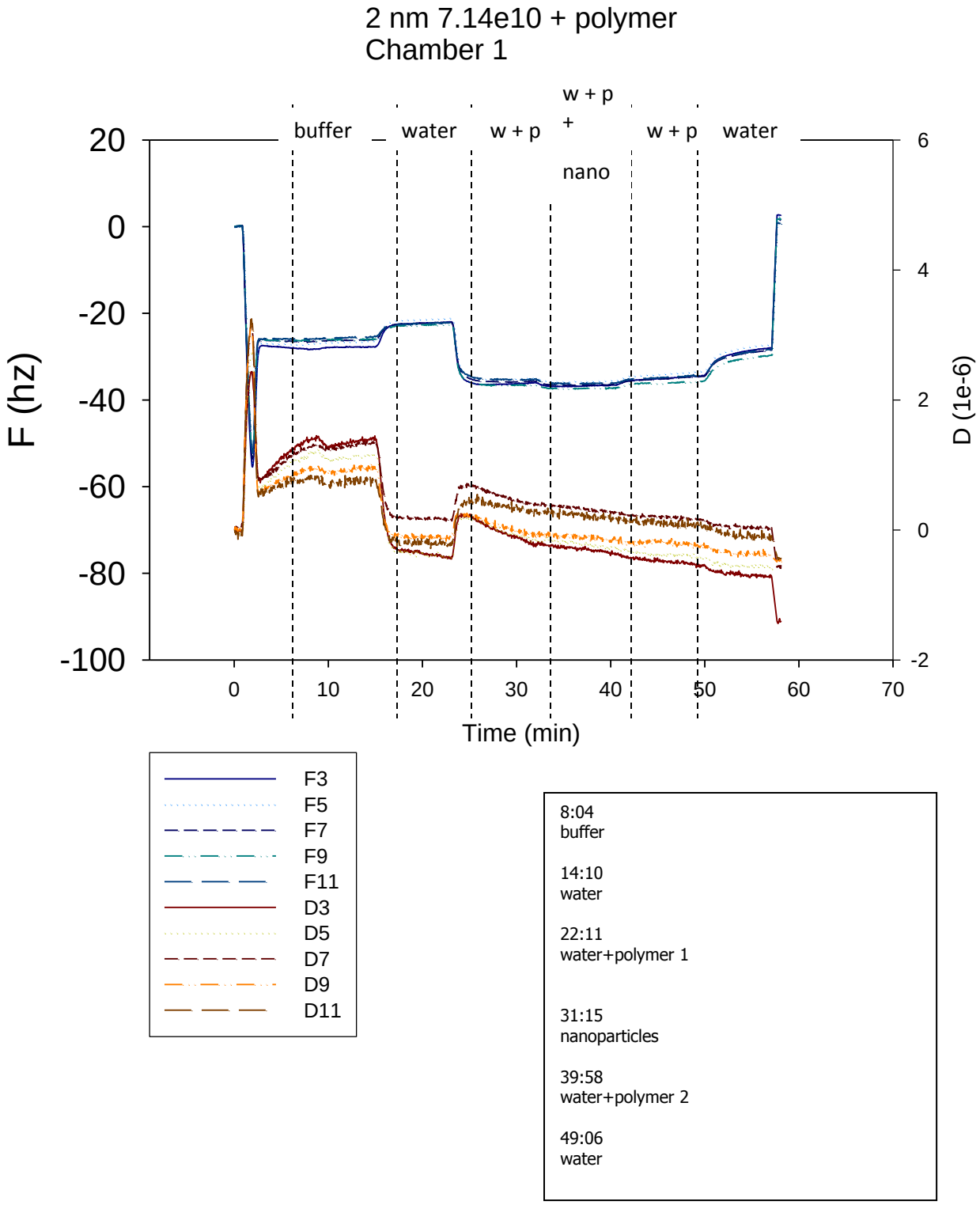
2 nm 7.14e10 + polymer
Chamber 1
buffer
water
w + p
w + p
+
nano
water
F (hz)
D (1e-6)
Time (min)
F3
F5
F7
F9
F11
D3
D5
D7
D9
D11
8:04
buffer
14:10
water
22:11
water+polymer 1
31:15
nanoparticles
39:58
water+polymer 2
49:06
water

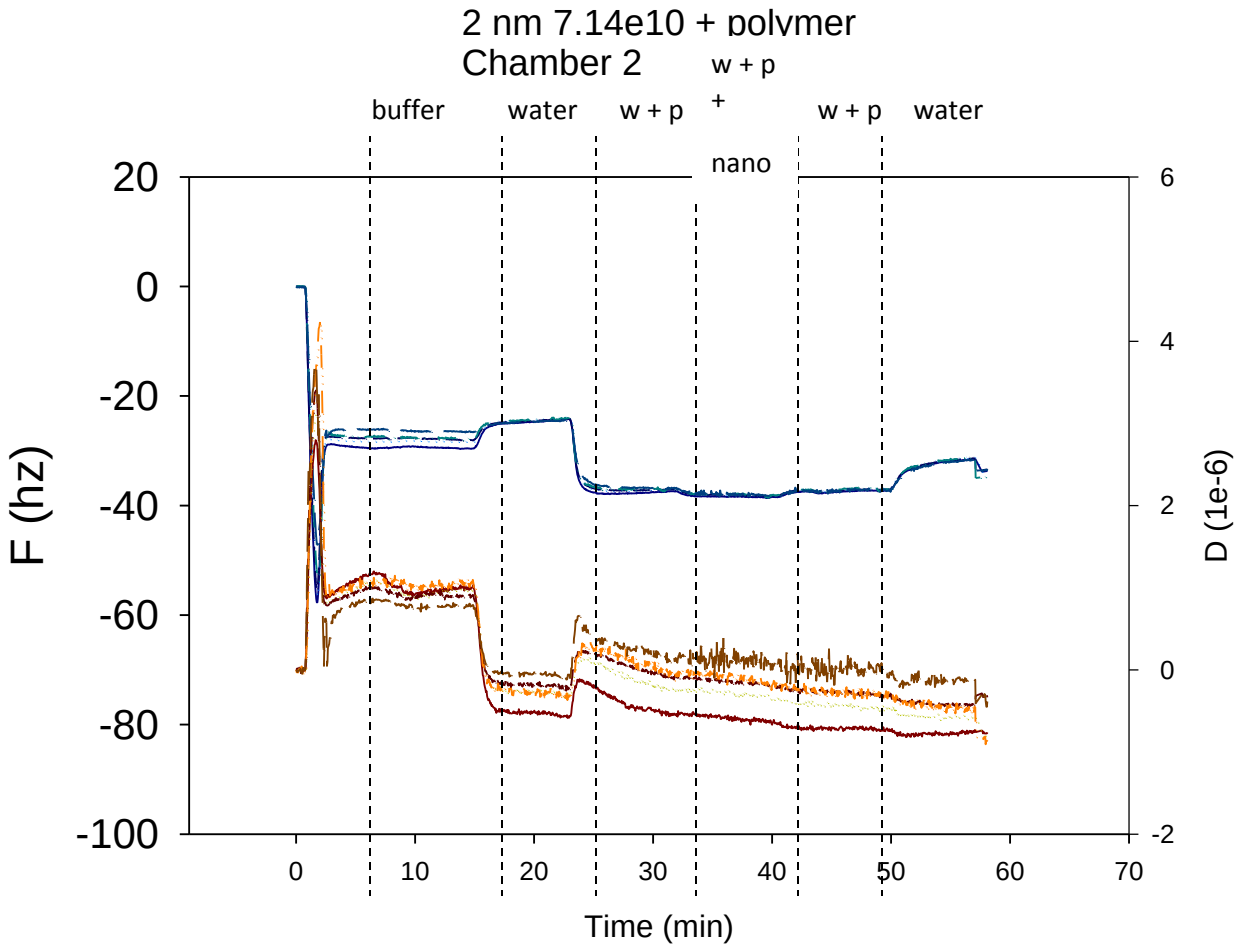

F3
F5
F7
F9
F11
D3
D5
D7
D9
D11

8:04
buffer

14:10
water

22:11
water+polymer 1

31:15
nanoparticles

39:58
water+polymer 2

49:06
water

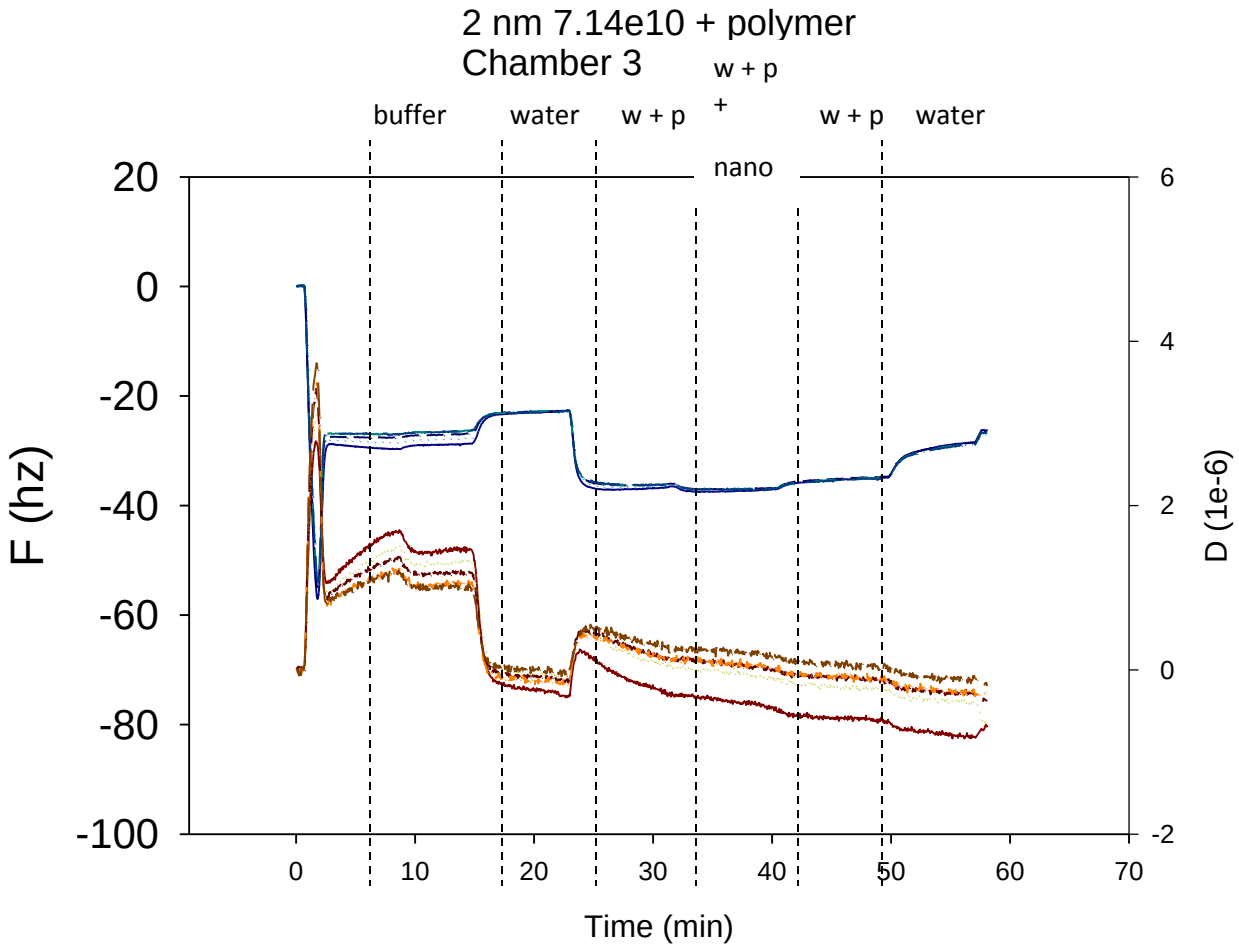

F3
F5
F7
F9
F11
D3
D5
D7
D9
D11

8:04
buffer

14:10
water

22:11
water+polymer 1

31:15
nanoparticles

39:58
water+polymer 2

49:06
water

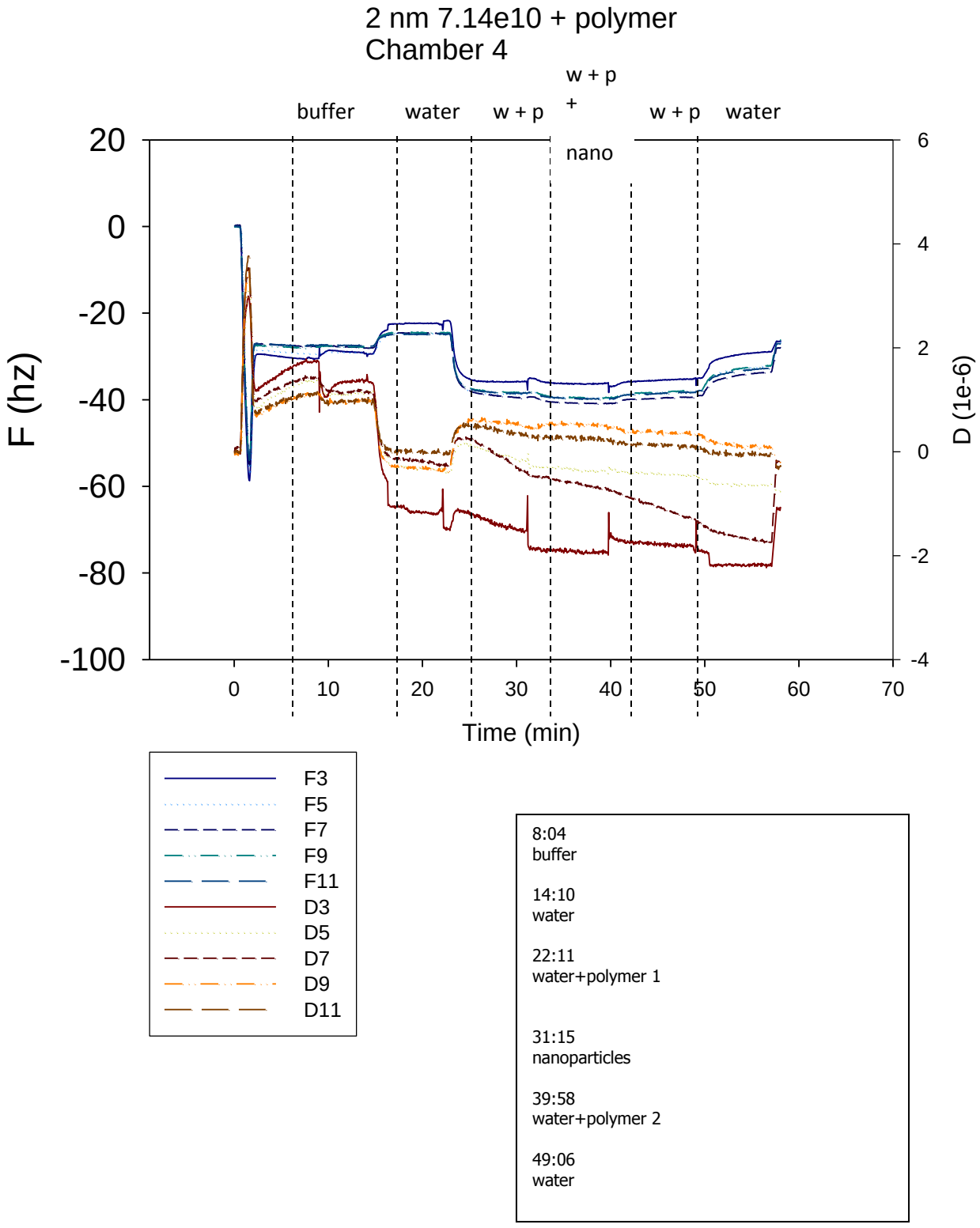
2 nm 7.14e10 + polymer
Chamber 4
buffer
water
w + p
w + p
+
nano
w + p
water
F (hz)
D (1e-6)
Time (min)
20
0
-20
-40
-60
-80
-100
6
4
2
0
-2
-4
0
10
20
30
40
50
60
70
F3
F5
F7
F9
F11
D3
D5
D7
D9
D11
8:04
buffer
14:10
water
22:11
water+polymer 1
31:15
nanoparticles
39:58
water+polymer 2
49:06
water

2 nm 2-28-2012 QCM-D Results

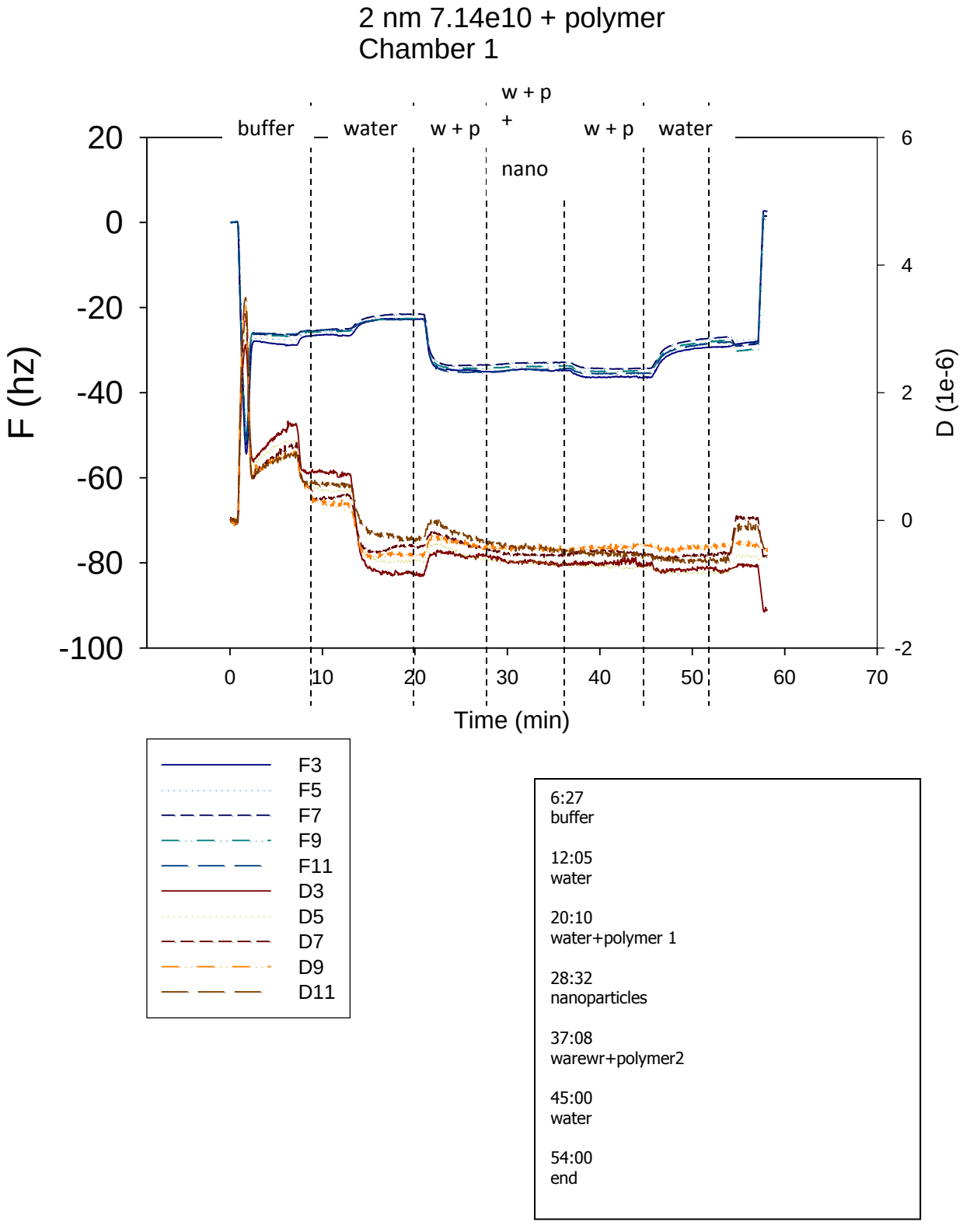
2 nm 7.14e10 + polymer
Chamber 1
buffer
water
w + p
w + p
+
nano
water
F (hz)
D (1e-6)
Time (min)
20
0
-20
-40
-60
-80
-100
6
4
2
0
-2
0
10
20
30
40
50
60
70
F3
F5
F7
F9
F11
D3
D5
D7
D9
D11
6:27
buffer
12:05
water
20:10
water+polymer 1
28:32
nanoparticles
37:08
warewr+polymer2
45:00
water
54:00
end

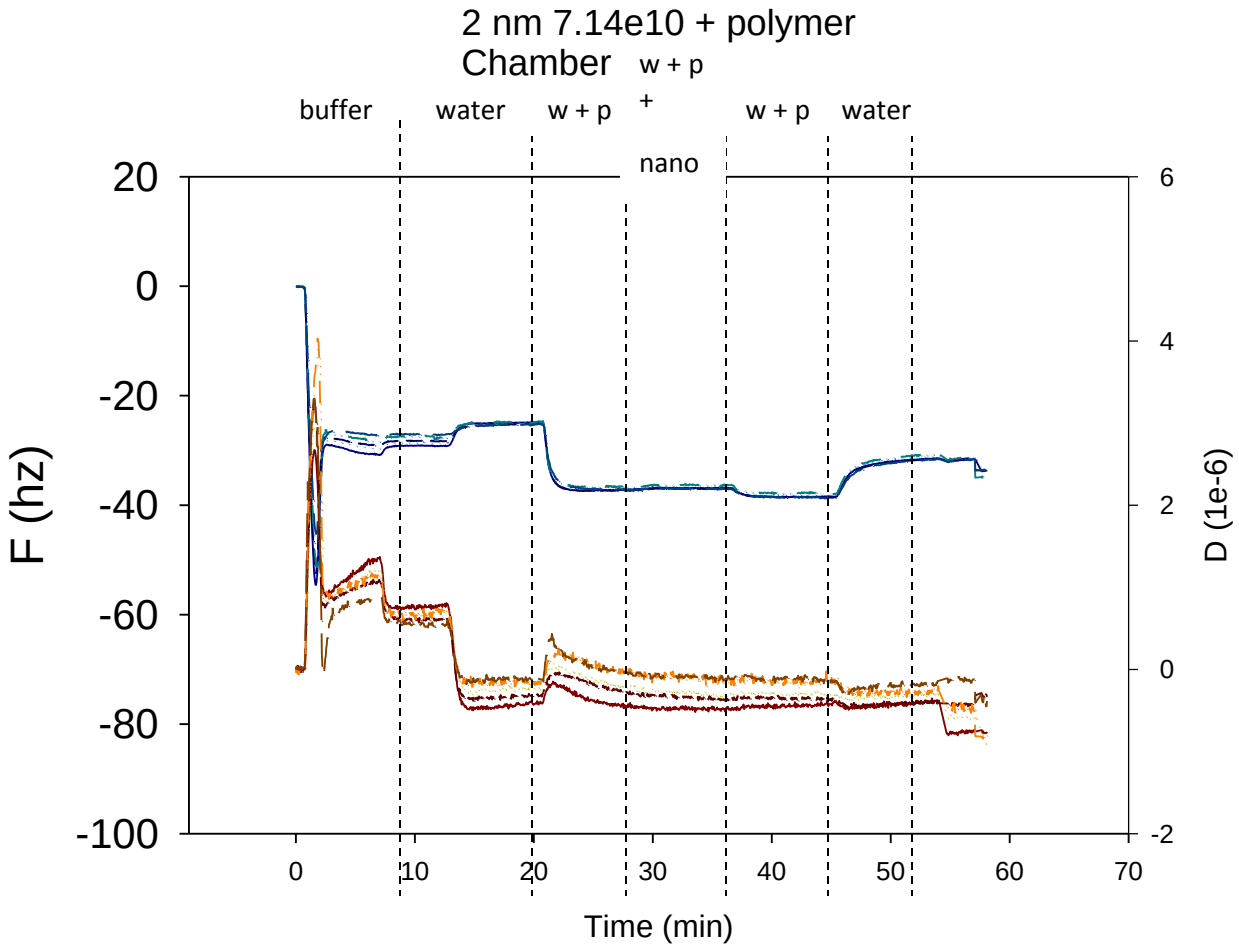

F3
F5
F7
F9
F11
D3
D5
D7
D9
D11

6:27
buffer

12:05
water

20:10
water+polymer 1

28:32
nanoparticles

37:08
warewr+polymer2

45:00
water

54:00
end

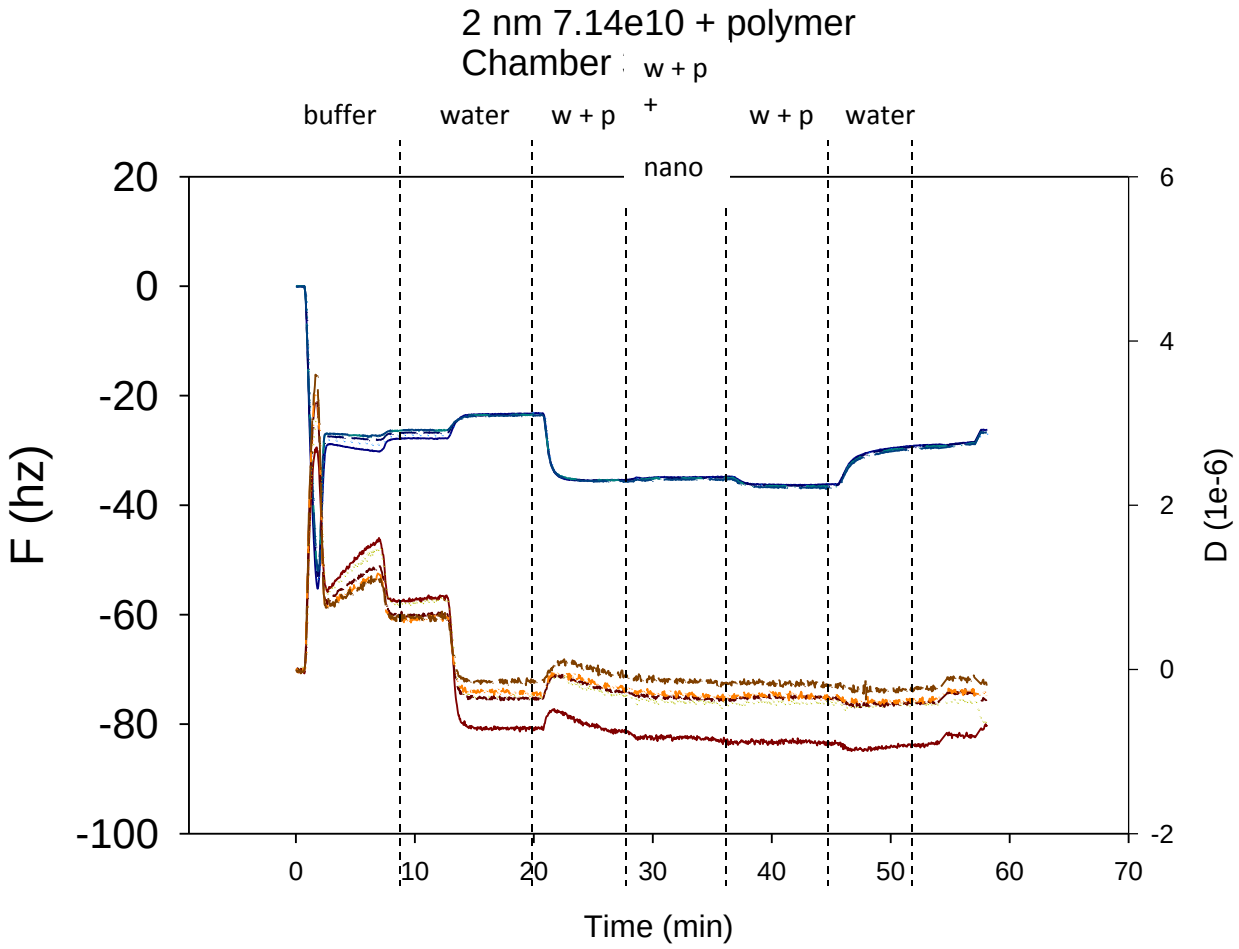

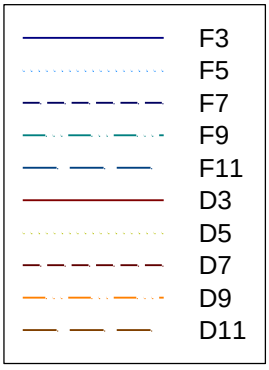

6:27
buffer

12:05
water

20:10
water+polymer 1

28:32
nanoparticles

37:08
warewr+polymer2

45:00
water

54:00
end

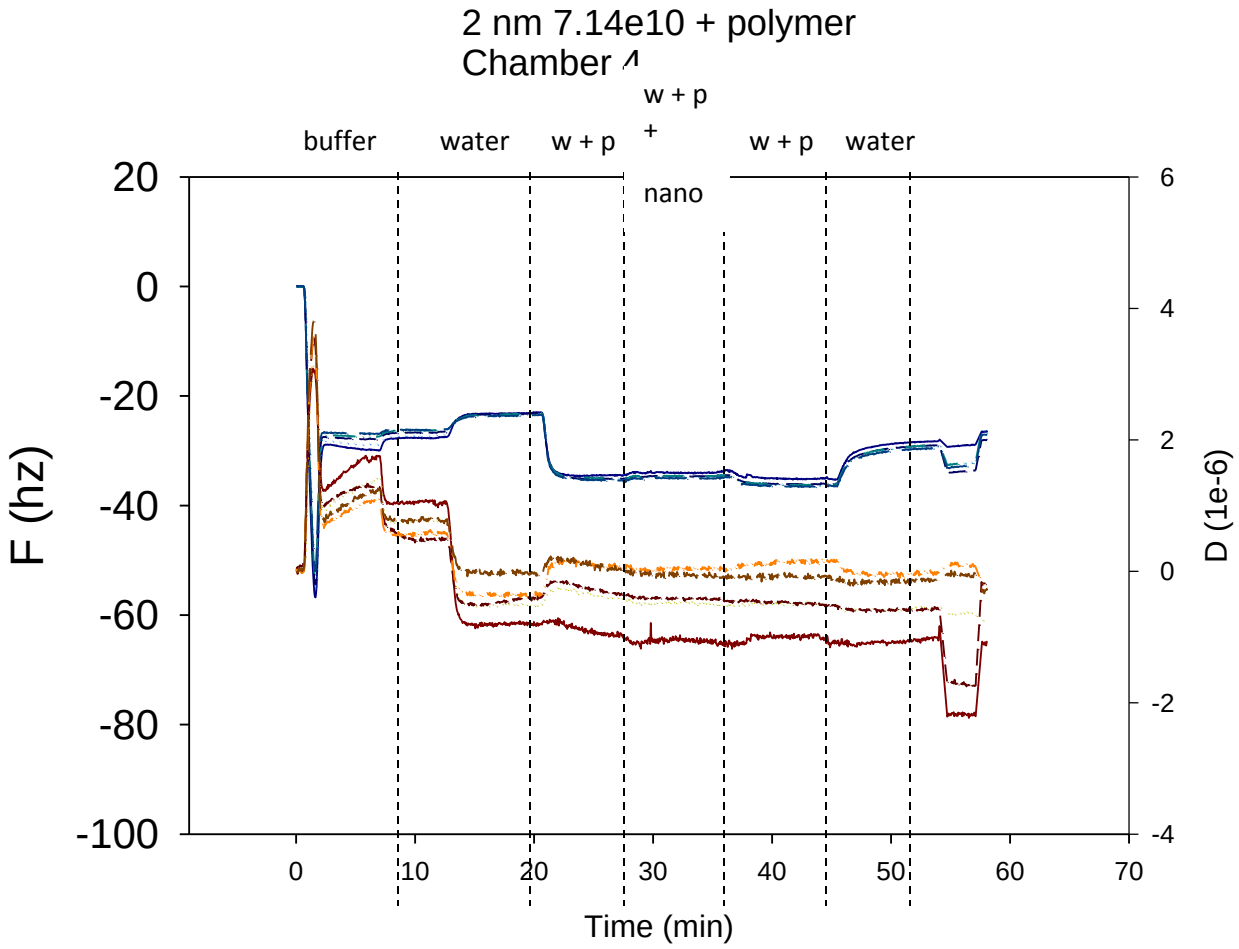

F3
F5
F7
F9
F11
D3
D5
D7
D9
D11

6:27
buffer

12:05
water

20:10
water+polymer 1

28:32
nanoparticles

37:08
warewr+polymer2

45:00
water

54:00
end

5 Nm 2-2-2012 QCM-D Results

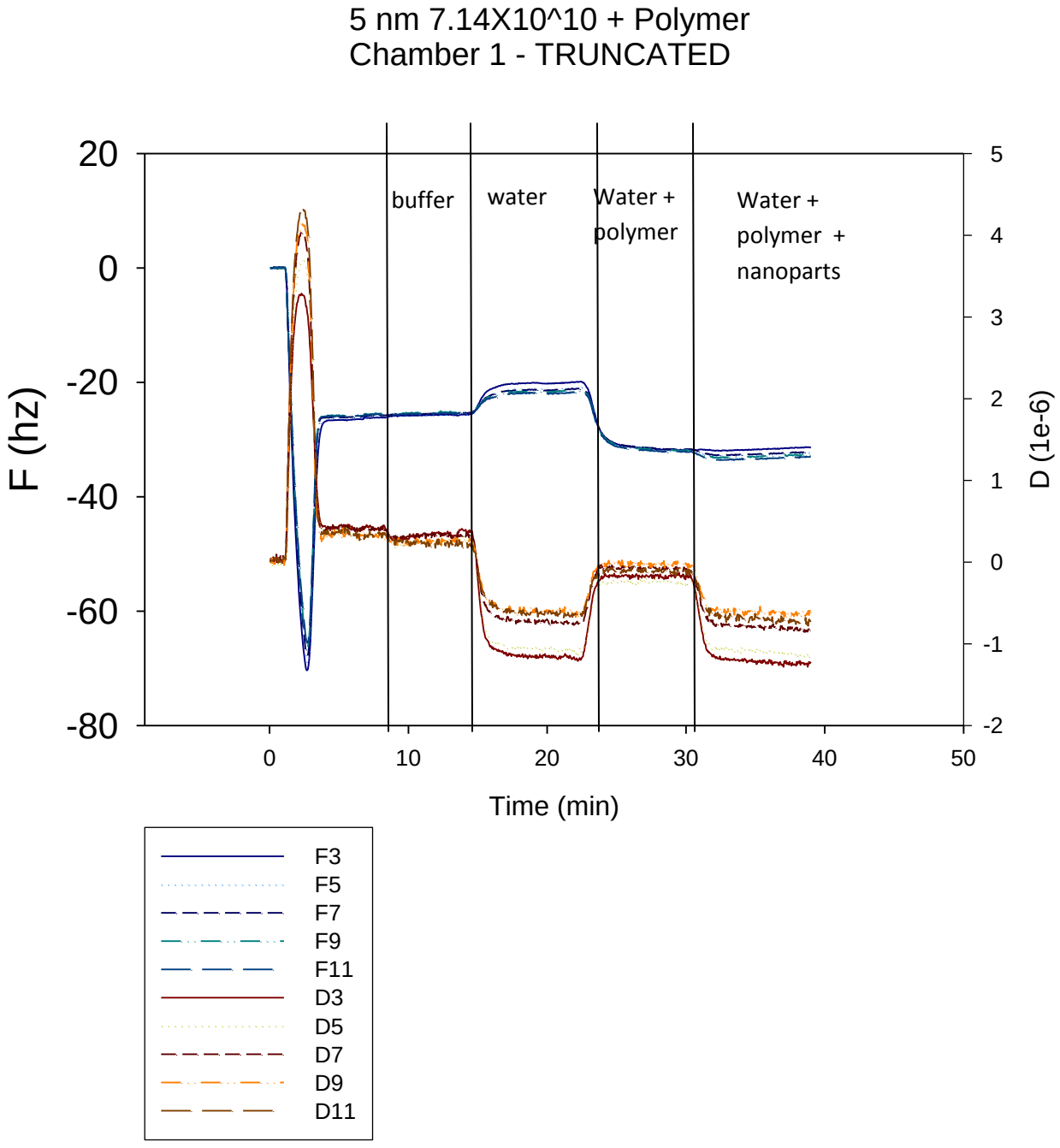

7:09
buffer

13:00
water

21:00
Polymer in Water

29:37 nps in polymer water

5 nm 7.14X10^10 + Polymer
Chamber 1

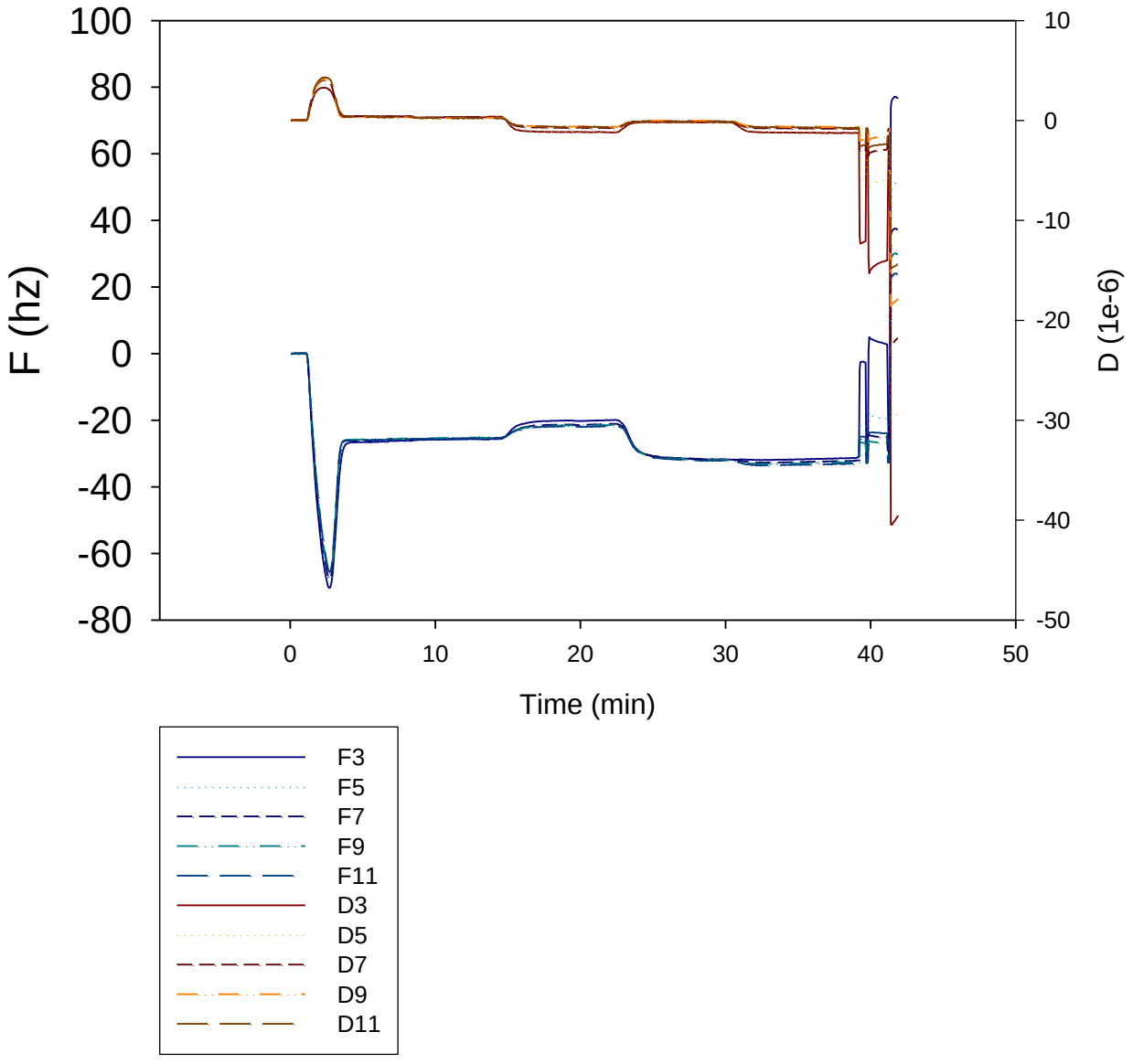

5 nm 7.14X10^10 + Polymer
Chamber 2

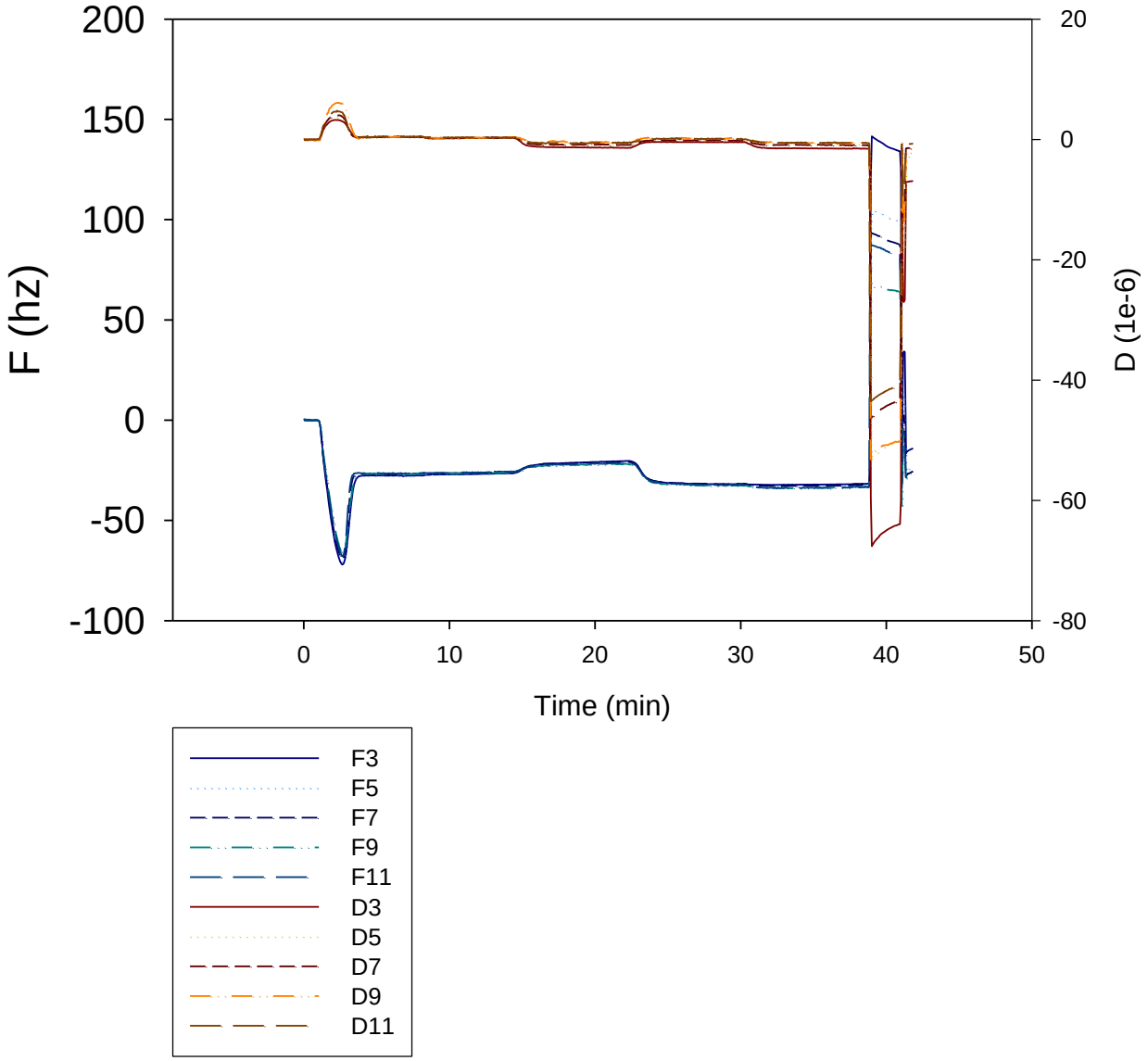

5 nm 7.14X10^10 + Polymer
Chamber 3

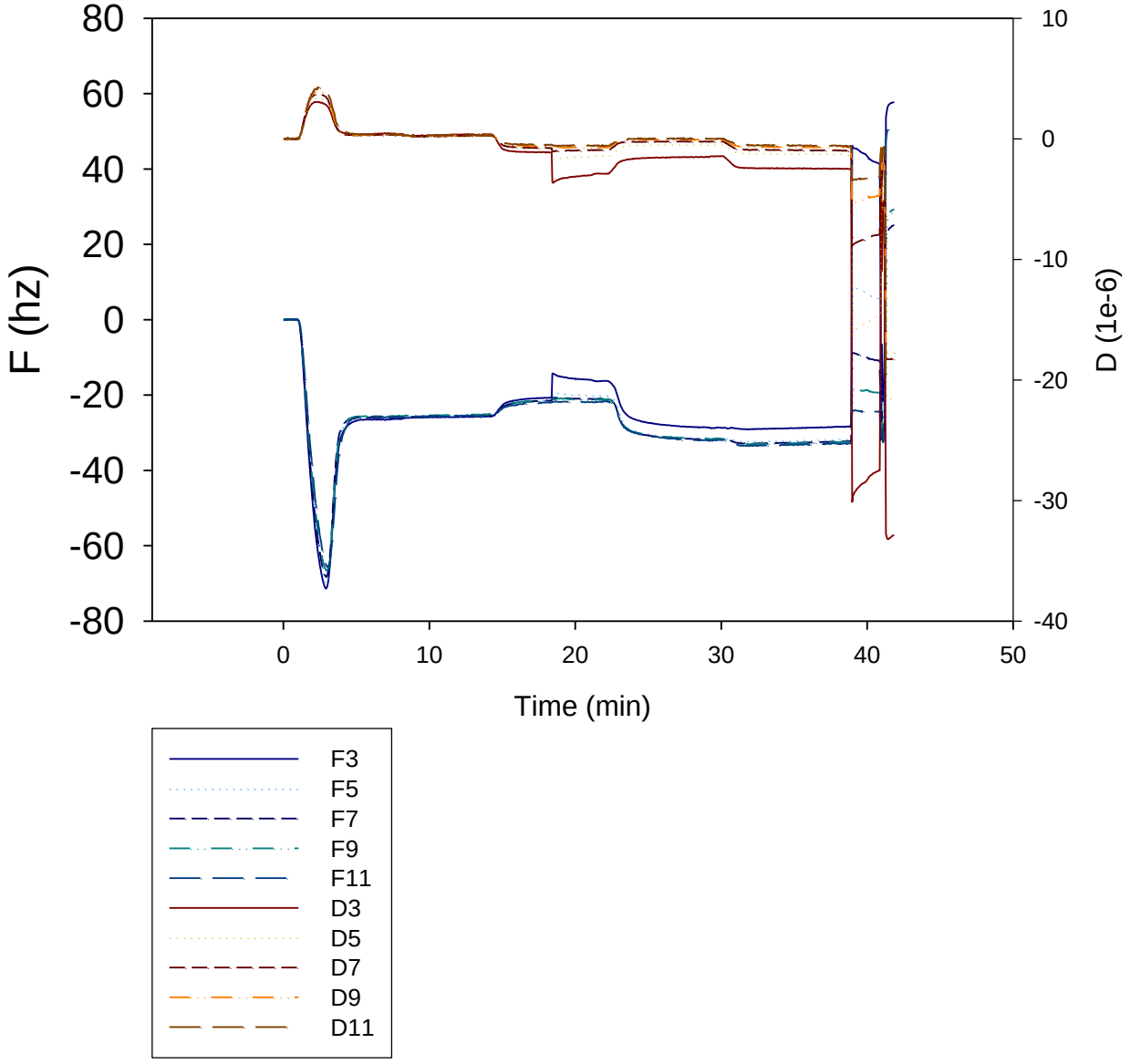

5 nm 7.14X10^10 + Polymer
Chamber 4

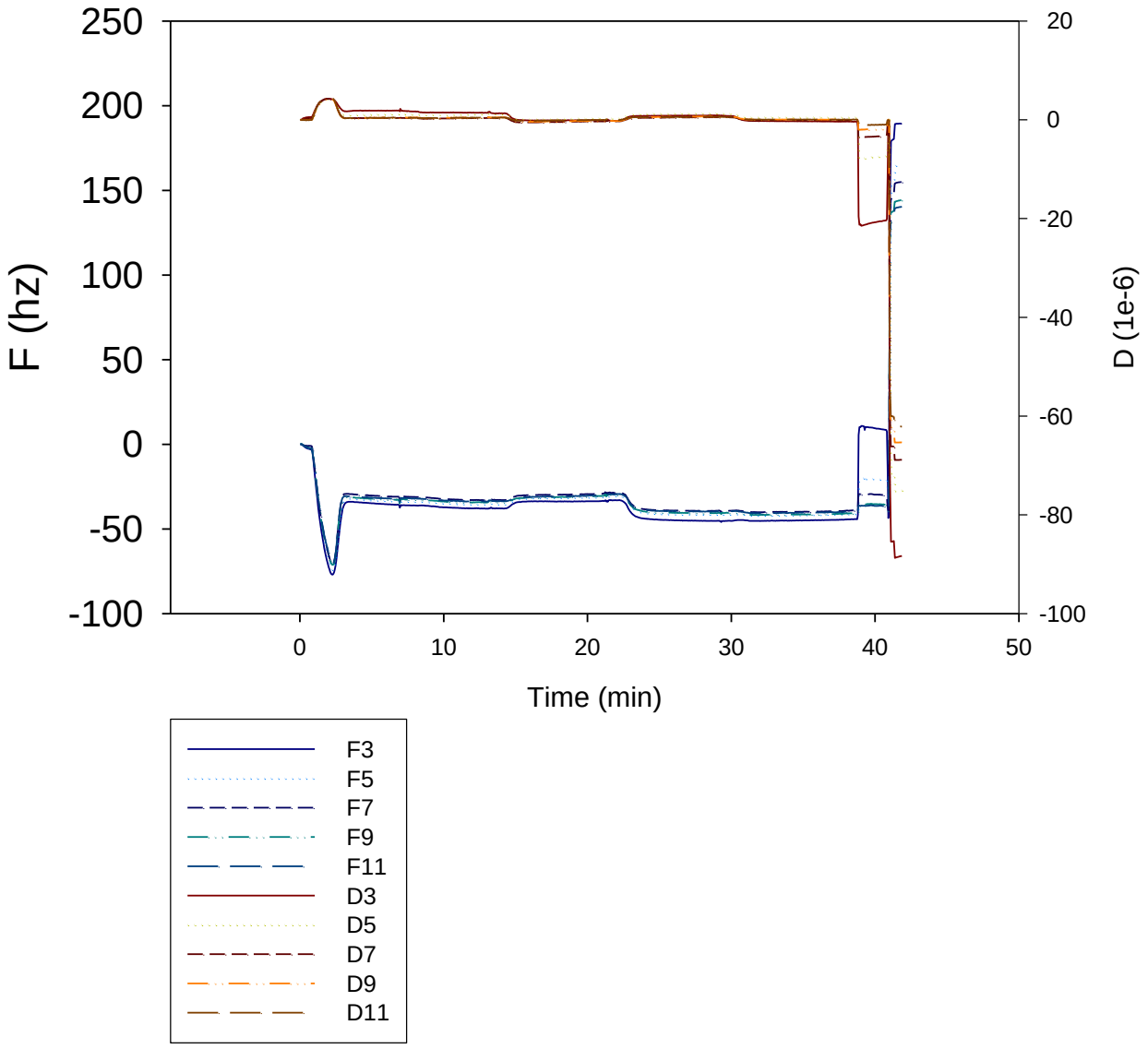

5 Nm 2-7-2012 QCM-D Results

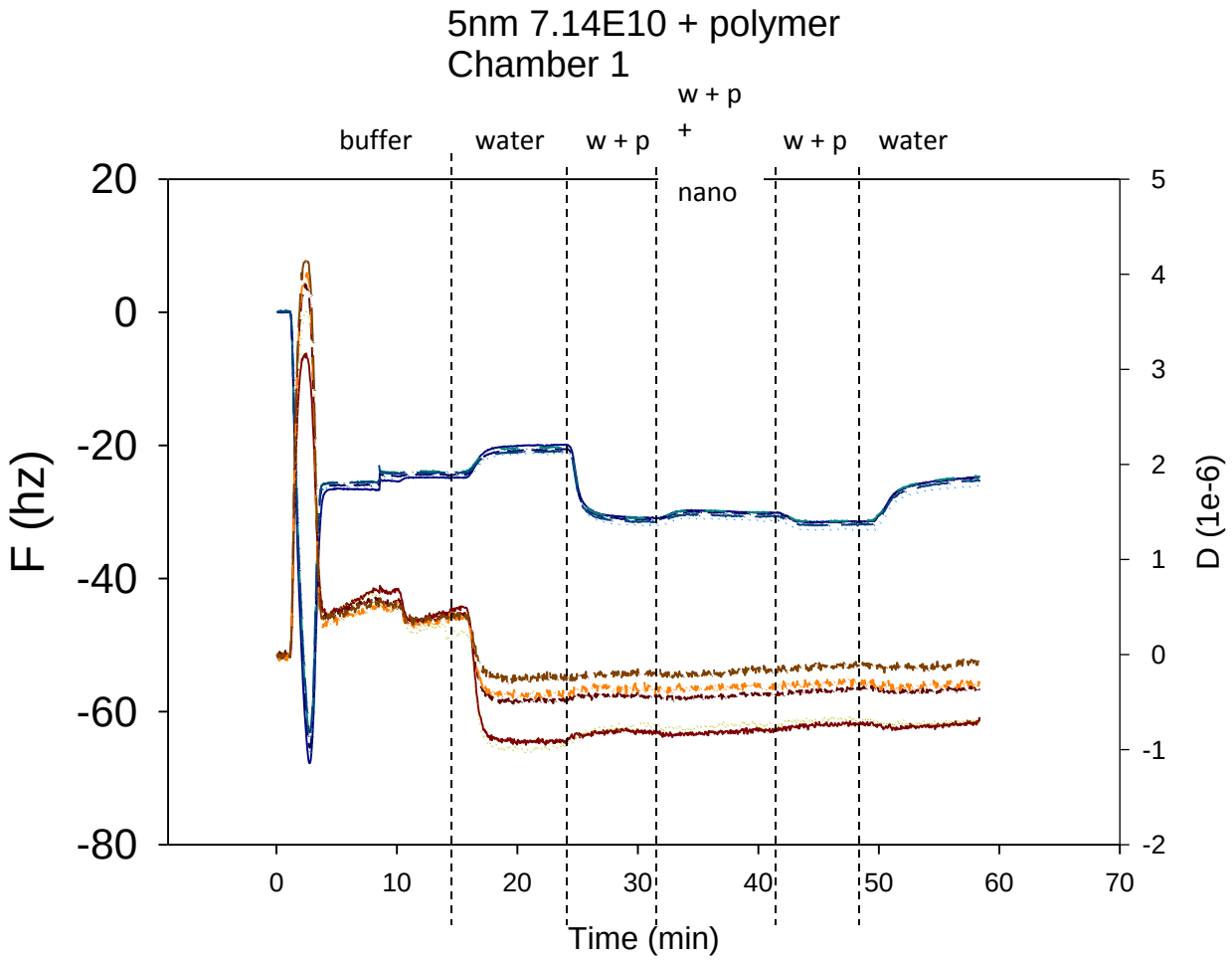

7:59
buffer rinse

14:00
water rinse

22:00
water+polymer #1

30:00
water+polymer+Nps

40:00
water+polymer #2

48:02
water rinse

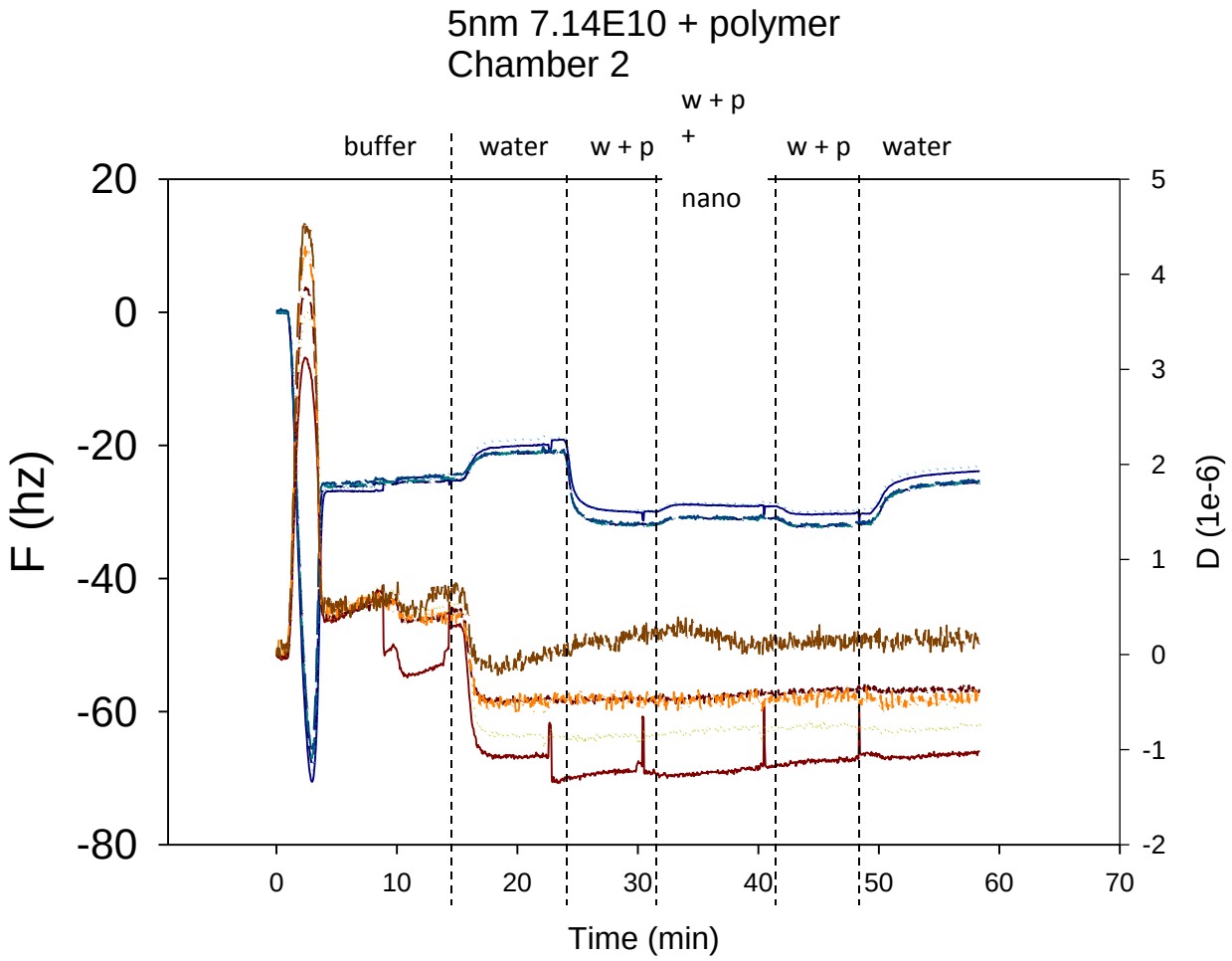

F3
F5
F7
F9
F11
D3
D5
D7
D9
D11

7:59
buffer rinse

14:00
water rinse

22:00
water+polymer #1

30:00
water+polymer+Nps

40:00
water+polymer #2

48:02
water rinse

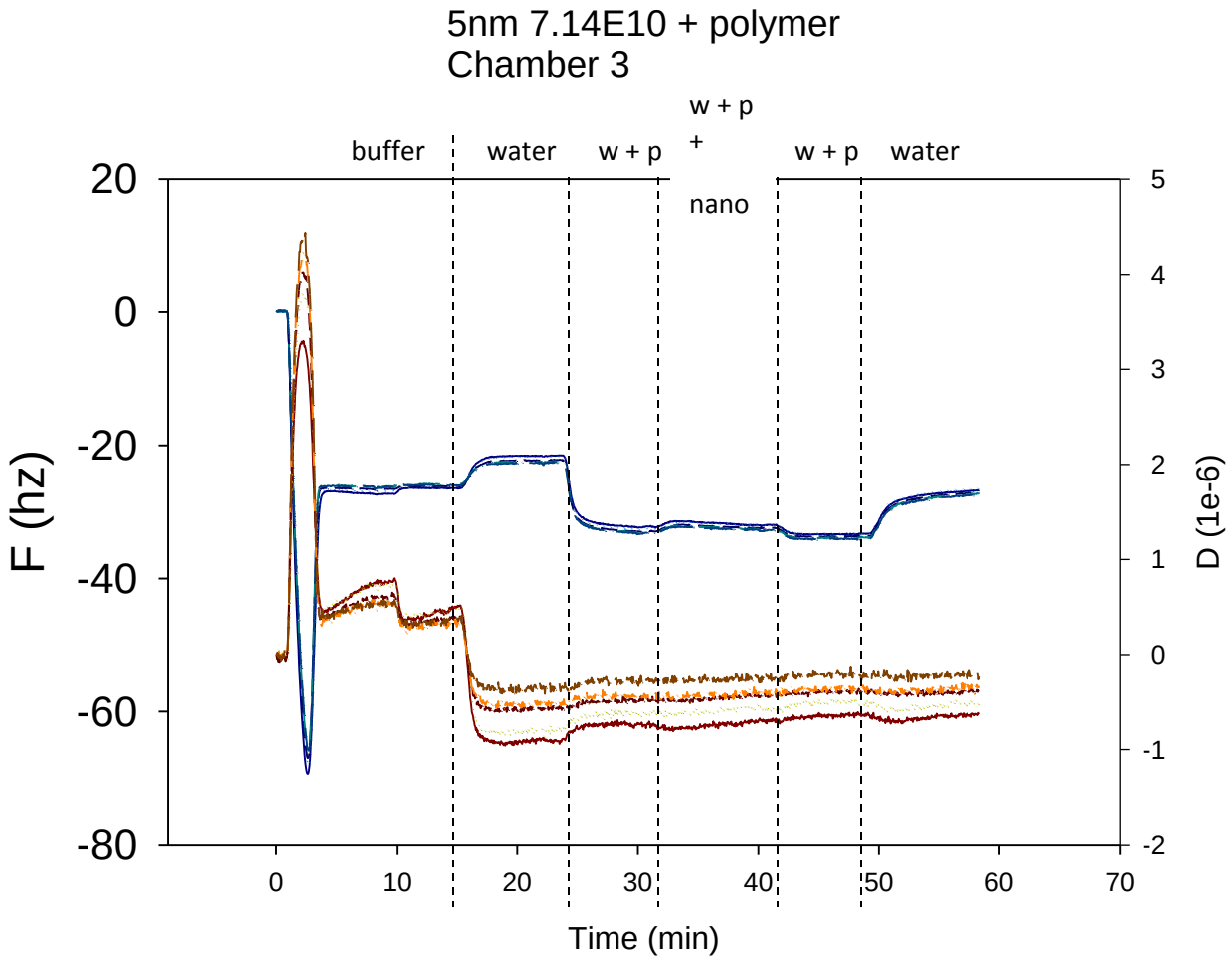

7:59
buffer rinse

14:00
water rinse

22:00
water+polymer #1

30:00
water+polymer+Nps

40:00
water+polymer #2

48:02
water rinse

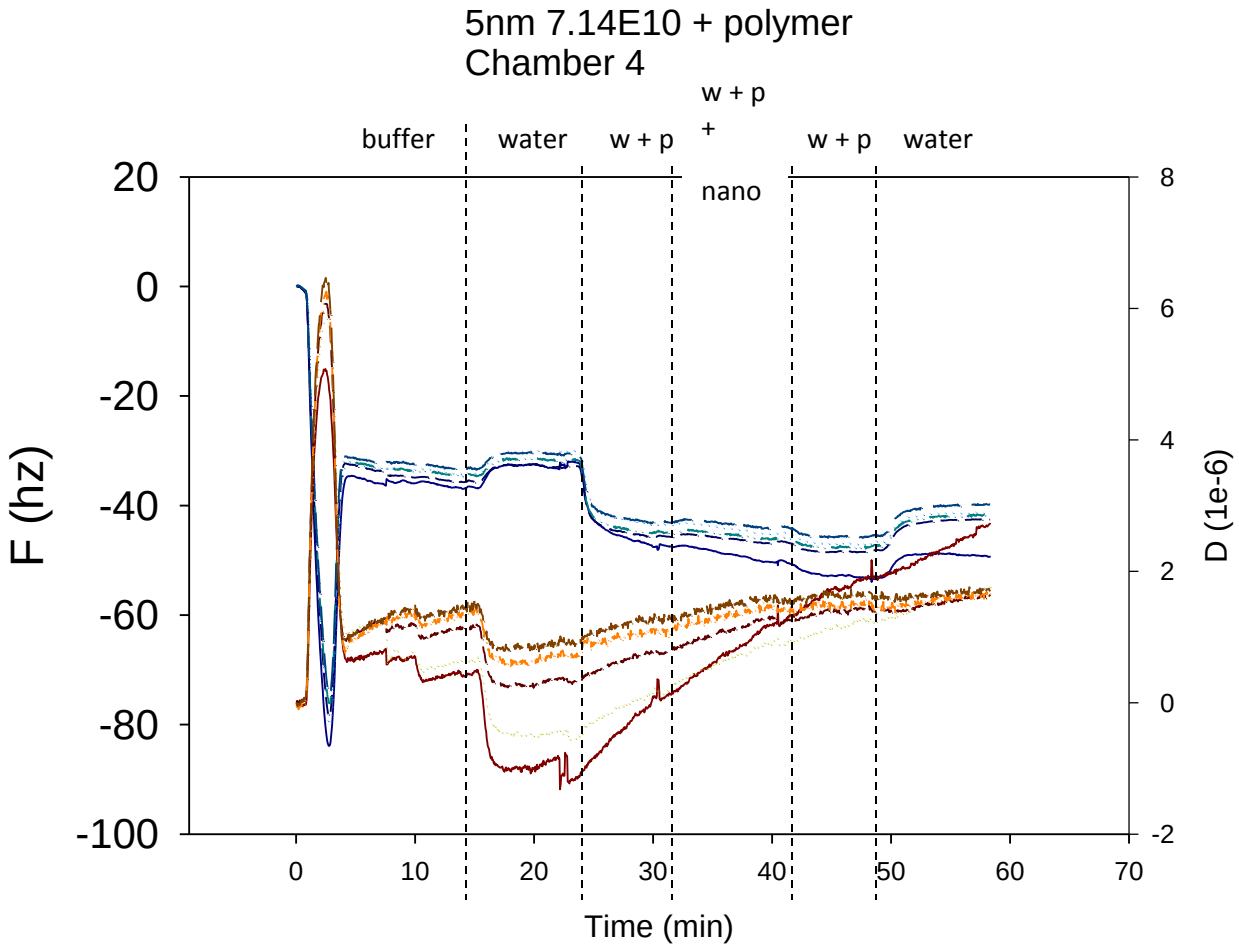

F3
F5
F7
F9
F11
D3
D5
D7
D9
D11

7:59
buffer rinse

14:00
water rinse

22:00
water+polymer #1

30:00
water+polymer+Nps

40:00
water+polymer #2

48:02
water rinse

5 Nm 2-9-2012 QCM-D Results

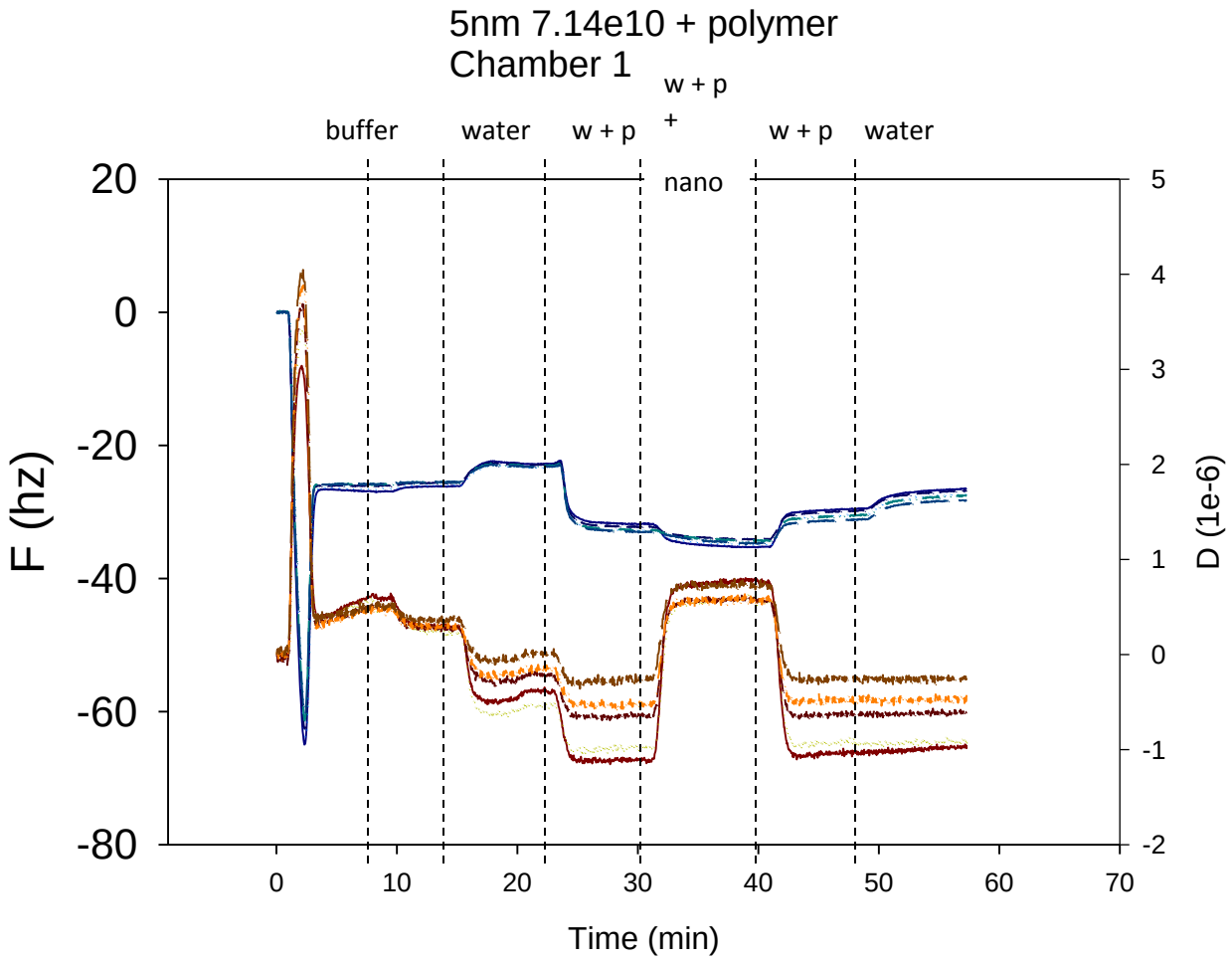

F3
F5
F7
F9
F11
D3
D5
D7
D9
D11

8:30
buffer

14:11
water

22:07
water + polymer

30:20
water + polymer + nanoparticles

40:18
water + polymer

48:08
water

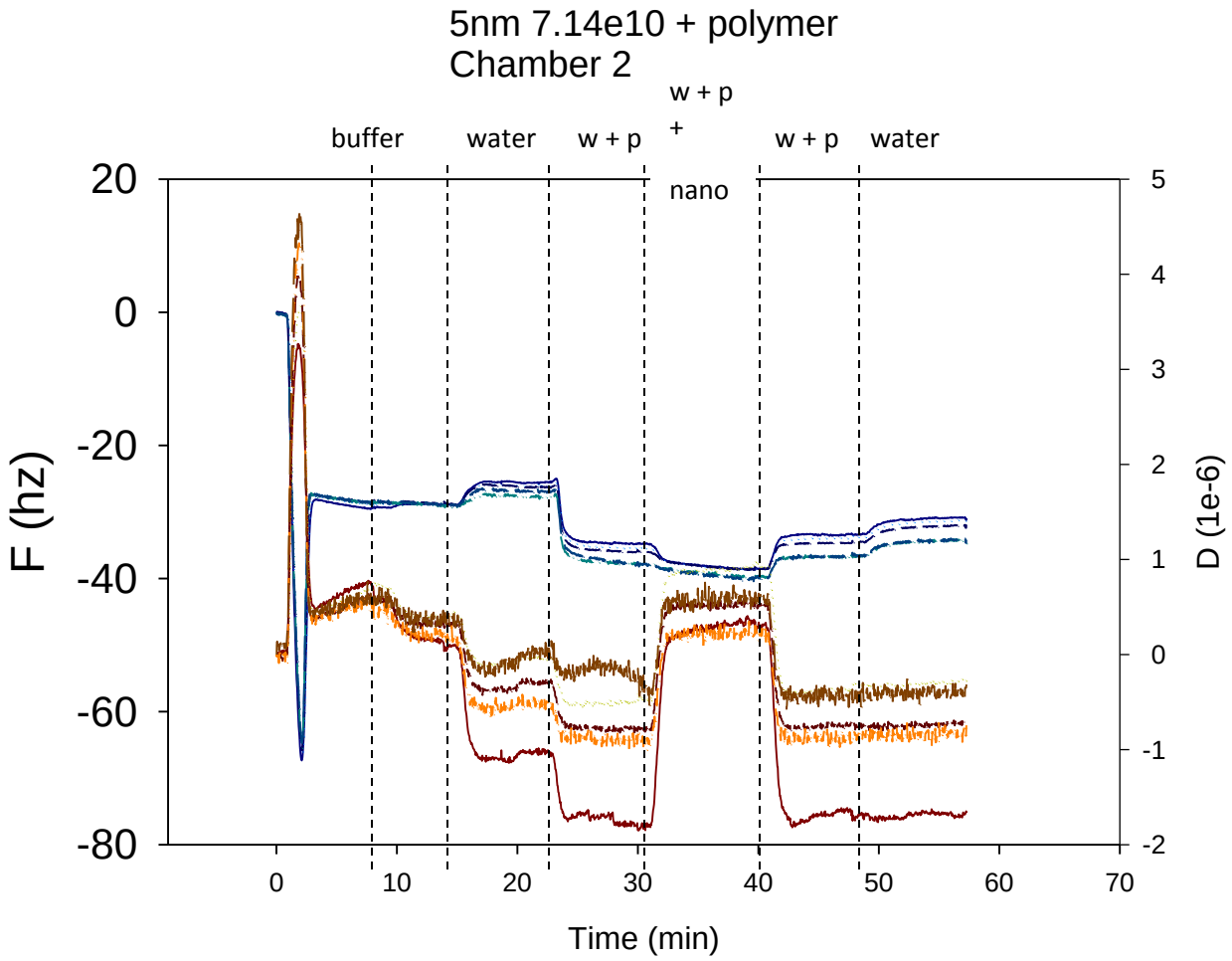

8:30
buffer

14:11
water

22:07
water + polymer

30:20
water + polymer + nanoparticles

40:18
water + polymer

48:08
water

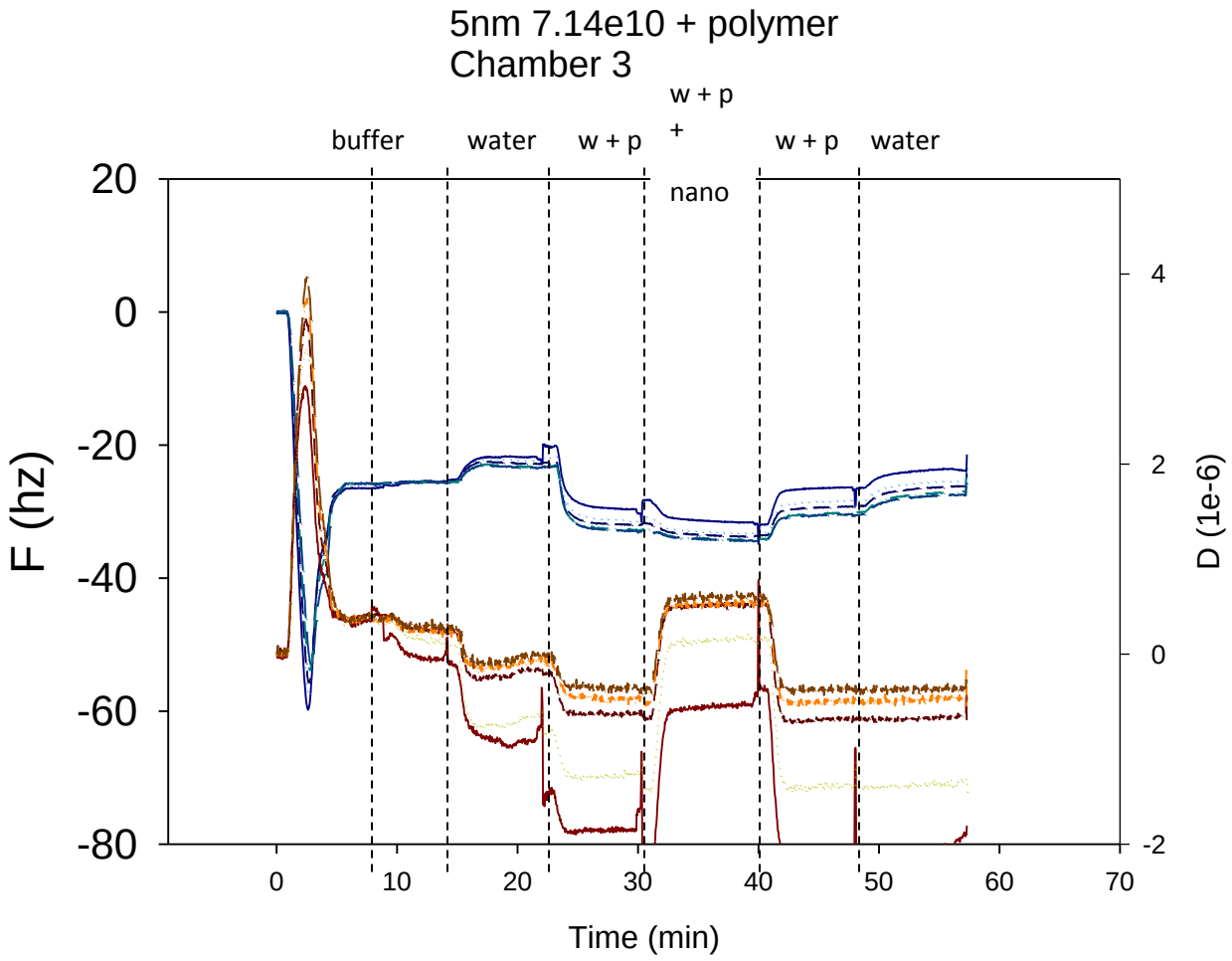

F3
F5
F7
F9
F11
D3
D5
D7
D9
D11

8:30
buffer

14:11
water

22:07
water + polymer

30:20
water + polymer + nanoparticles

40:18
water + polymer

48:08
water

5 Nm 2-10-2012 QCM-D Results

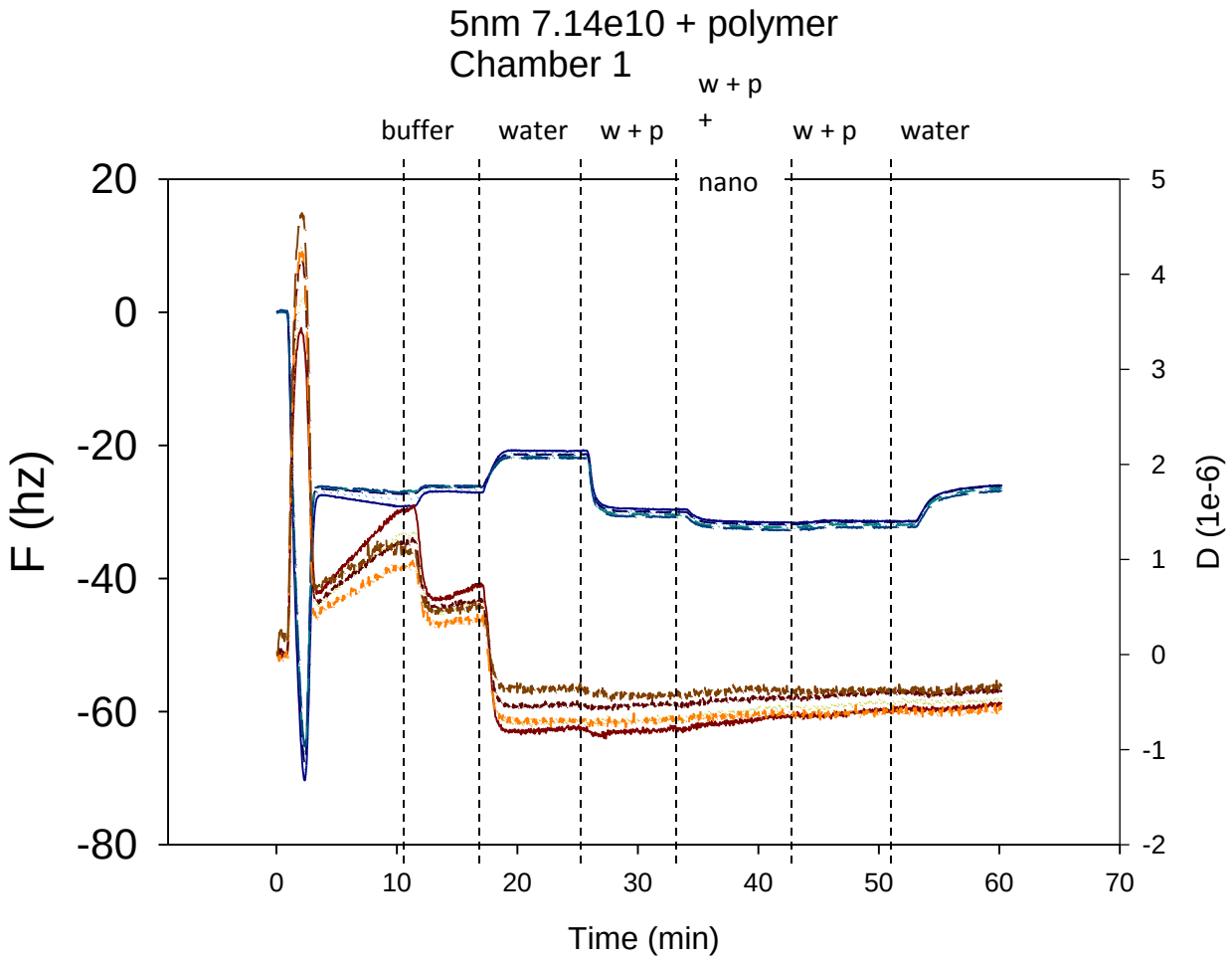

F3
F5
F7
F9
F11
D3
D5
D7
D9
D11

10:28
buffer

16:18
water

24:21
water + polymer

32:41
water+polymer+NPs

43:36
water + polymer

51:42
water

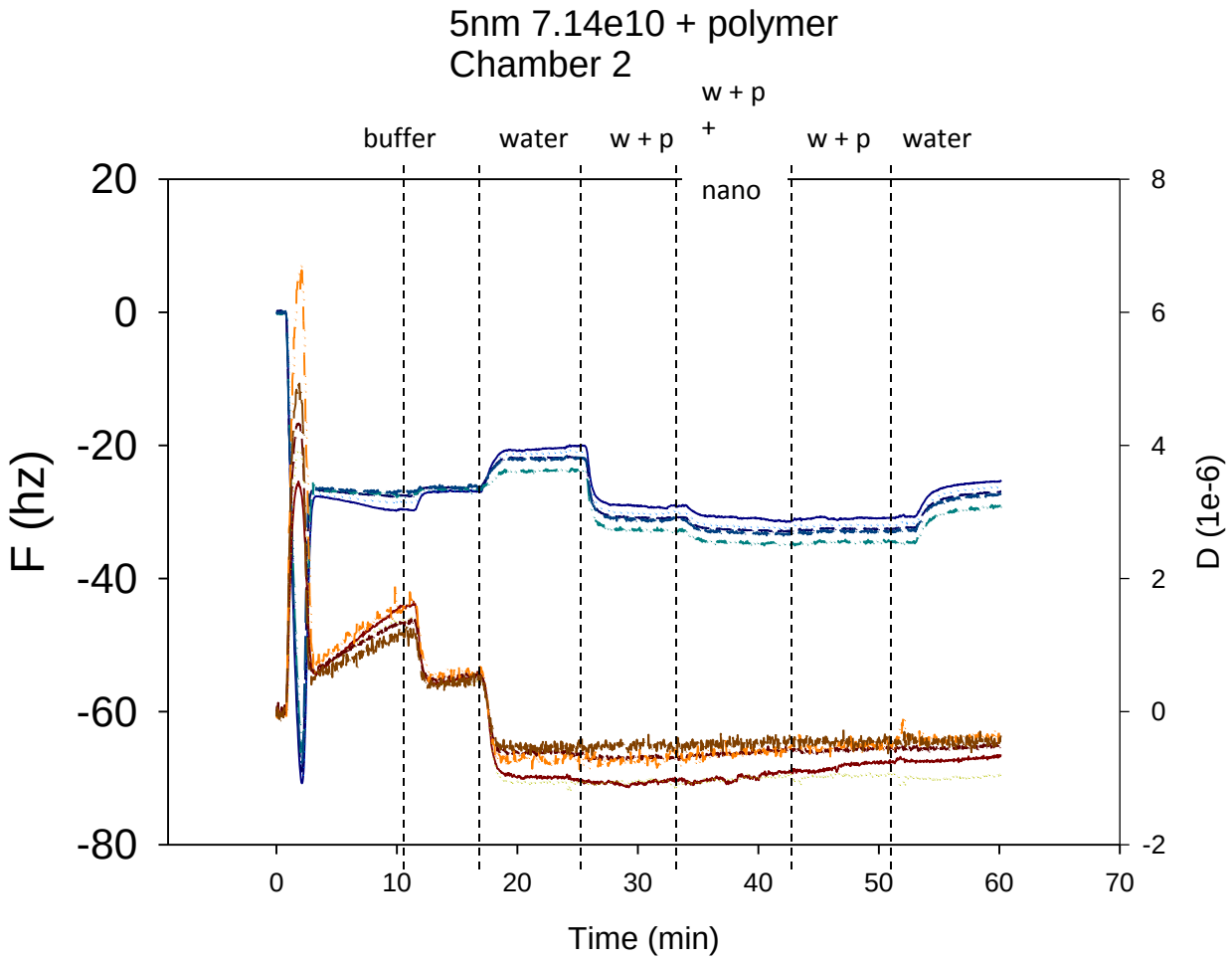

F3
F5
F7
F9
F11
D3
D5
D7
D9
D11

10:28
buffer

16:18
water

24:21
water + polymer

32:41
water+polymer+NPs

43:36
water + polymer

51:42
water

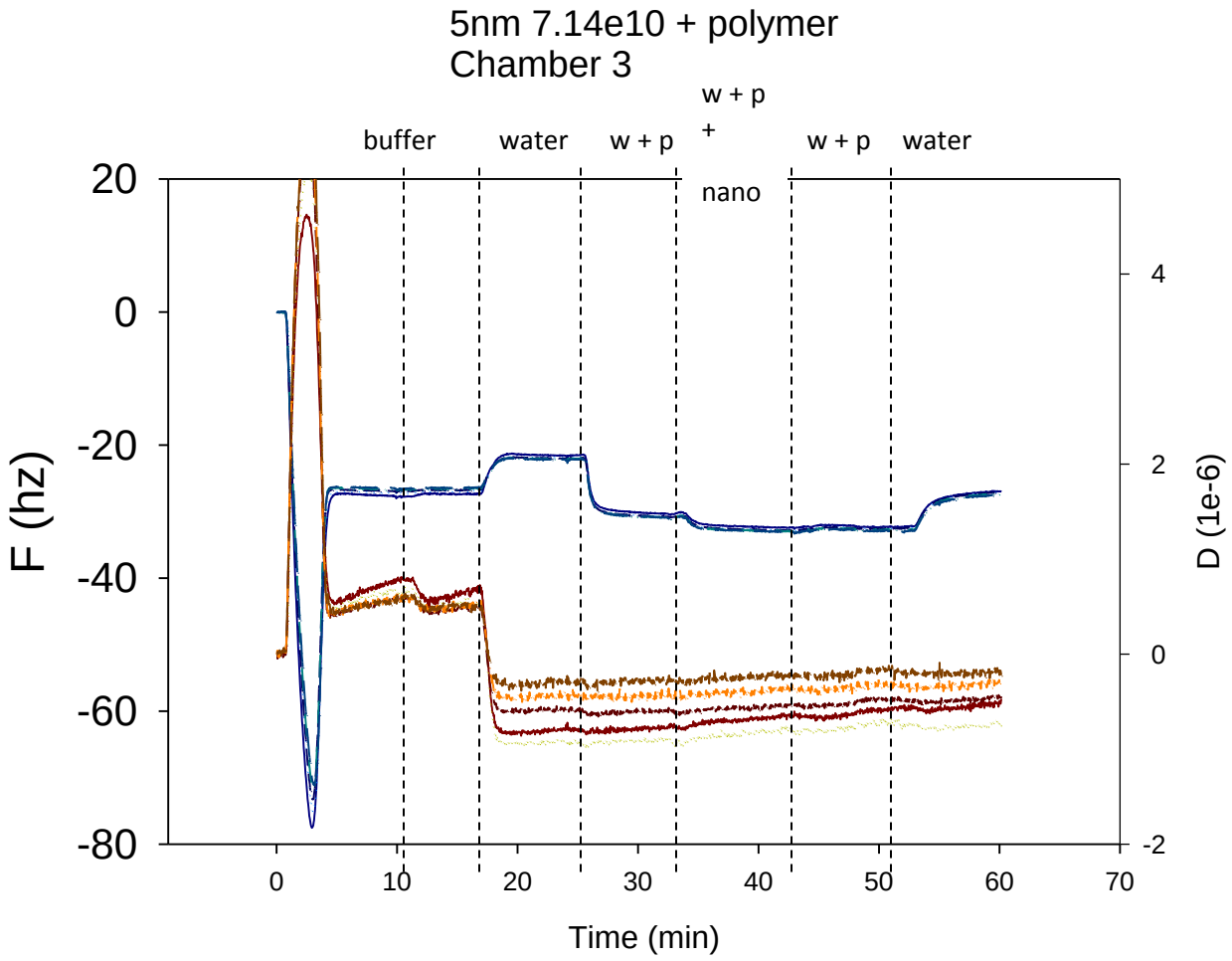

F3
F5
F7
F9
F11
D3
D5
D7
D9
D11

10:28
buffer

16:18
water

24:21
water + polymer

32:41
water+polymer+NPs

43:36
water + polymer

51:42
water

5 Nm 2-14-2012 QCM-D Results

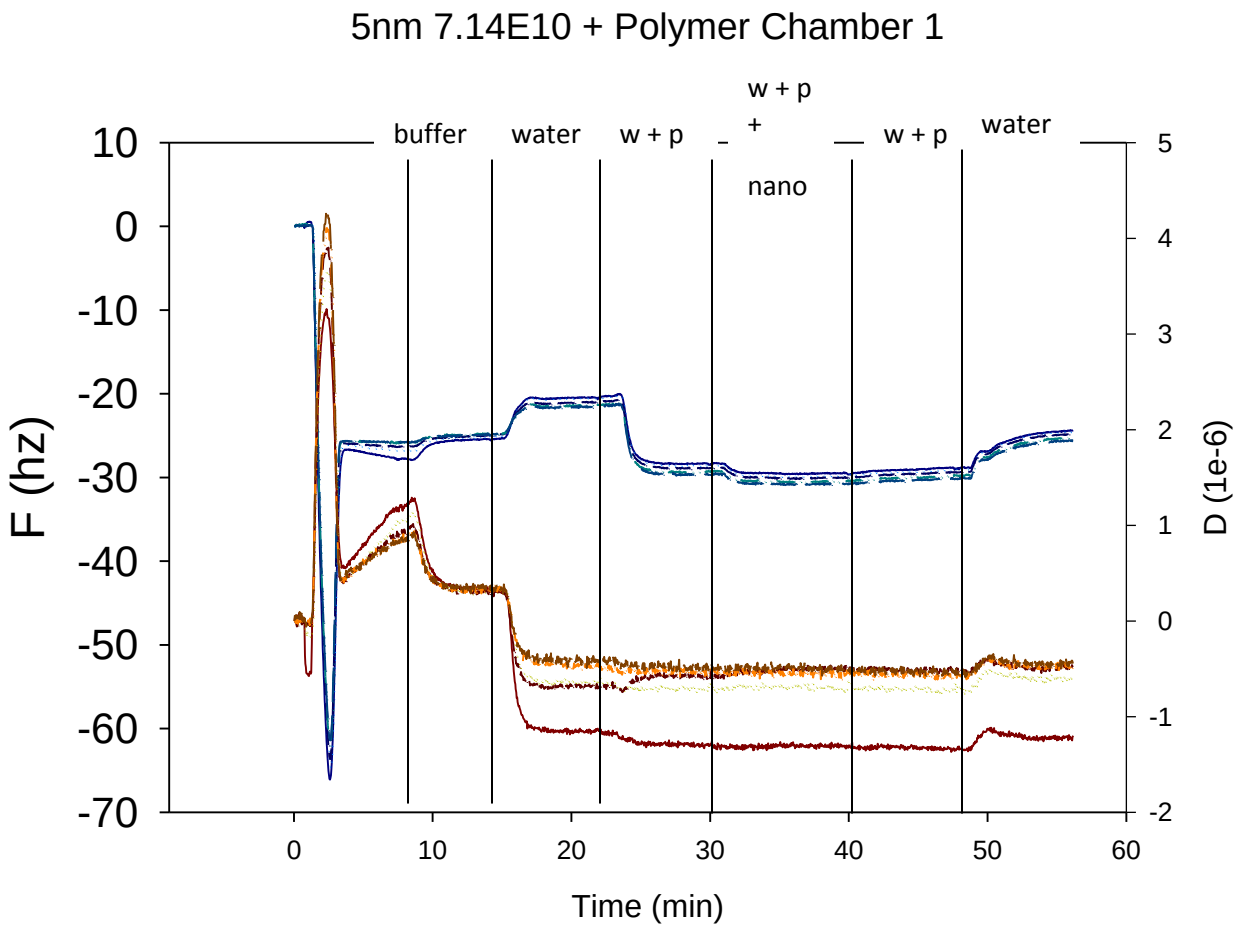

F3
F5
F7
F9
F11
D3
D5
D7
D9
D11

8:00
buffer

14:15
water

22:08
water+polymer

30:07
nanoparticles

40:15
water+polymer 2

47:58
water

56:00
End

10 NM 3-1-2012 QCM-D Results

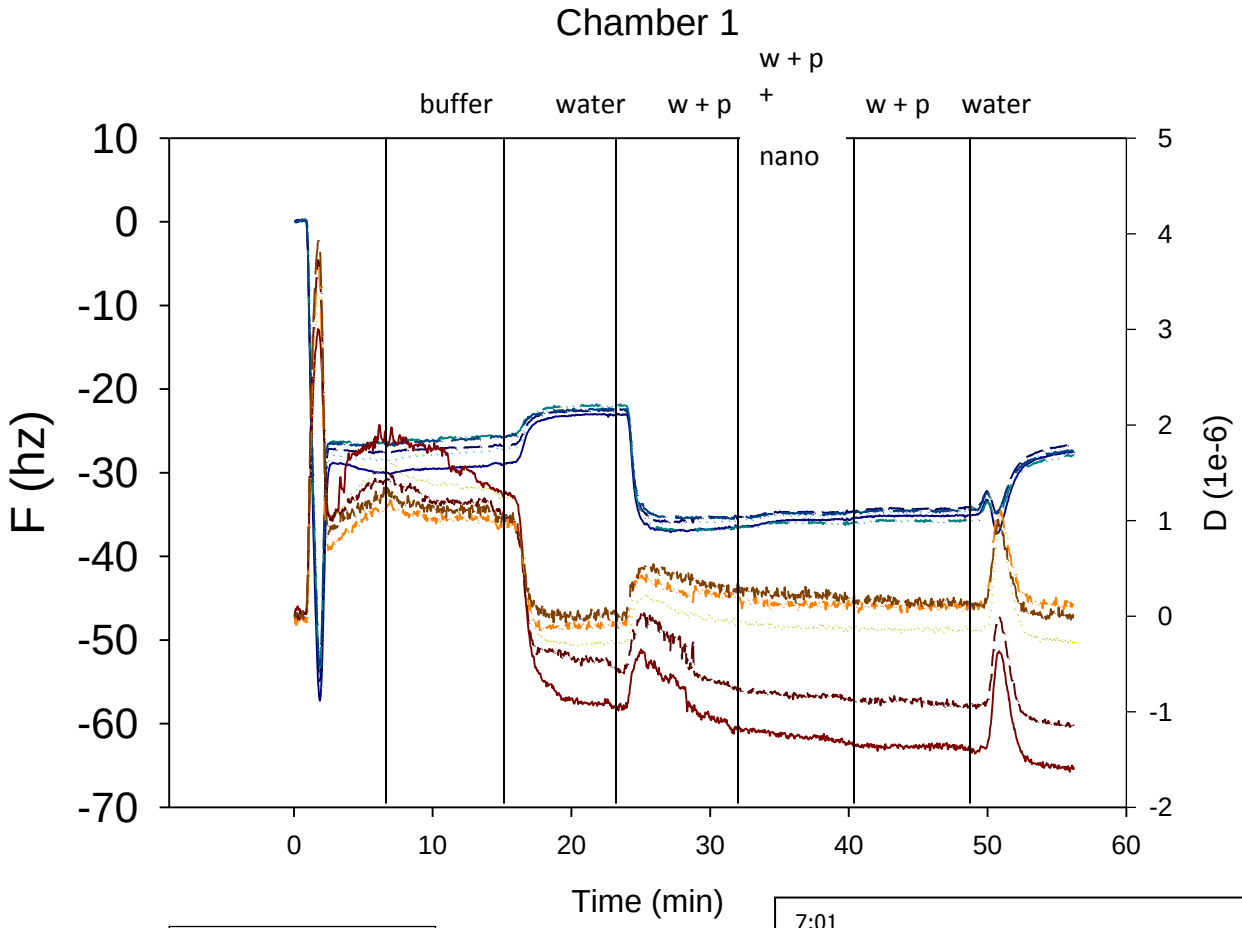

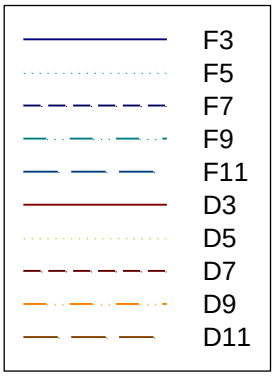

7:01
buffer

15:11
water

23:06
water+polymer 1

32:09
gold nanoparticles

40:43
water+polymer 2

48:34
water

56:04
End

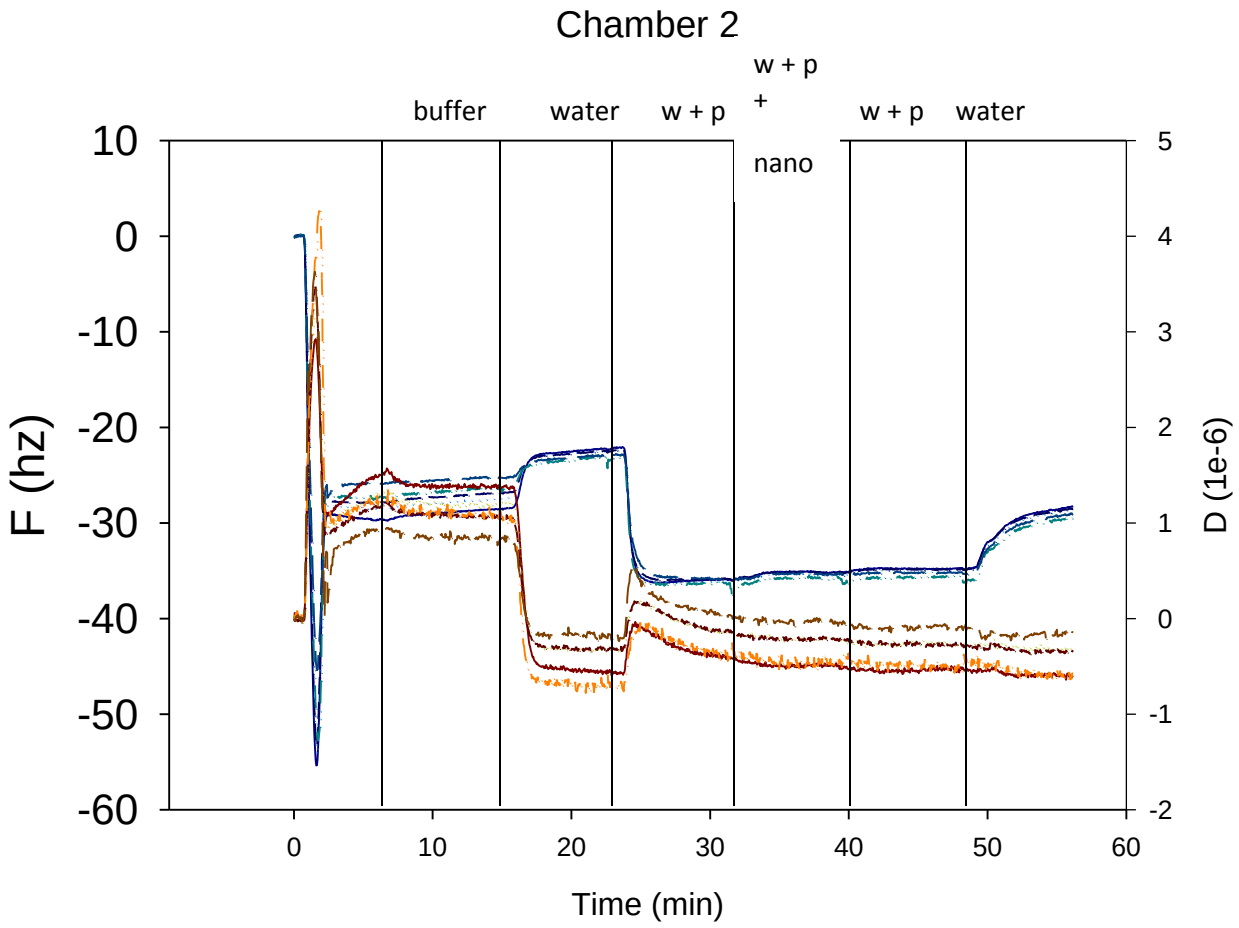

F3
F5
F7
F9
F11
D3
D5
D7
D9
D11

7:01
buffer

15:11
water

23:06
water+polymer 1

32:09
gold nanoparticles

40:43
water+polymer 2

48:34
water

56:04
End

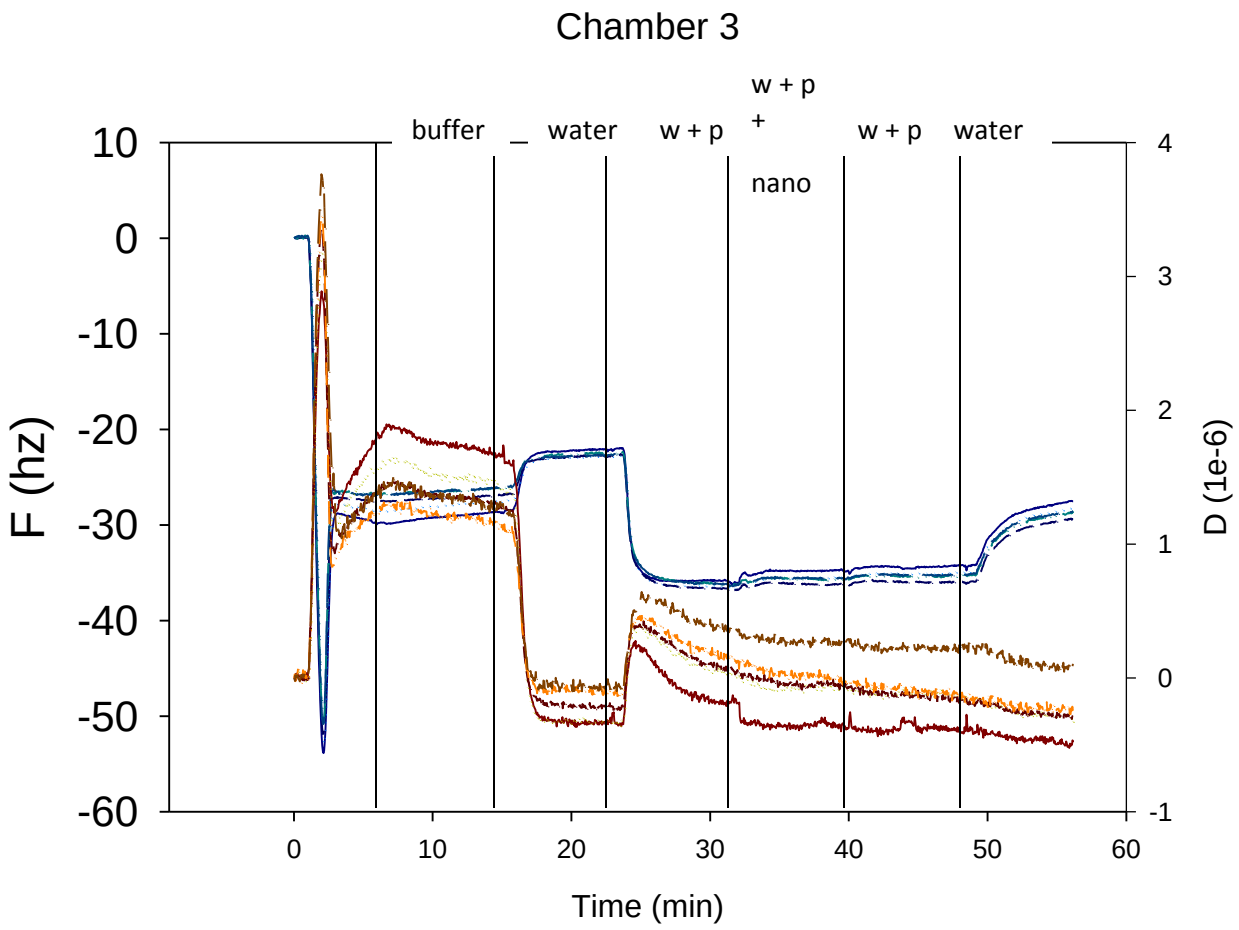

F3
F5
F7
F9
F11
D3
D5
D7
D9
D11

7:01
buffer

15:11
water

23:06
water+polymer 1

32:09
gold nanoparticles

40:43
water+polymer 2

48:34
water

56:04
End

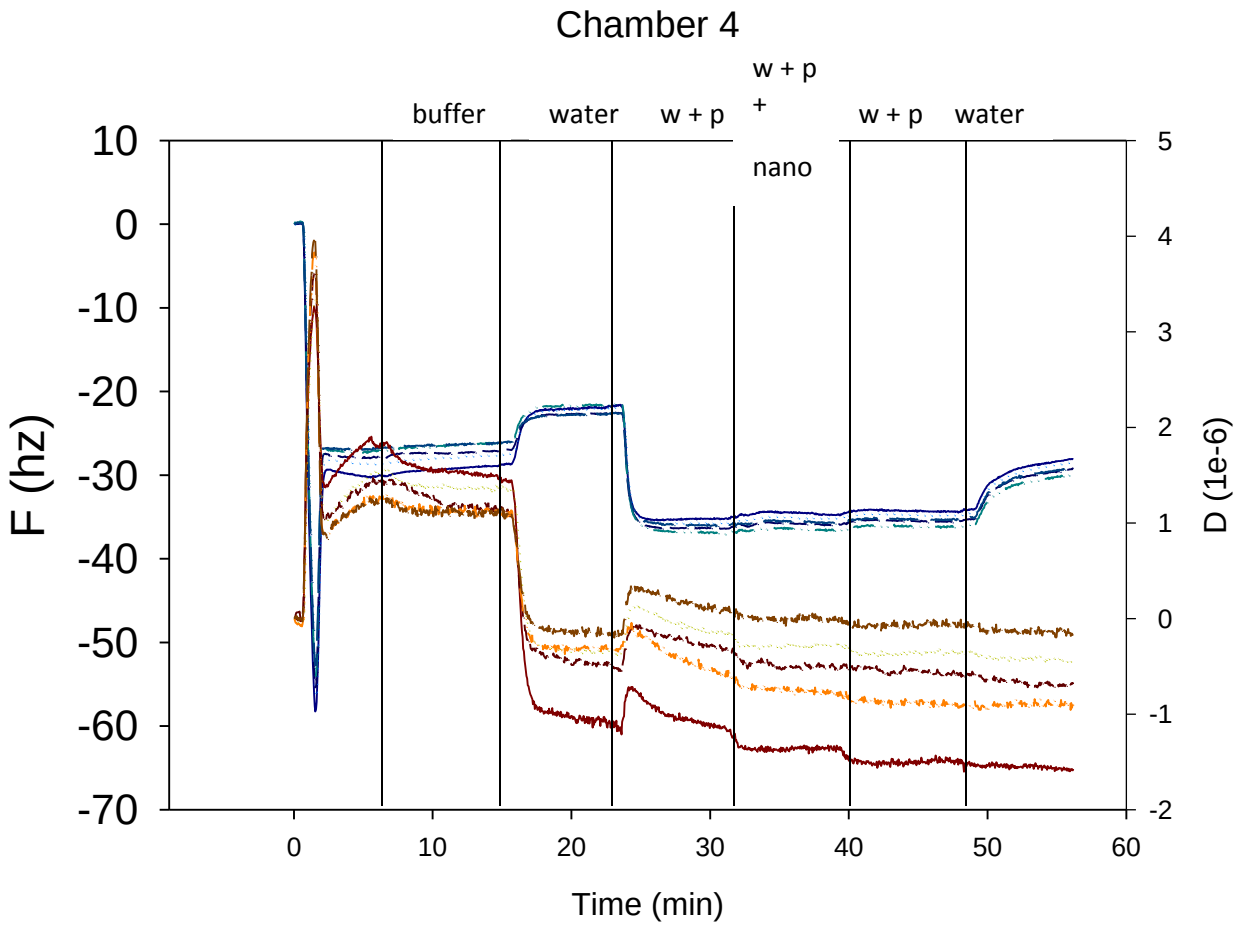

F3
F5
F7
F9
F11
D3
D5
D7
D9
D11

7:01
buffer

15:11
water

23:06
water+polymer 1

32:09
gold nanoparticles

40:43
water+polymer 2

48:34
water

56:04
End

10 NM 3-14-2012 QCM-D Results

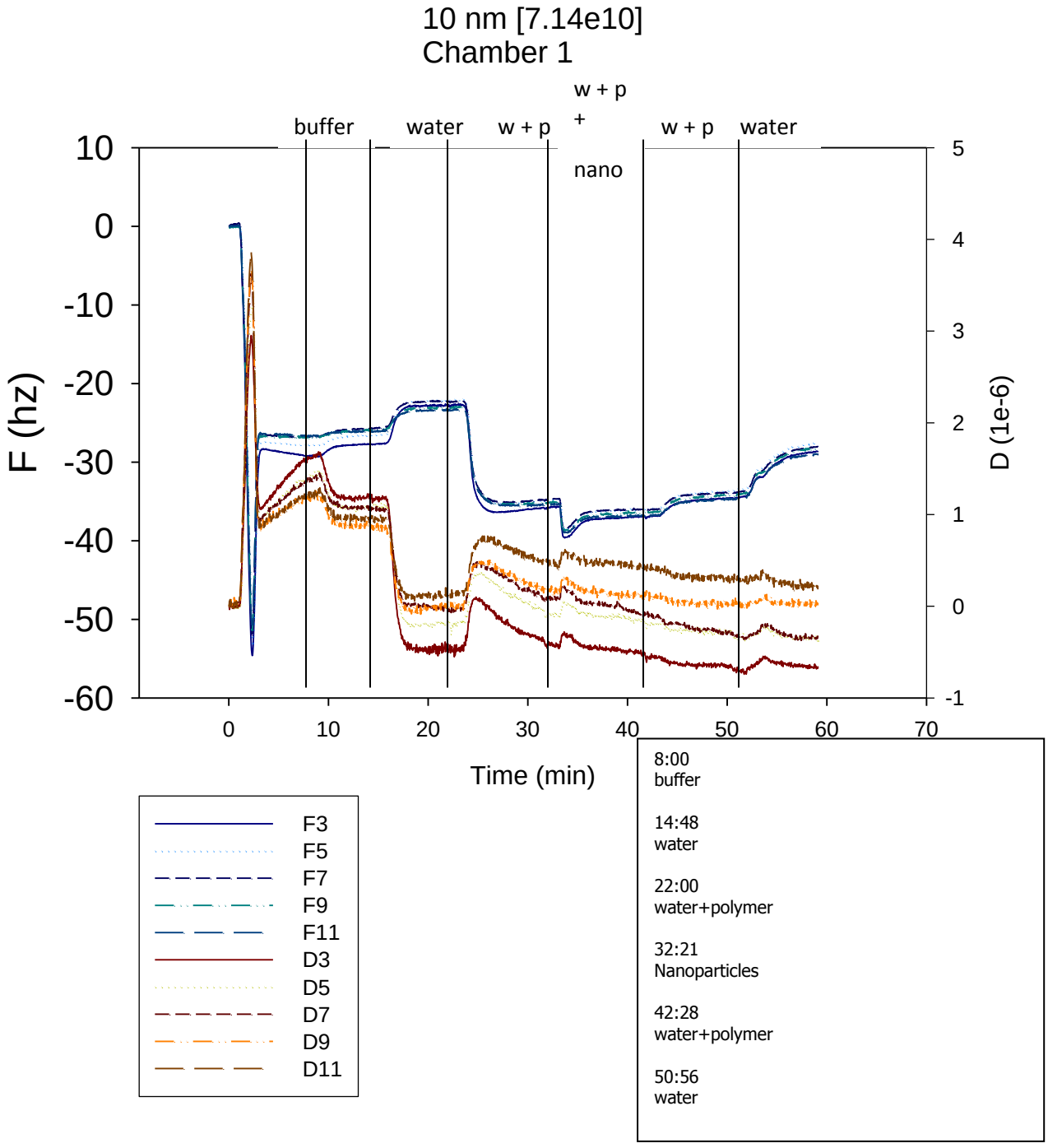

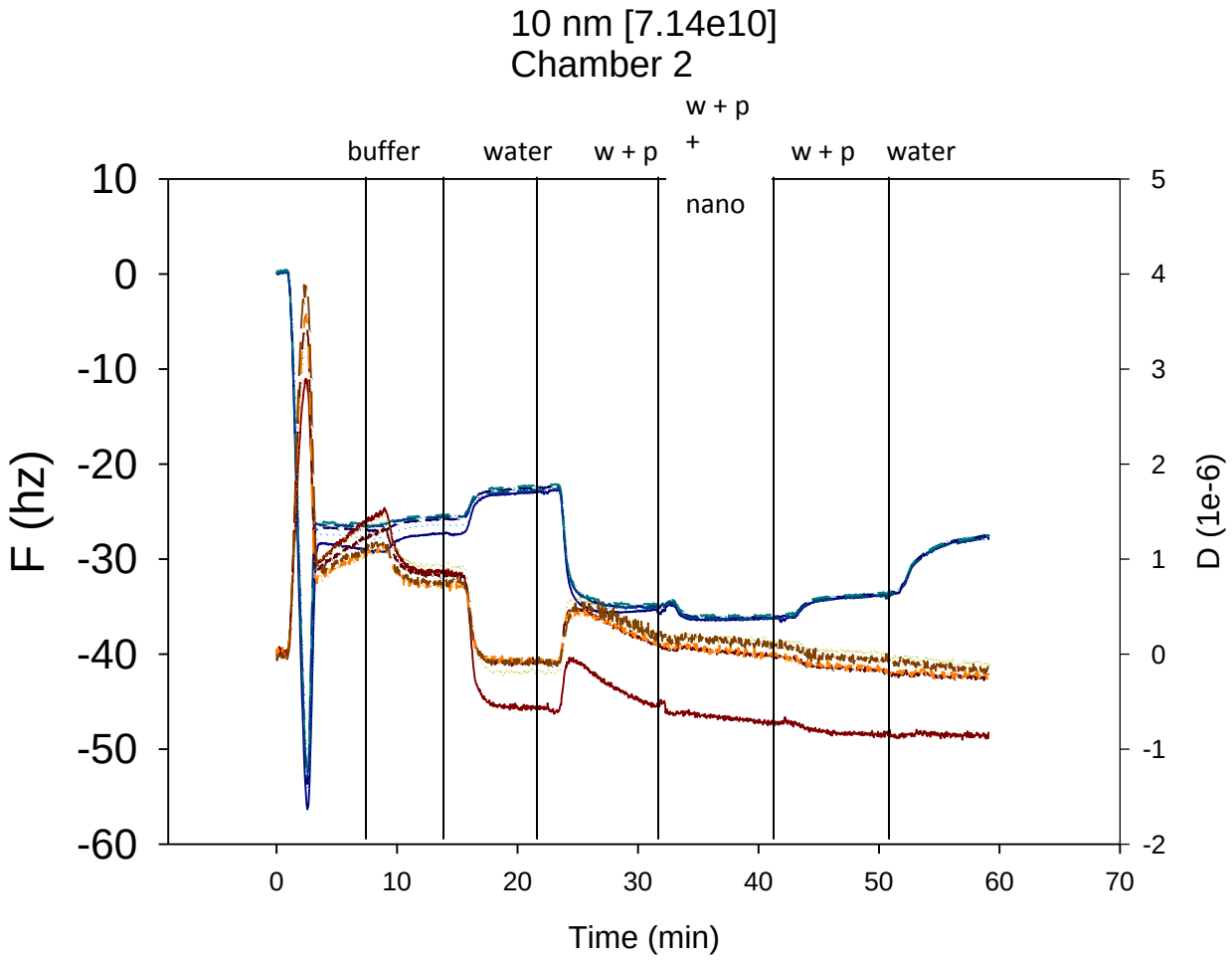

8:00
buffer

14:48
water

22:00
water+polymer

32:21
Nanoparticles

42:28
water+polymer

50:56
water

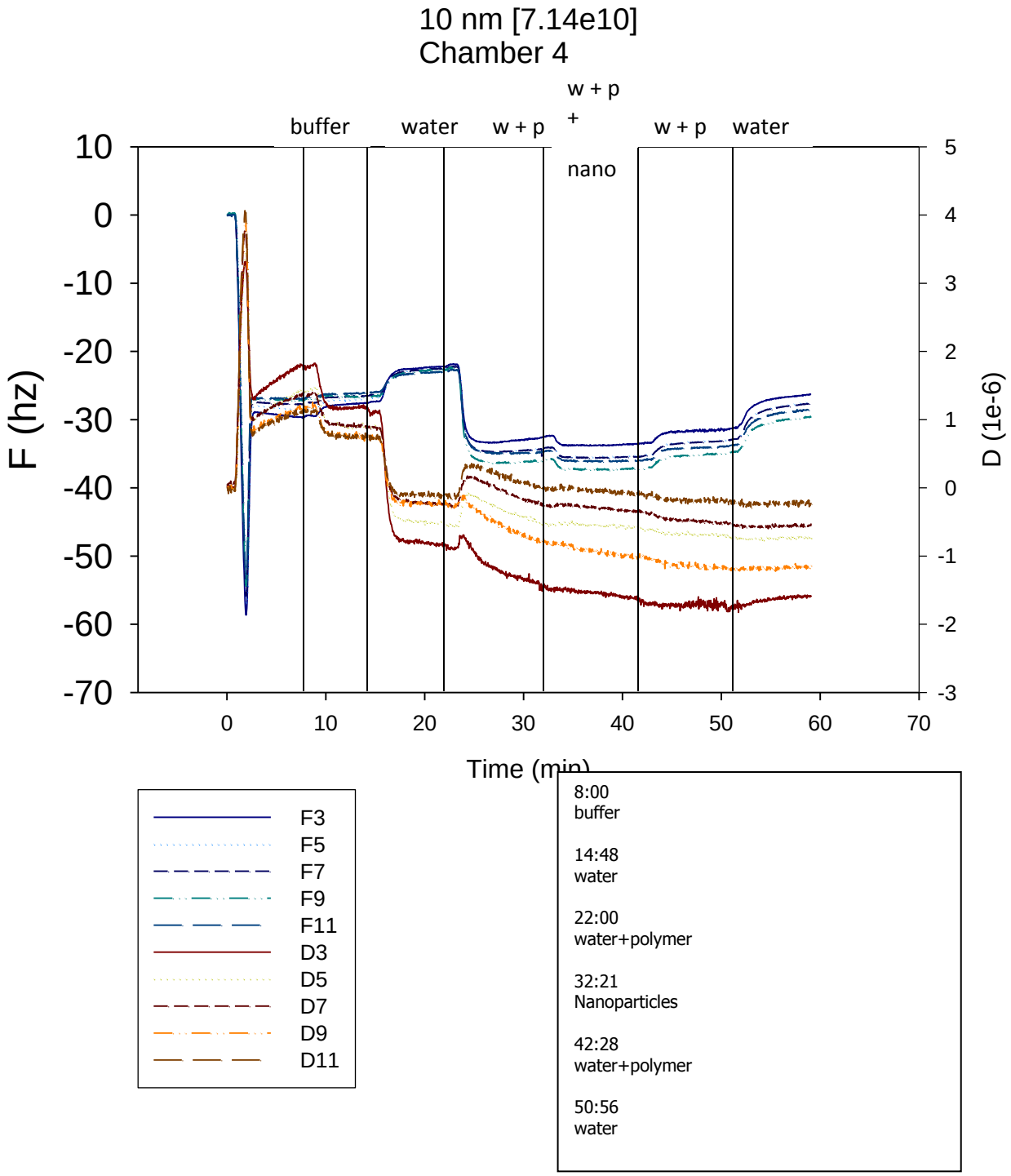
10 nm [7.14e10]
Chamber 4
buffer
water
w + p
w + p
+
nano
water
F (hz)
D (1e-6)
Time (min)
F3
F5
F7
F9
F11
D3
D5
D7
D9
D11
8:00
buffer
14:48
water
22:00
water+polymer
32:21
Nanoparticles
42:28
water+polymer
50:56
water

10 NM 3-23-2012 QCM-D Results

Chamber 1 10 nm

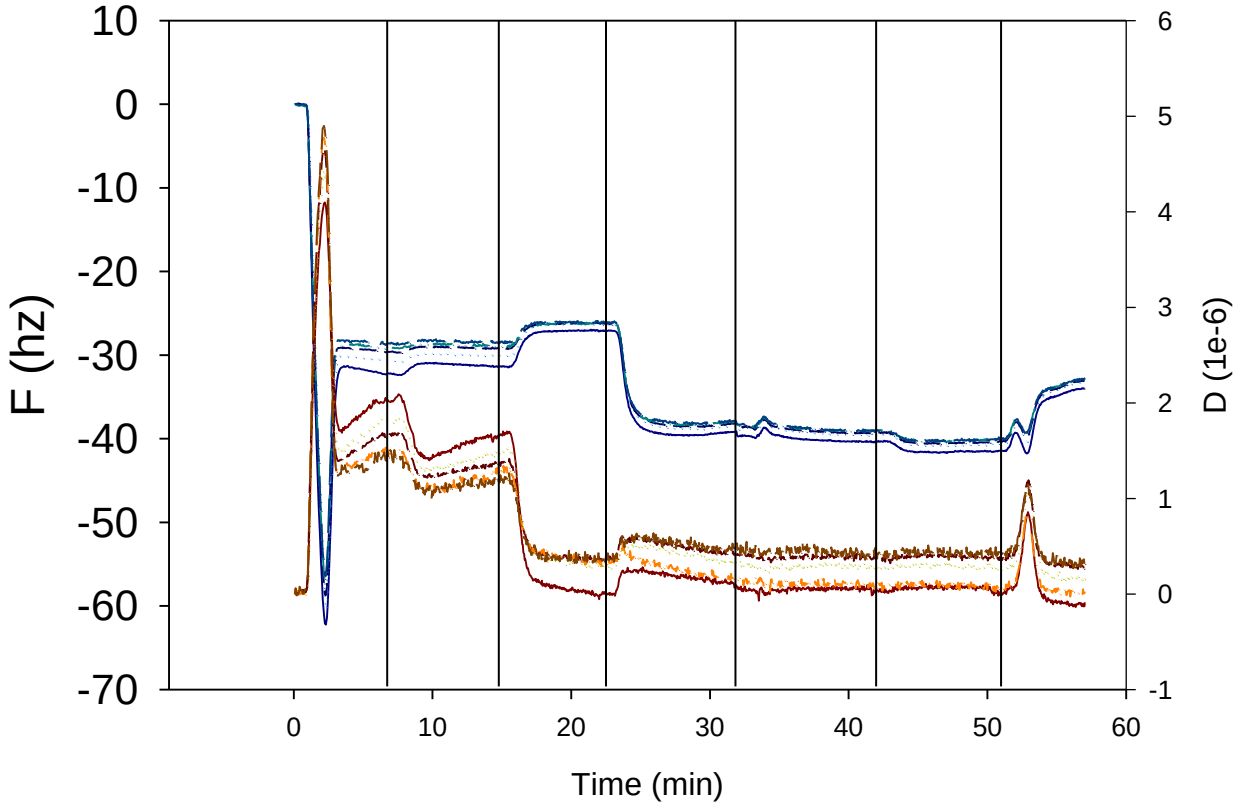

F3
F5
F7
F9
F11
D3
D5
D7
D9
D11

6:59
buffer

14:04
water

22:12
water +polymer

32:40
nanoparticles

42:00
water + polymer

49:58
water

56:55
end

Chamber 2 10 nm

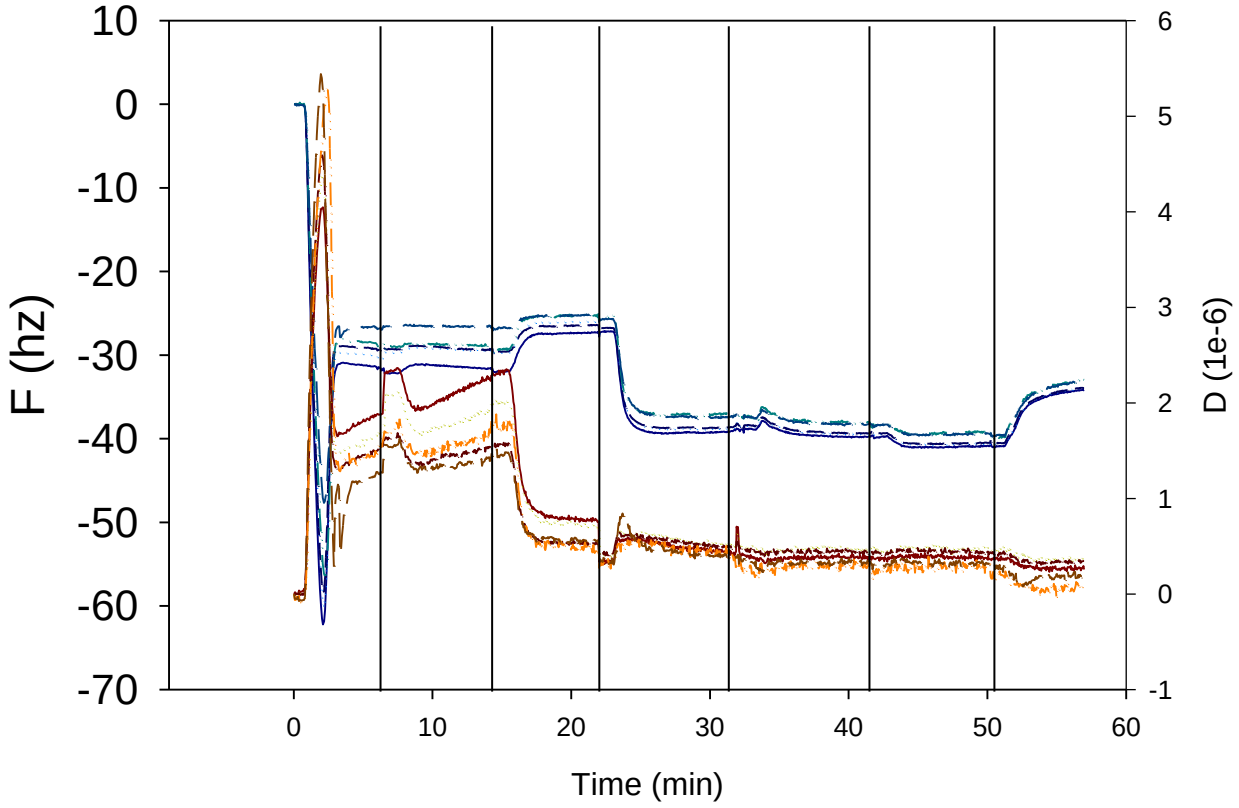

F3
F5
F7
F9
F11
D3
D5
D7
D9
D11

6:59
buffer

14:04
water

22:12
water +polymer

32:40
nanoparticles

42:00
water + polymer

49:58
water

56:55
end

Chamber 3 10 nm

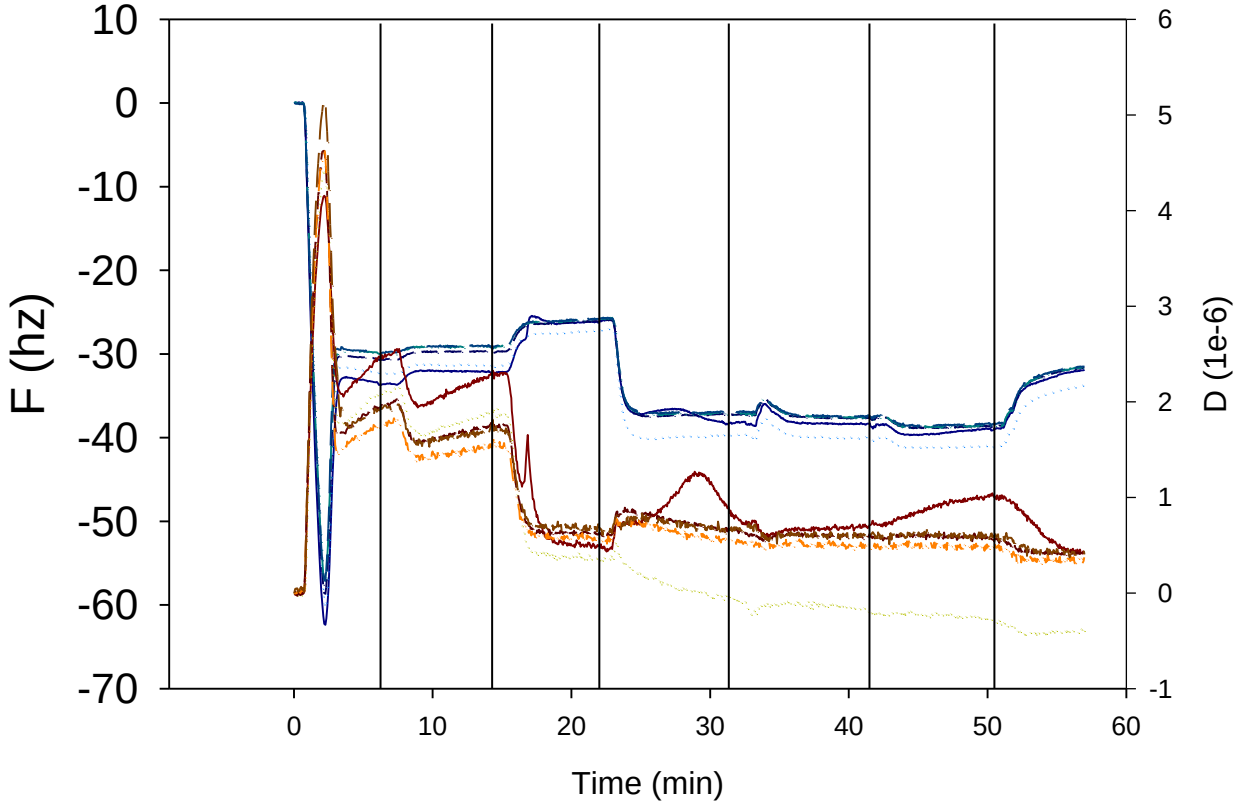

F3
F5
F7
F9
F11
D3
D5
D7
D9
D11

6:59
buffer

14:04
water

22:12
water +polymer

32:40
nanoparticles

42:00
water + polymer

49:58
water

56:55
end

10 NM 3-30-2012 QCM-D Results

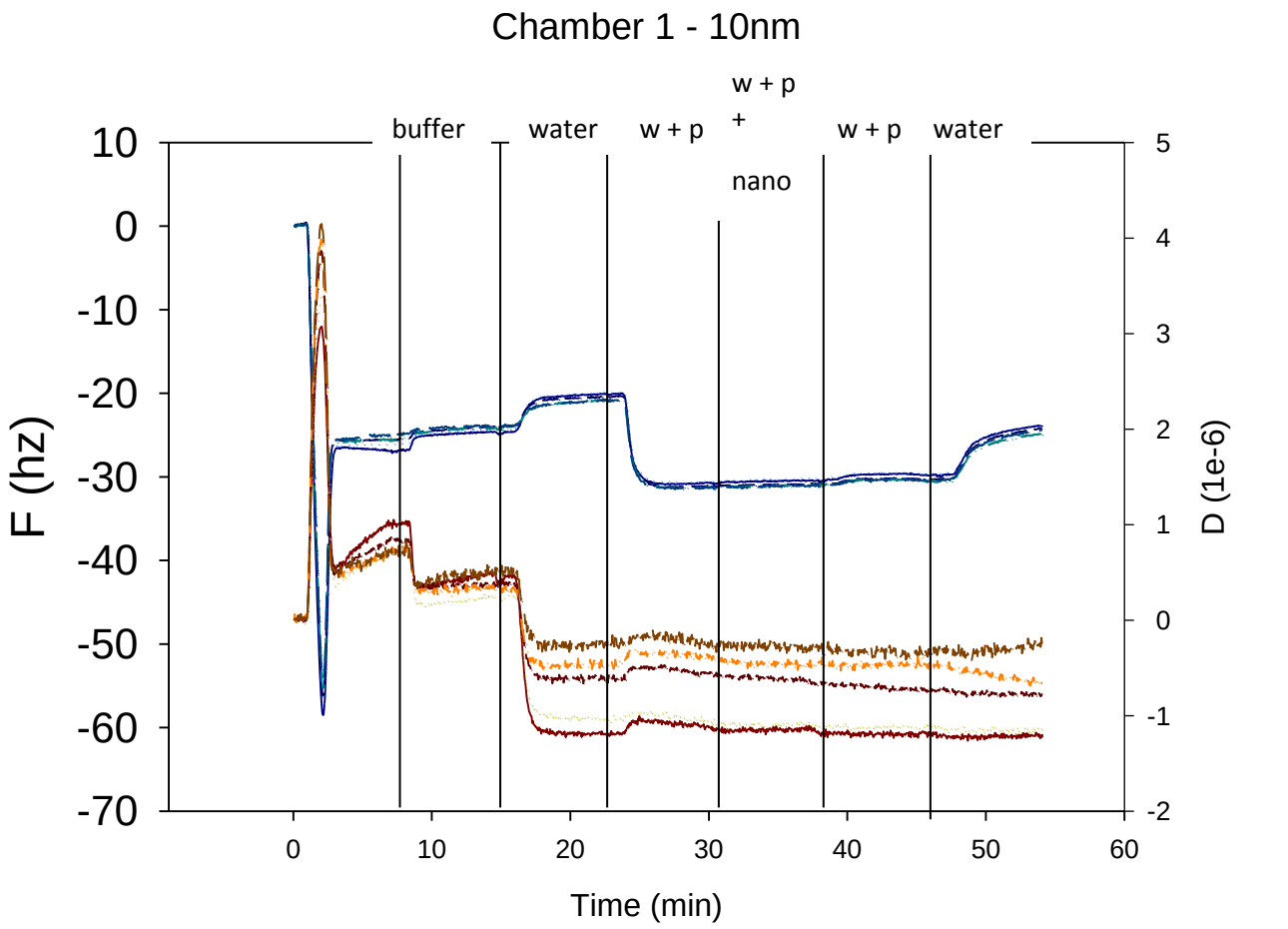

F3
F5
F7
F9
F11
D3
D5
D7
D9
D11

7:24
buffer

15:07
water

22:56
polymer

30:54
nanoparticles

38:14
water+polymer 2

46:25
water

54:00
end

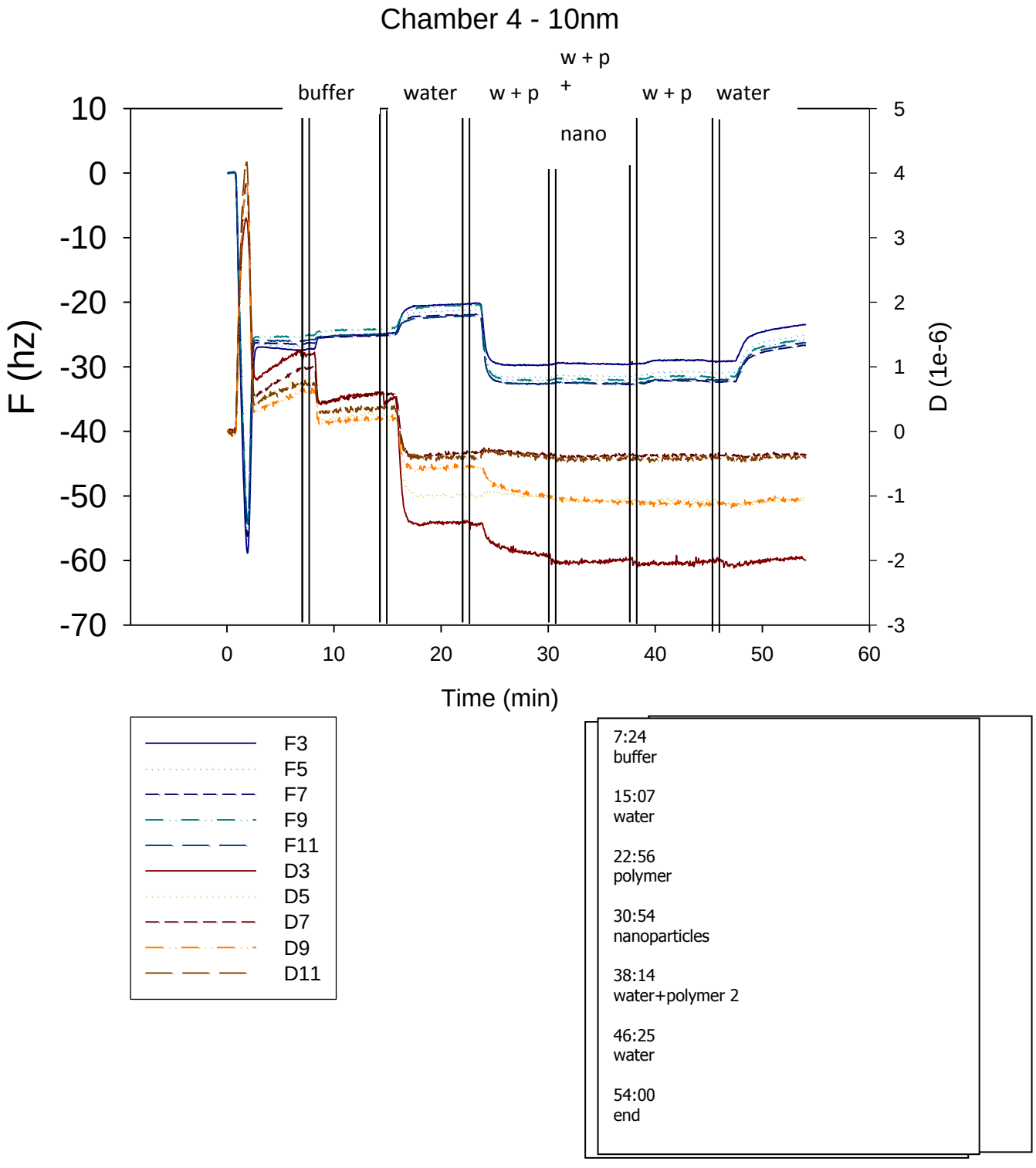
Chamber 4 - 10nm
buffer
water
w + p
w + p
+
nano
w + p
water
F (hz)
D (1e-6)
Time (min)
10
0
-10
-20
-30
-40
-50
-60
-70
5
4
3
2
1
0
-1
-2
-3
0
10
20
30
40
50
60
F3
F5
F7
F9
F11
D3
D5
D7
D9
D11
7:24
buffer
15:07
water
22:56
polymer
30:54
nanoparticles
38:14
water+polymer 2
46:25
water
54:00
end

10 NM 3-30-2012 QCM-D Results

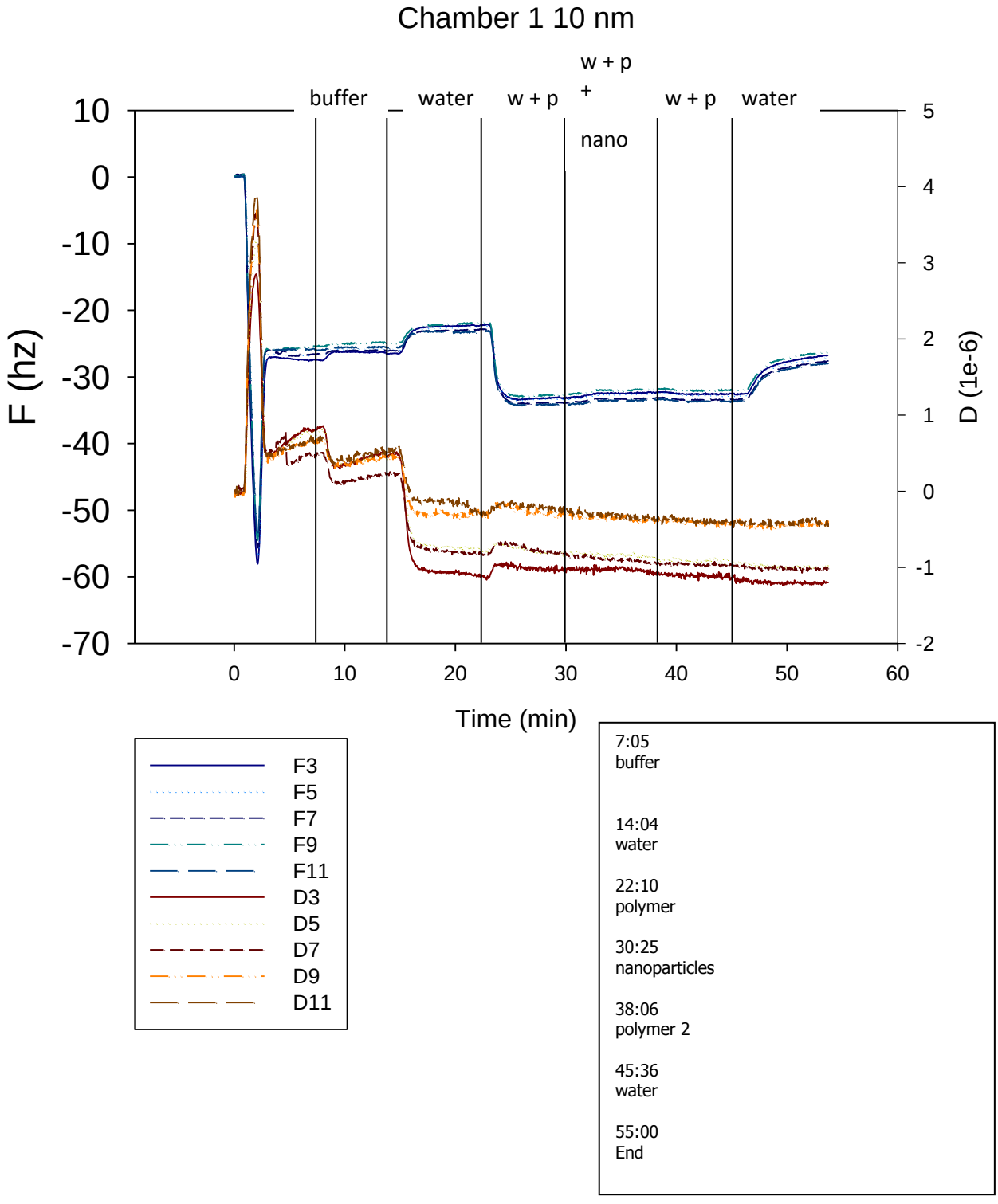
Chamber 1 10 nm
buffer
water
w + p
w + p
+
nano
w + p
water
F (hz)
D (1e-6)
Time (min)
10
0
-10
-20
-30
-40
-50
-60
-70
5
4
3
2
1
0
-1
-2
0
10
20
30
40
50
60
F3
F5
F7
F9
F11
D3
D5
D7
D9
D11
7:05
buffer
14:04
water
22:10
polymer
30:25
nanoparticles
38:06
polymer 2
45:36
water
55:00
End

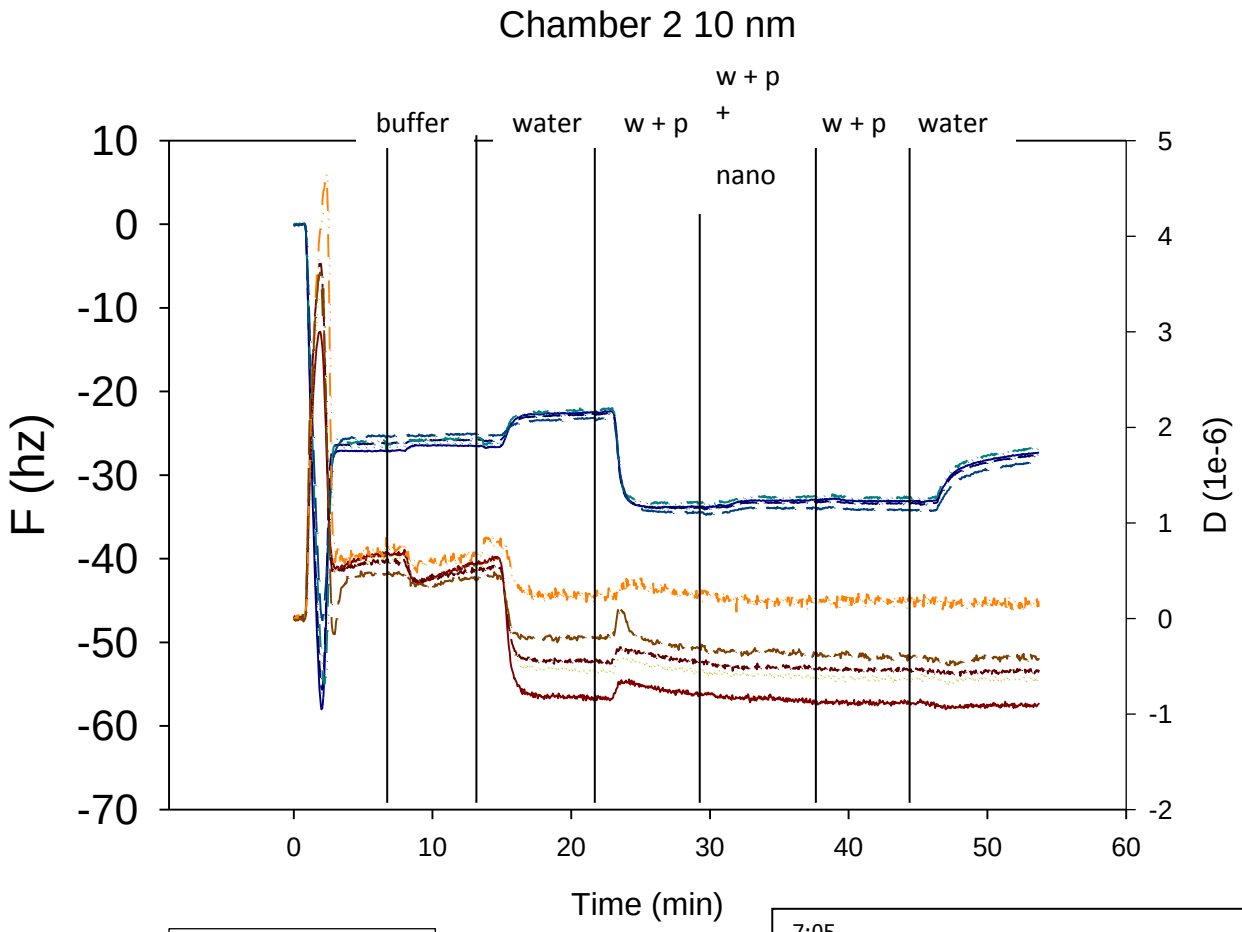

F3
F5
F7
F9
F11
D3
D5
D7
D9
D11

7:05
buffer

14:04
water

22:10
polymer

30:25
nanoparticles

38:06
polymer 2

45:36
water

55:00
End

Chamber 3 10nm

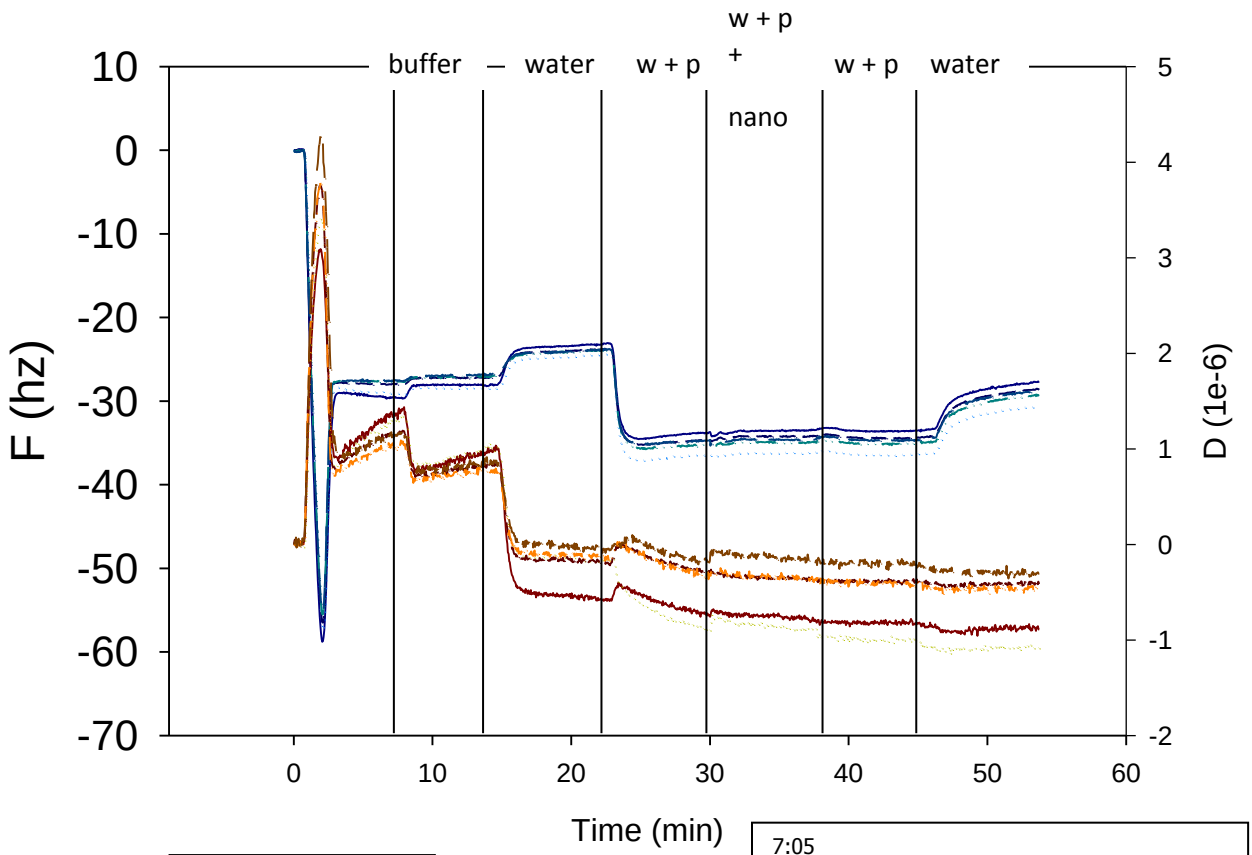

F3
F5
F7
F9
F11
D3
D5
D7
D9
D11

7:05
buffer

14:04
water

22:10
polymer

30:25
nanoparticles

38:06
polymer 2

45:36
water

55:00
End

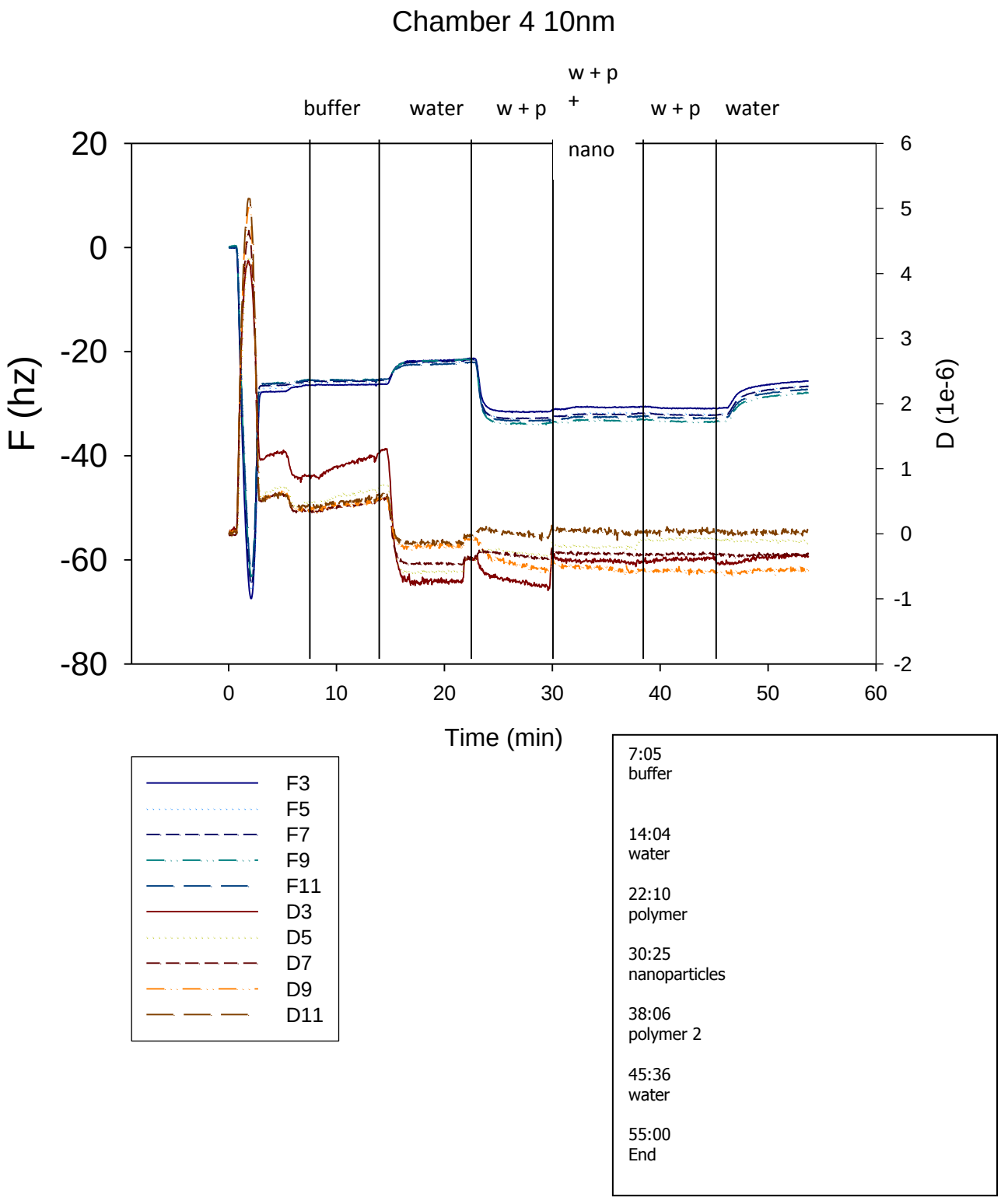
Chamber 4 10nm
buffer
water
w + p
w + p
+
nano
w + p
water
F (hz)
D (1e-6)
Time (min)
20
0
-20
-40
-60
-80
6
5
4
3
2
1
0
-1
-2
0
10
20
30
40
50
60
F3
F5
F7
F9
F11
D3
D5
D7
D9
D11
7:05
buffer
14:04
water
22:10
polymer
30:25
nanoparticles
38:06
polymer 2
45:36
water
55:00
End

40 NM 4-3-2012 QCM-D Results

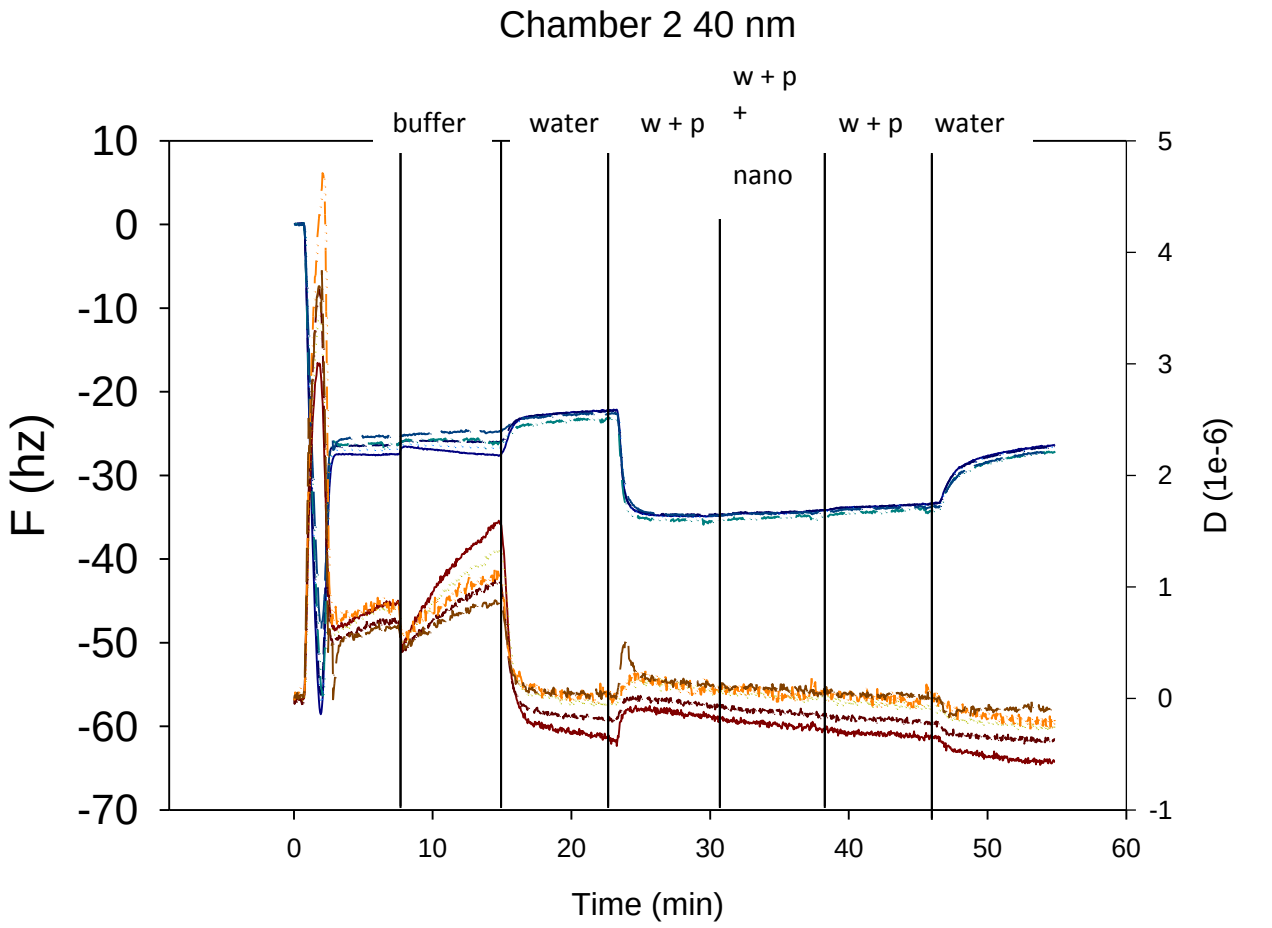

buffer
6:49

water
14:12

polymer
22:22

nanoparts
30:01

polymer
37:46

water
45:51

end
54:46

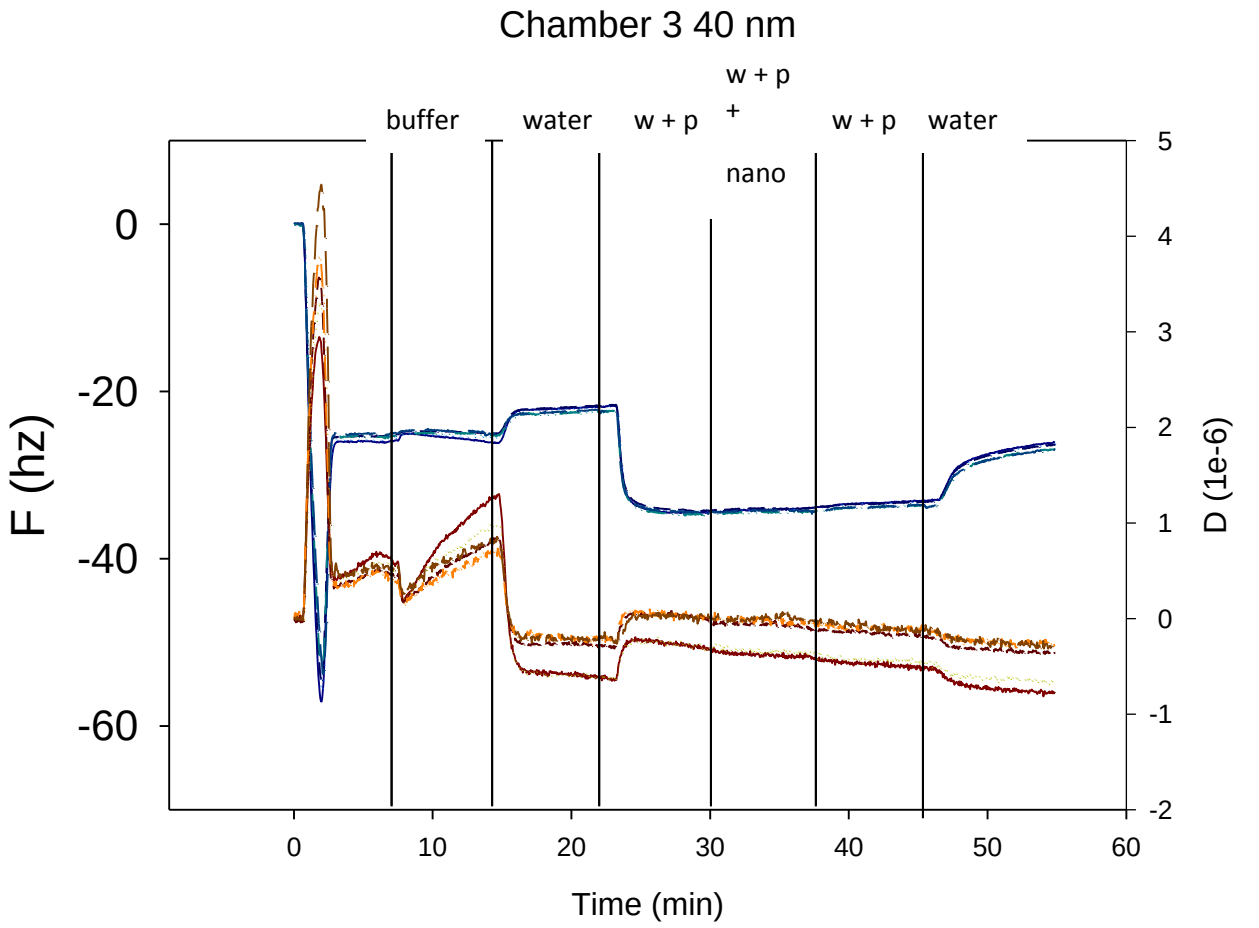

F3
F5
F7
F9
F11
D3
D5
D7
D9
D11

buffer
6:49

water
14:12

polymer
22:22

nanoparts
30:01

polymer
37:46

water
45:51

end
54:46

40 NM 4-3-2012 QCM-D Results

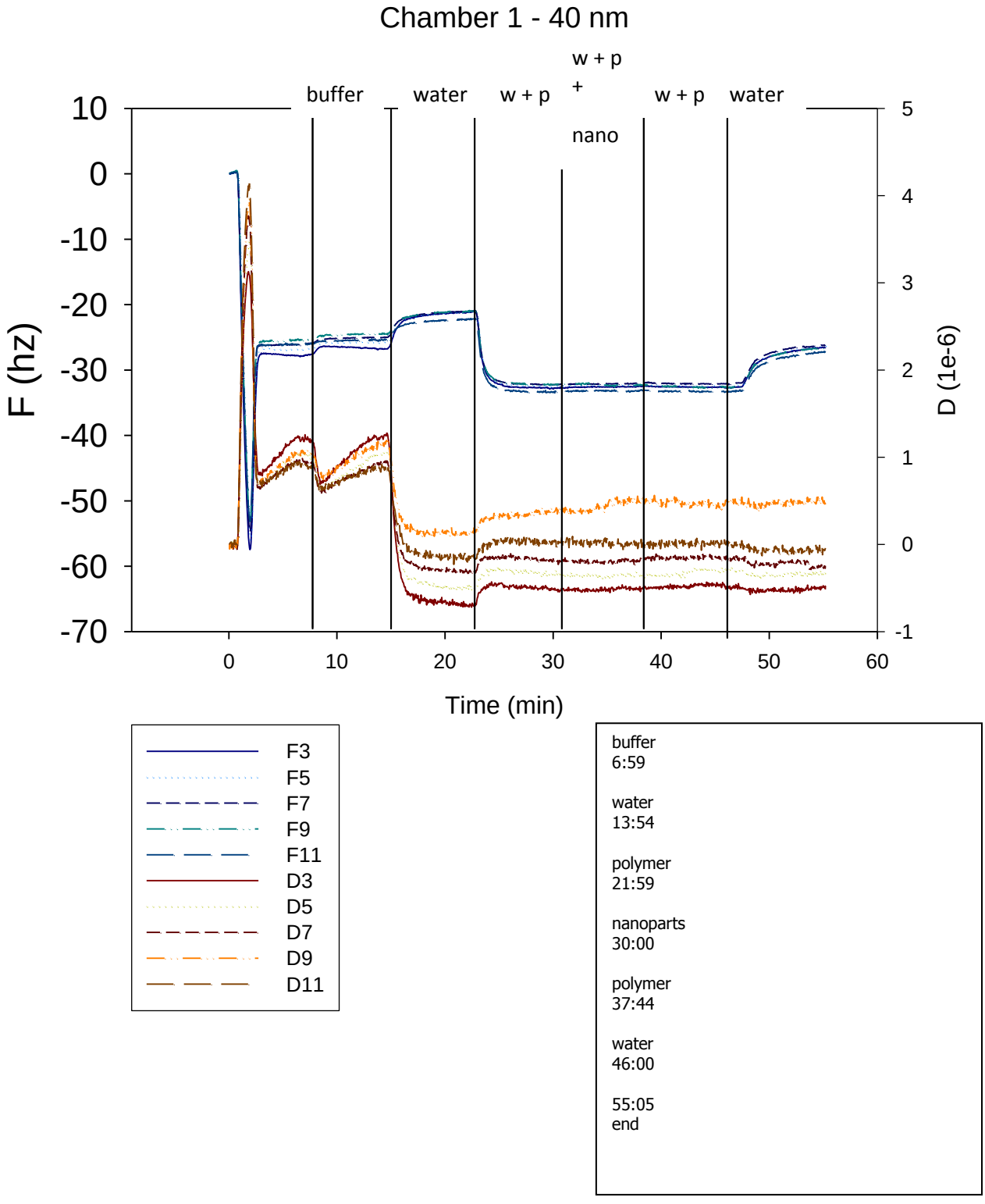
Chamber 1 - 40 nm
buffer
water
w + p
w + p
+
nano
w + p
water
F (hz)
D (1e-6)
Time (min)
10
0
-10
-20
-30
-40
-50
-60
-70
5
4
3
2
1
0
-1
0
10
20
30
40
50
60
F3
F5
F7
F9
F11
D3
D5
D7
D9
D11
buffer
6:59
water
13:54
polymer
21:59
nanoparts
30:00
polymer
37:44
water
46:00
55:05
end

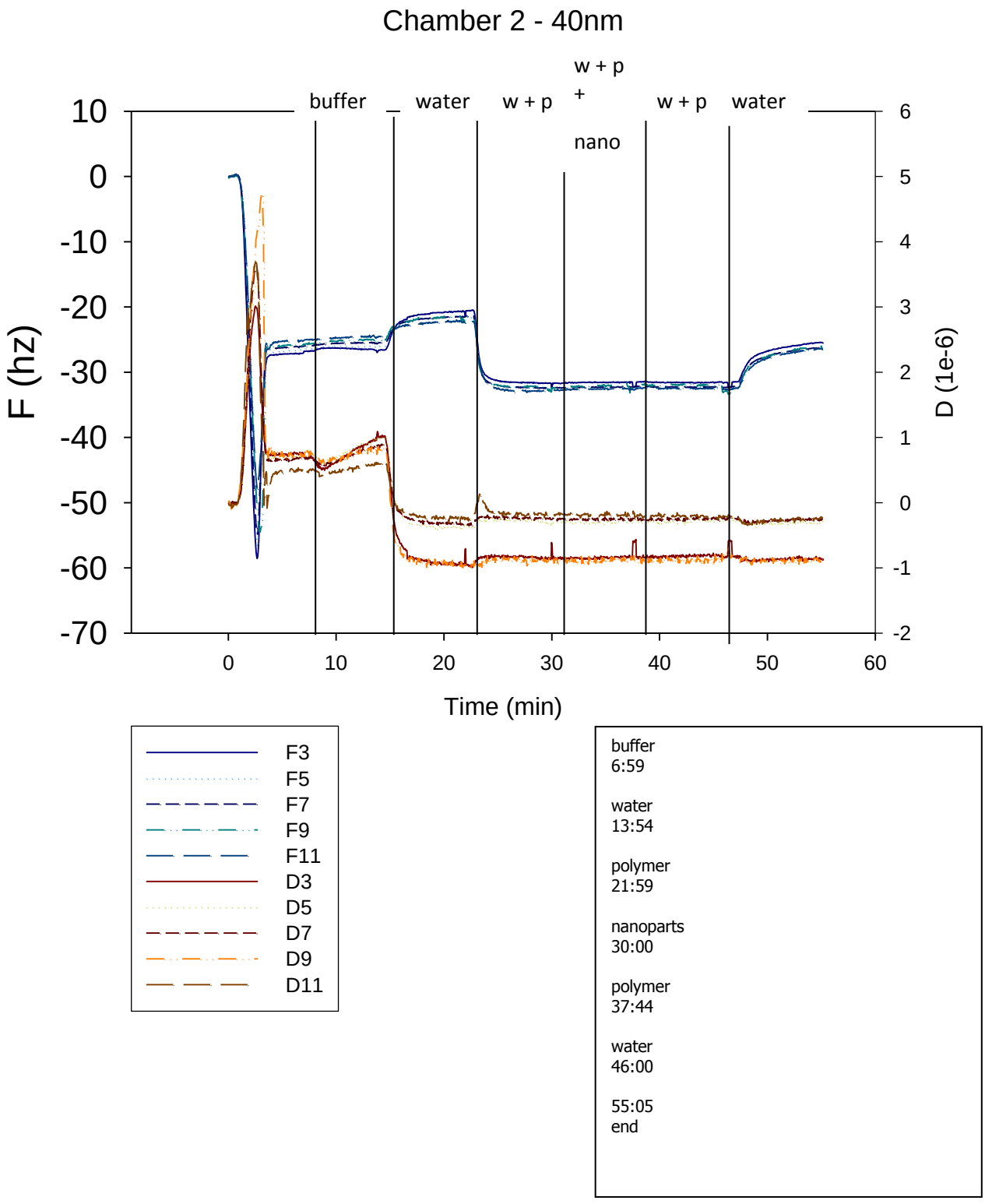
Chamber 2 - 40nm
buffer
water
w + p
w + p
+
nano
water
F (hz)
D (1e-6)
Time (min)
10
0
-10
-20
-30
-40
-50
-60
-70
6
5
4
3
2
1
0
-1
-2
0
10
20
30
40
50
60
F3
F5
F7
F9
F11
D3
D5
D7
D9
D11
buffer
6:59
water
13:54
polymer
21:59
nanoparts
30:00
polymer
37:44
water
46:00
55:05
end

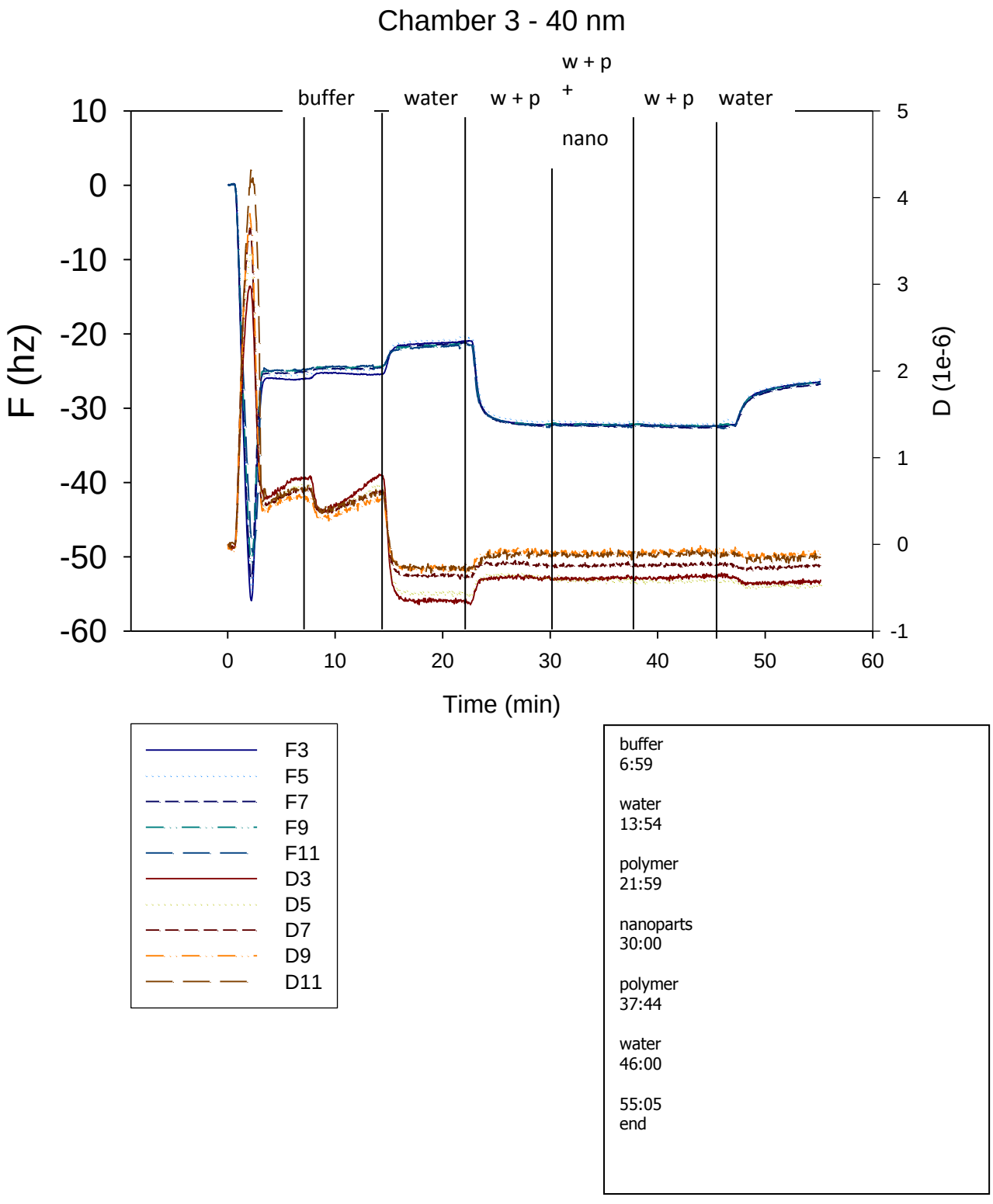
Chamber 3 - 40 nm
buffer
water
w + p
w + p
+
nano
w + p
water
F (hz)
D (1e-6)
Time (min)
10
0
-10
-20
-30
-40
-50
-60
5
4
3
2
1
0
-1
0
10
20
30
40
50
60
F3
F5
F7
F9
F11
D3
D5
D7
D9
D11
buffer
6:59
water
13:54
polymer
21:59
nanoparts
30:00
polymer
37:44
water
46:00
55:05
end

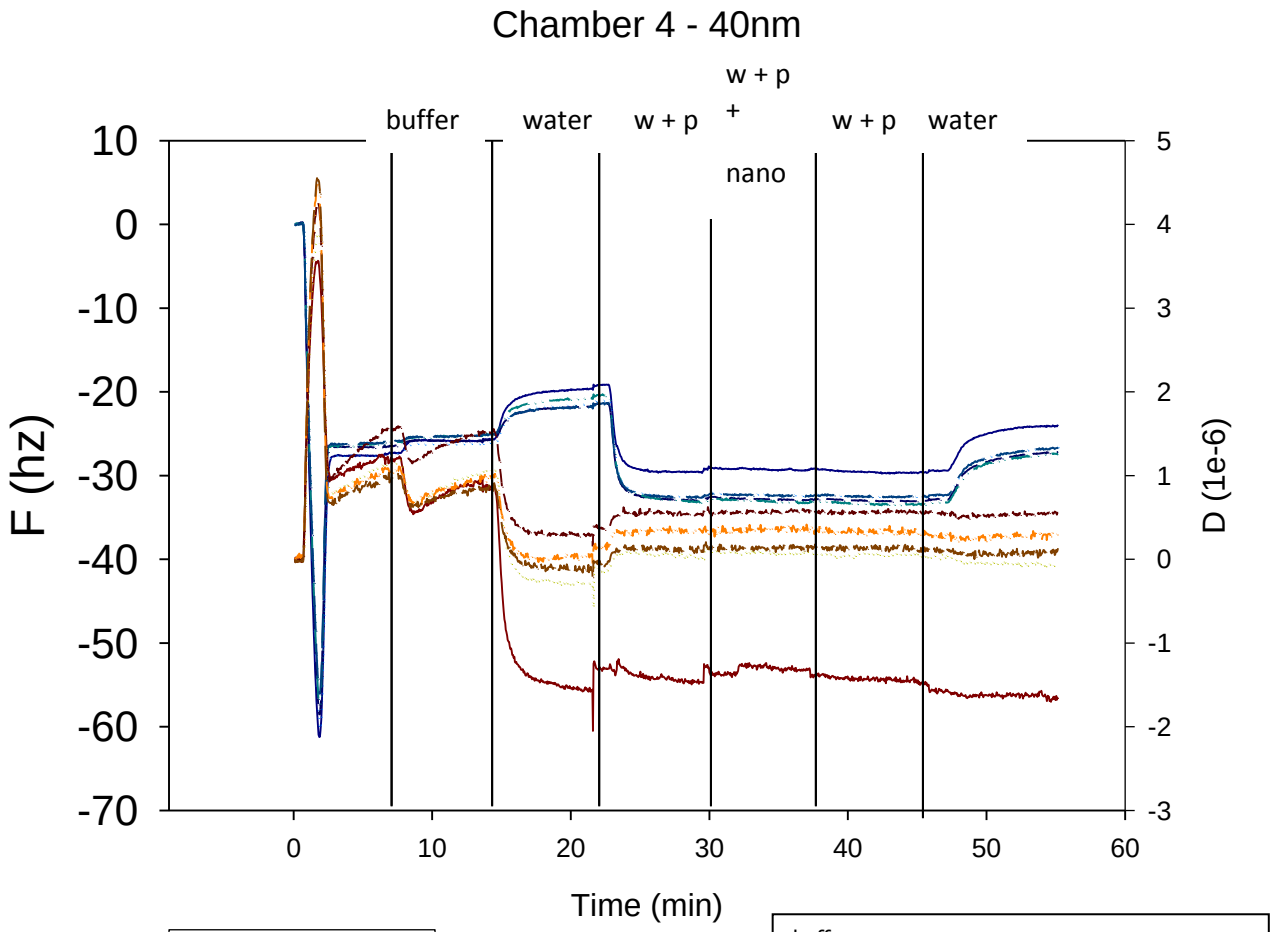

F3
F5
F7
F9
F11
D3
D5
D7
D9
D11

buffer
6:59

water
13:54

polymer
21:59

nanoparts
30:00

polymer
37:44

water
46:00

55:05
end

40 NM 4-3-2012 QCM-D Results

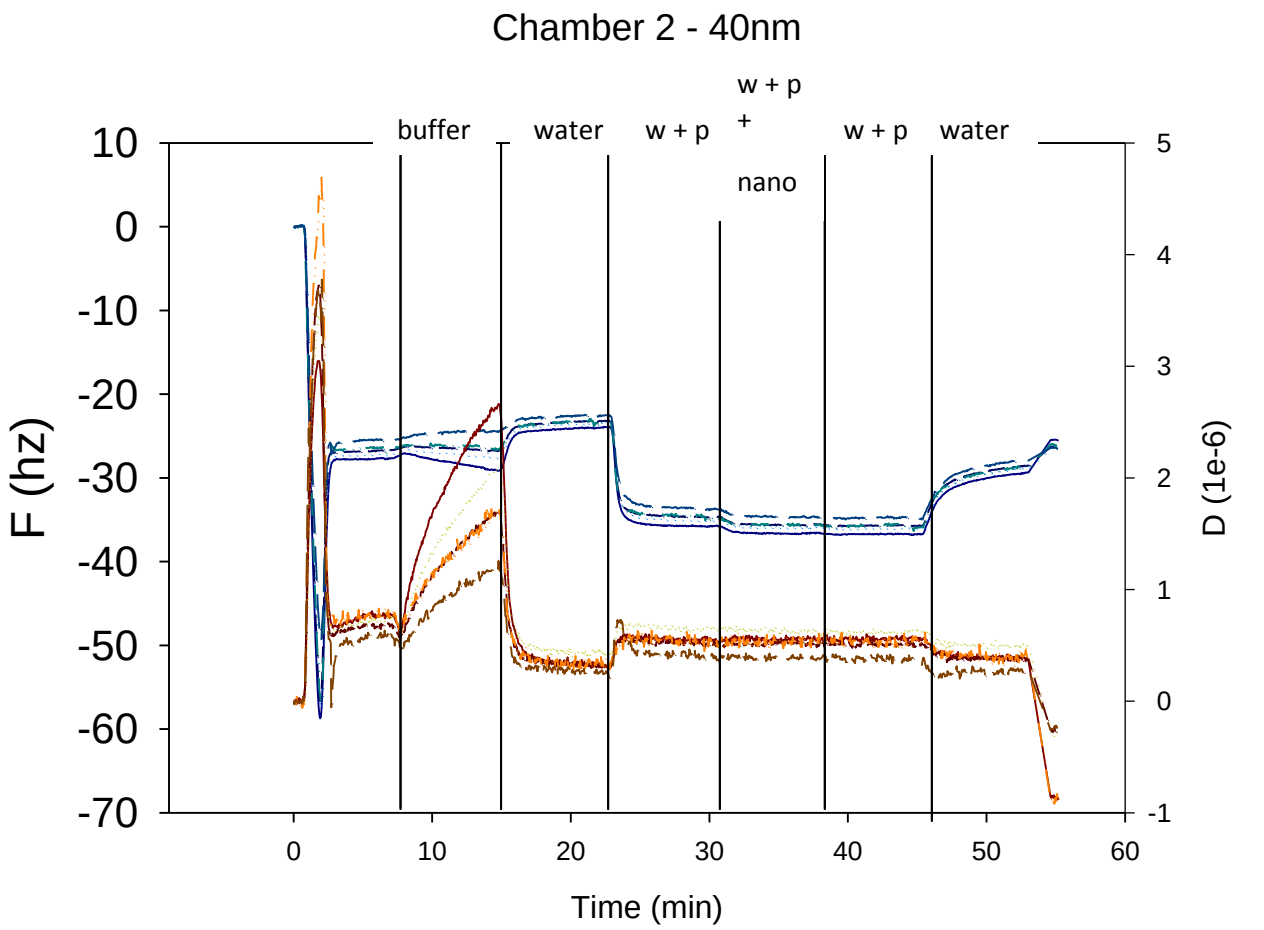

7:05
buffer

14:14
water

22:03
water+polymer

30:13
nanoparicles

37:18
water+polymer 2

45:00
water

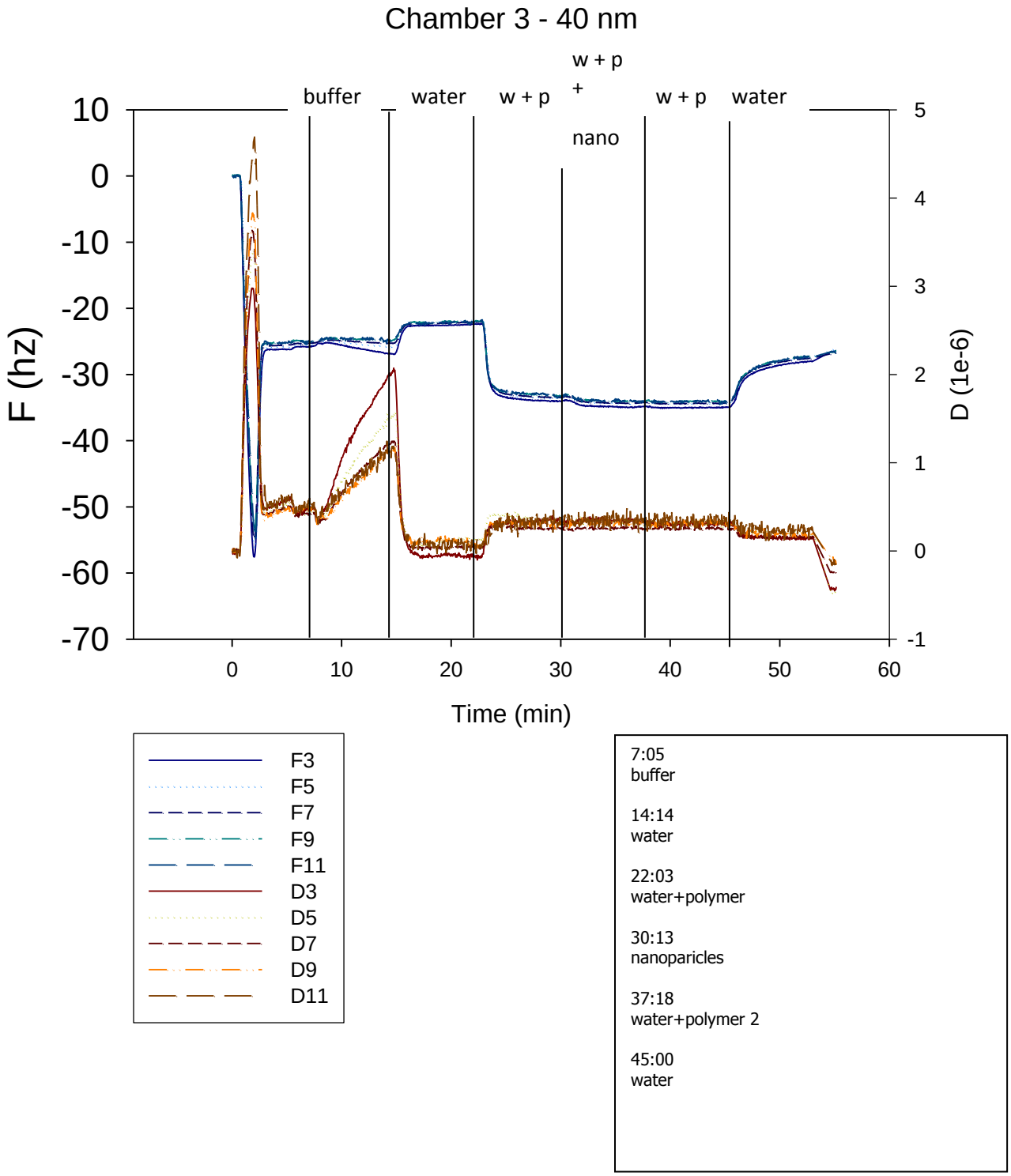
Chamber 3 - 40 nm
buffer
water
w + p
w + p
+
nano
w + p
water
F (hz)
D (1e-6)
Time (min)
10
0
-10
-20
-30
-40
-50
-60
-70
5
4
3
2
1
0
-1
0
10
20
30
40
50
60
F3
F5
F7
F9
F11
D3
D5
D7
D9
D11
7:05
buffer
14:14
water
22:03
water+polymer
30:13
nanoparicles
37:18
water+polymer 2
45:00
water

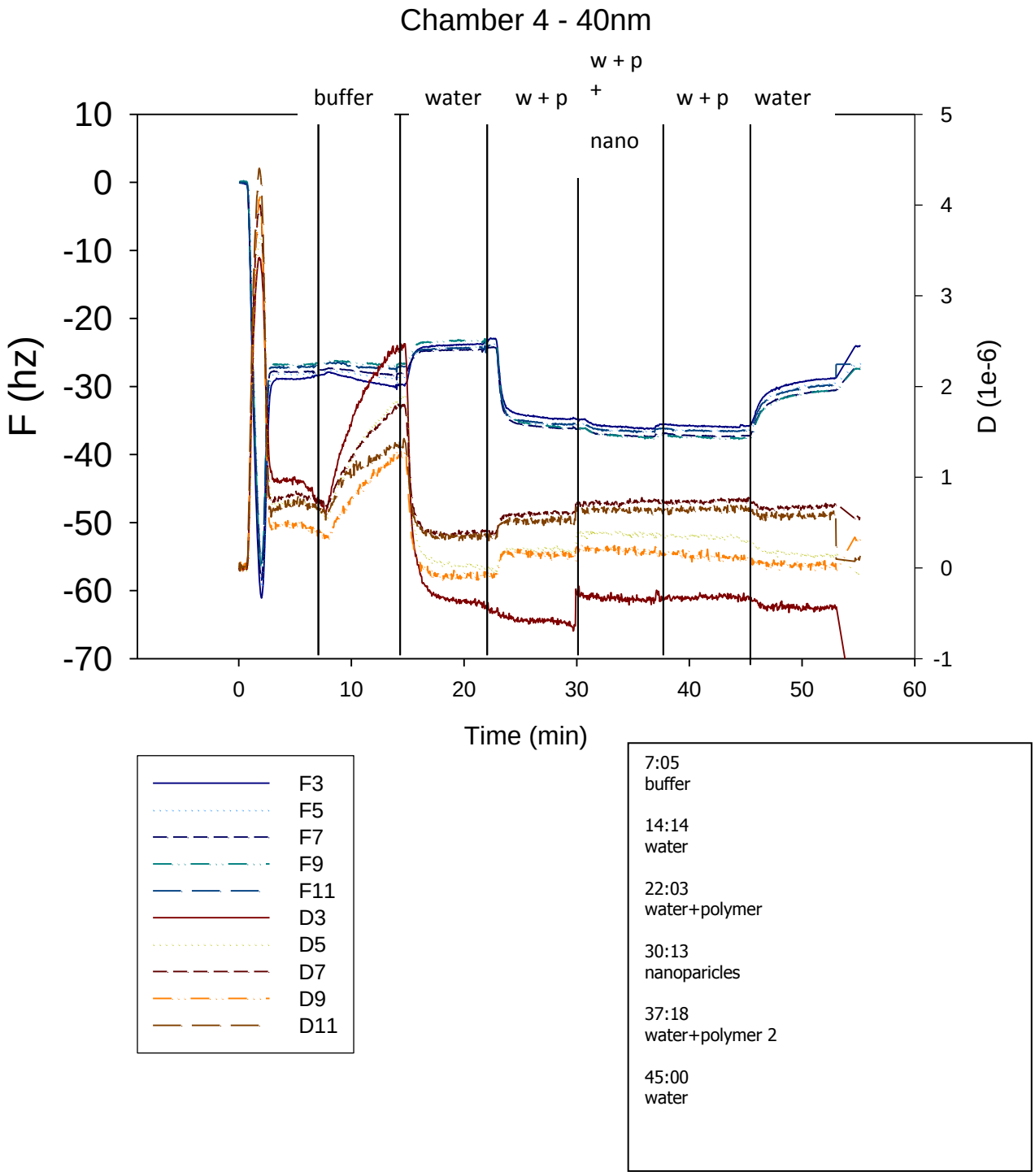
Chamber 4 - 40nm
buffer
water
w + p
w + p
+
nano
w + p
water
F (hz)
D (1e-6)
Time (min)
10
0
-10
-20
-30
-40
-50
-60
-70
5
4
3
2
1
0
-1
0
10
20
30
40
50
60
F3
F5
F7
F9
F11
D3
D5
D7
D9
D11
7:05
buffer
14:14
water
22:03
water+polymer
30:13
nanoparicles
37:18
water+polymer 2
45:00
water

40 NM 4-3-2012 QCM-D Results

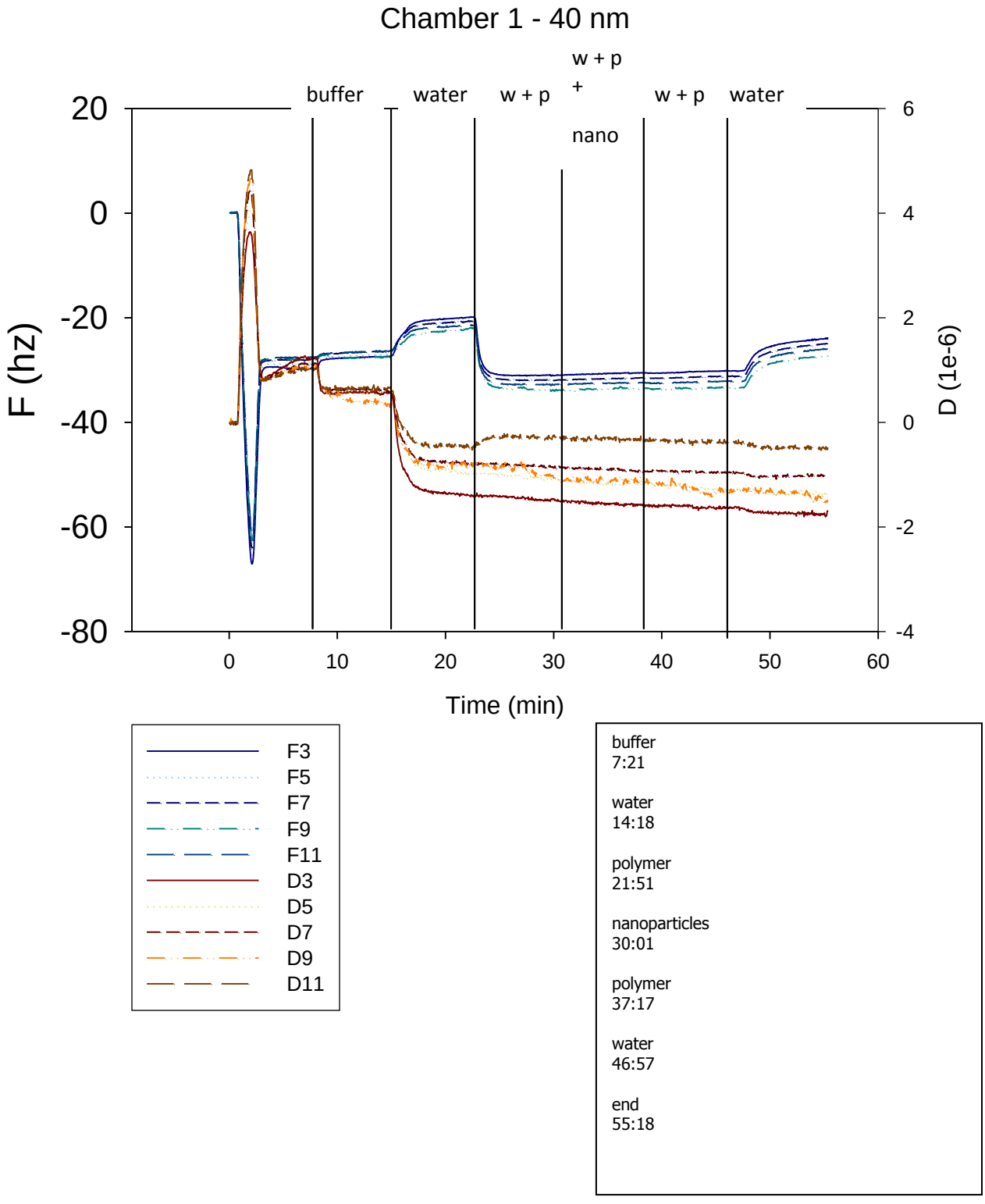
Chamber 1 - 40 nm
buffer
water
w + p
w + p
+
nano
w + p
water
F (hz)
D (1e-6)
Time (min)
20
0
-20
-40
-60
-80
6
4
2
0
-2
-4
0
10
20
30
40
50
60
F3
F5
F7
F9
F11
D3
D5
D7
D9
D11
buffer
7:21
water
14:18
polymer
21:51
nanoparticles
30:01
polymer
37:17
water
46:57
end
55:18

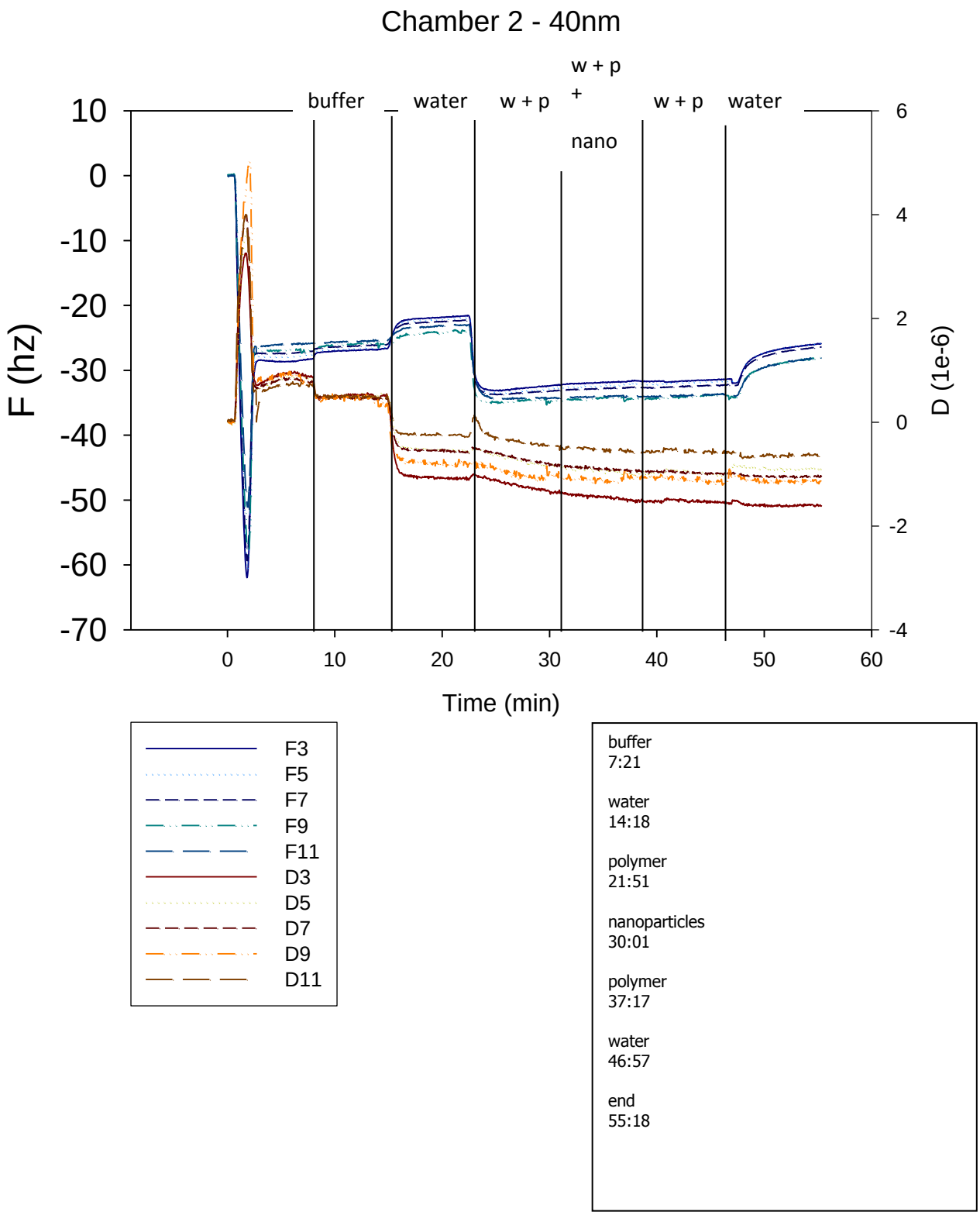
Chamber 2 - 40nm
buffer
water
w + p
w + p
+
nano
water
F (hz)
D (1e-6)
Time (min)
10
0
-10
-20
-30
-40
-50
-60
-70
6
4
2
0
-2
-4
0
10
20
30
40
50
60
F3
F5
F7
F9
F11
D3
D5
D7
D9
D11
buffer
7:21
water
14:18
polymer
21:51
nanoparticles
30:01
polymer
37:17
water
46:57
end
55:18

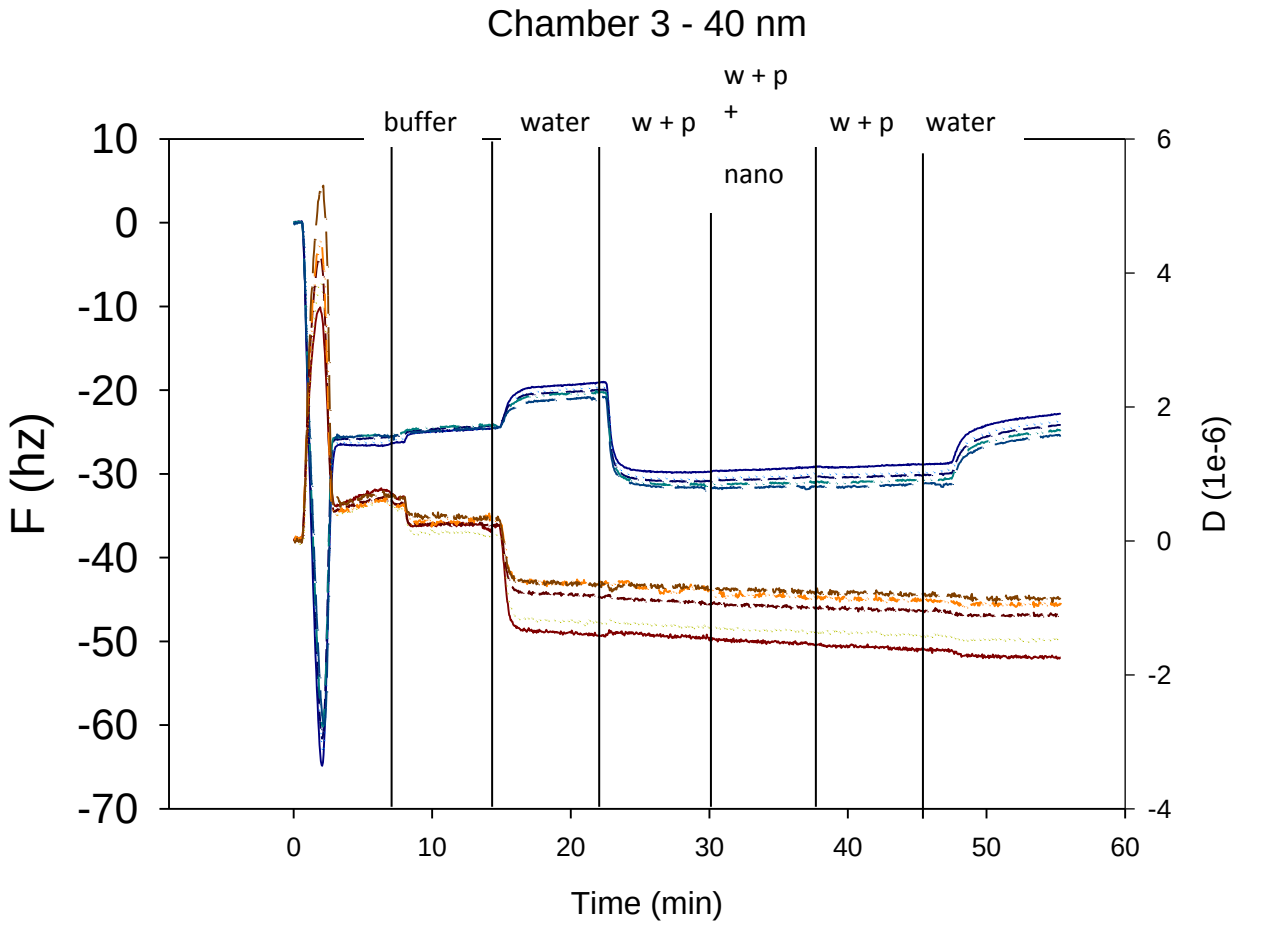

F3
F5
F7
F9
F11
D3
D5
D7
D9
D11

buffer
7:21

water
14:18

polymer
21:51

nanoparticles
30:01

polymer
37:17

water
46:57

end
55:18

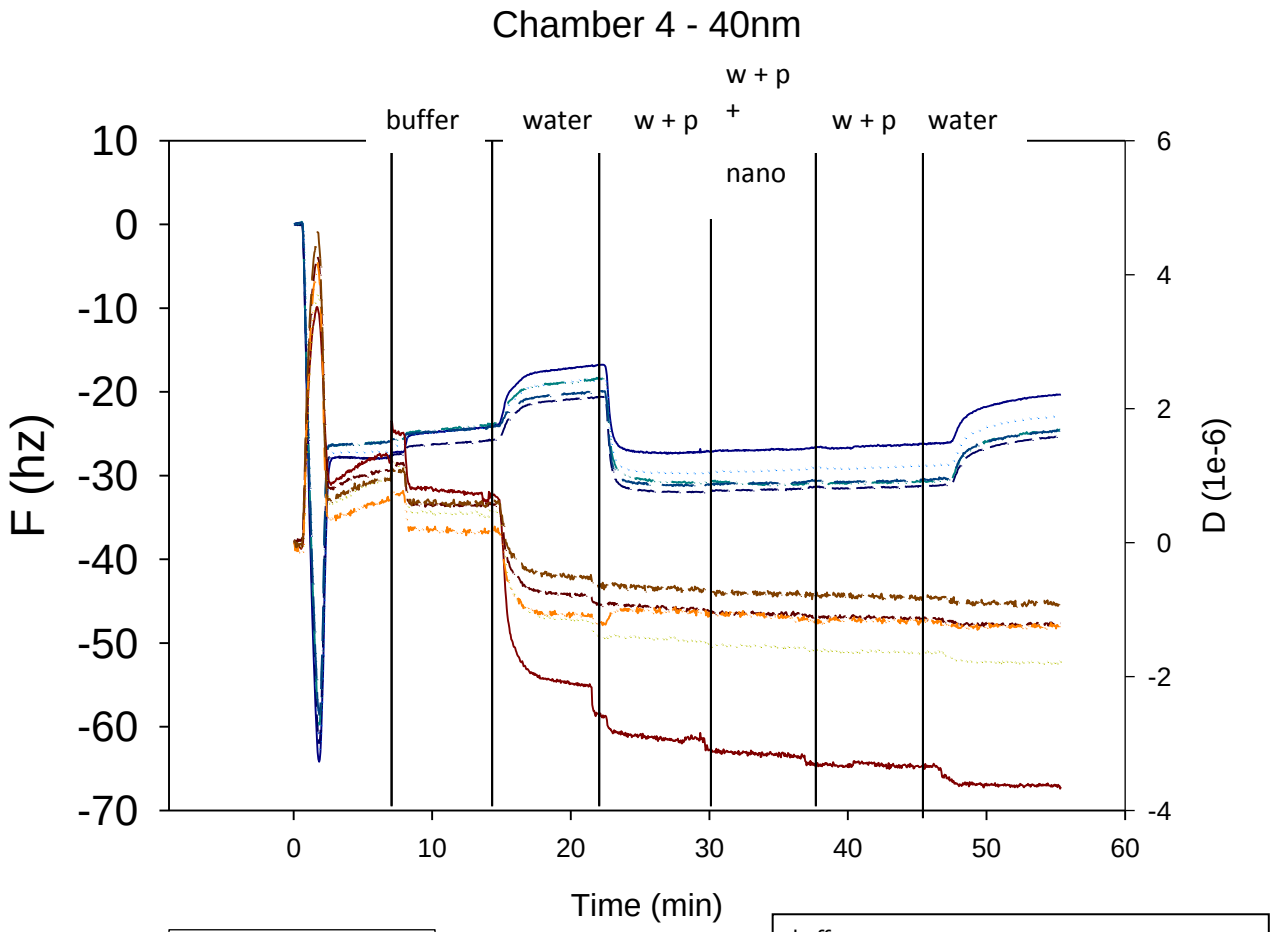

F3
F5
F7
F9
F11
D3
D5
D7
D9
D11

buffer
7:21

water
14:18

polymer
21:51

nanoparticles
30:01

polymer
37:17

water
46:57

end
55:18

APPENDIX C: ALL Overtone Analysis Bar Graphs

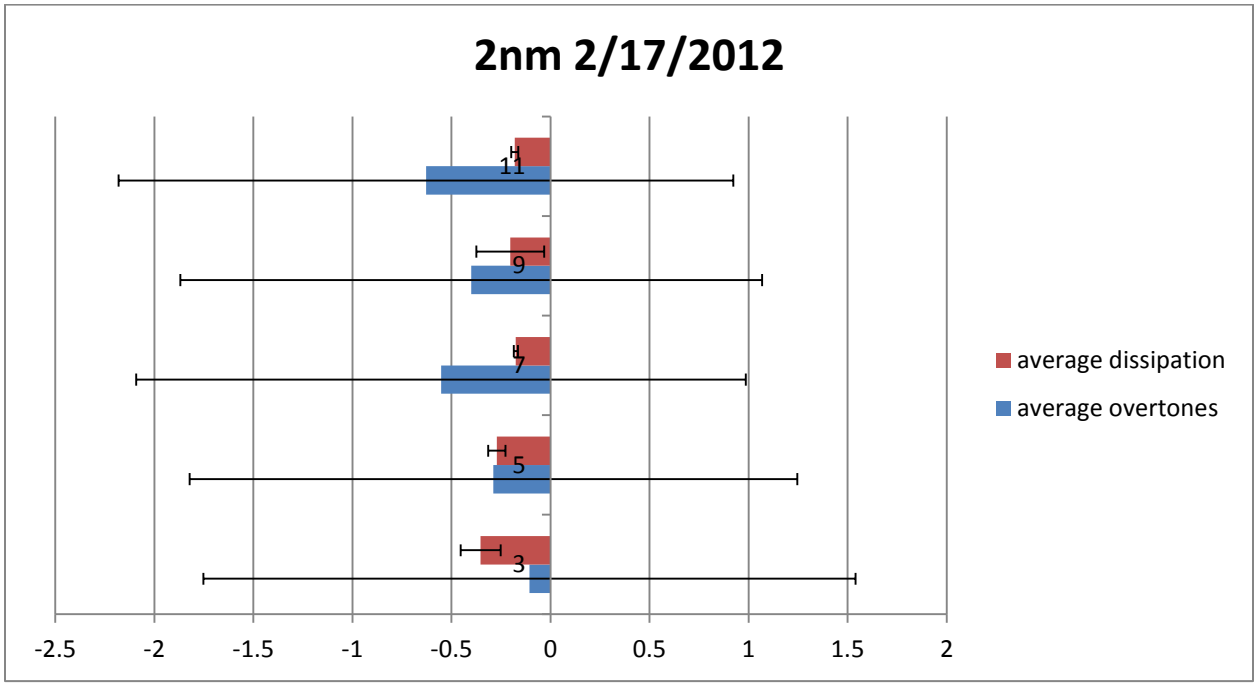

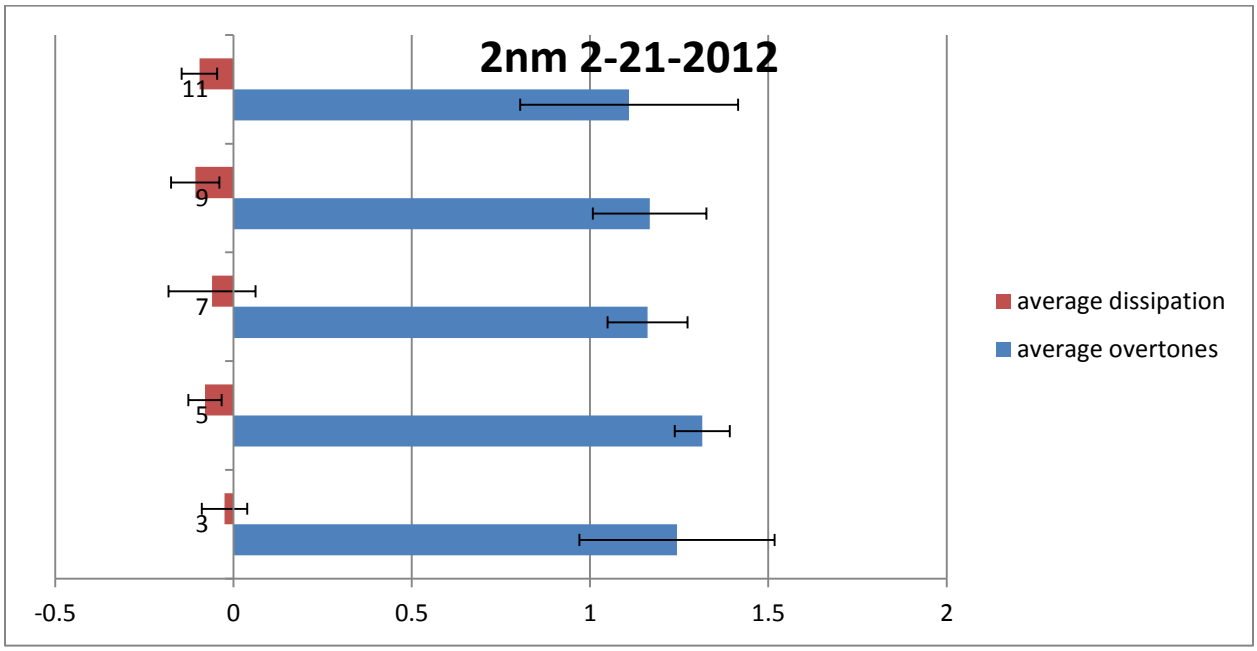

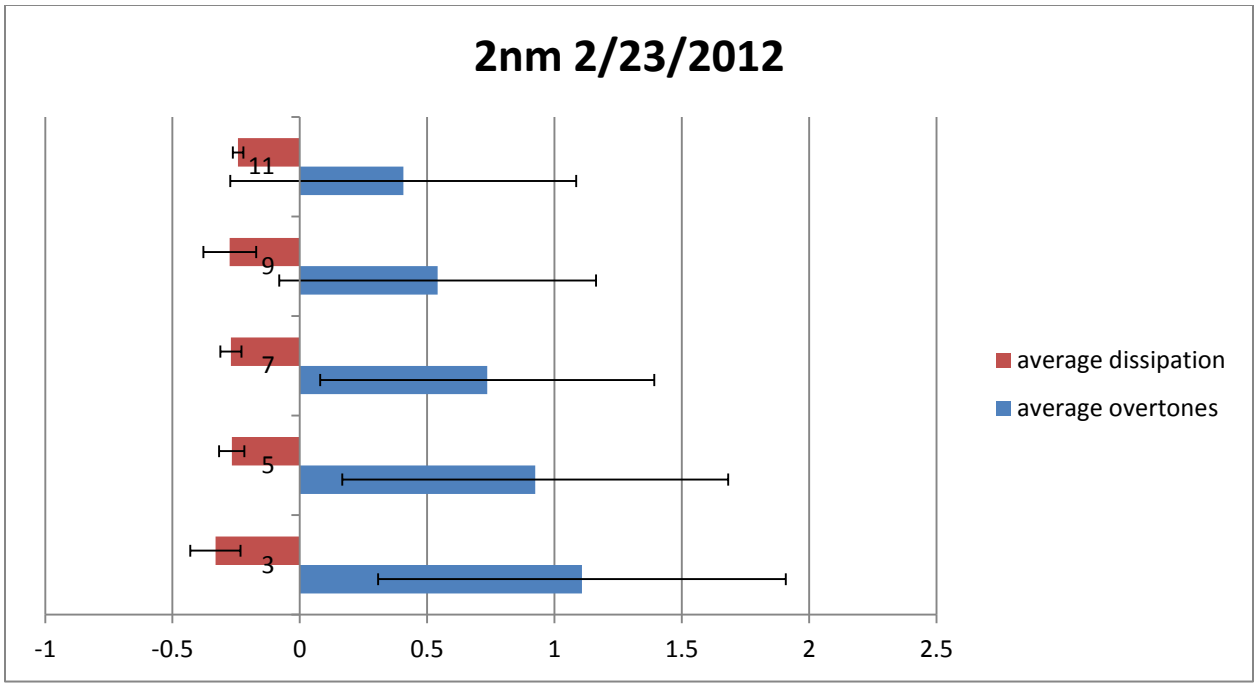
2nm 2/23/2012
11
9
7
5
3
-1
-0.5
0
0.5
1
1.5
2
2.5
average dissipation
average overtones

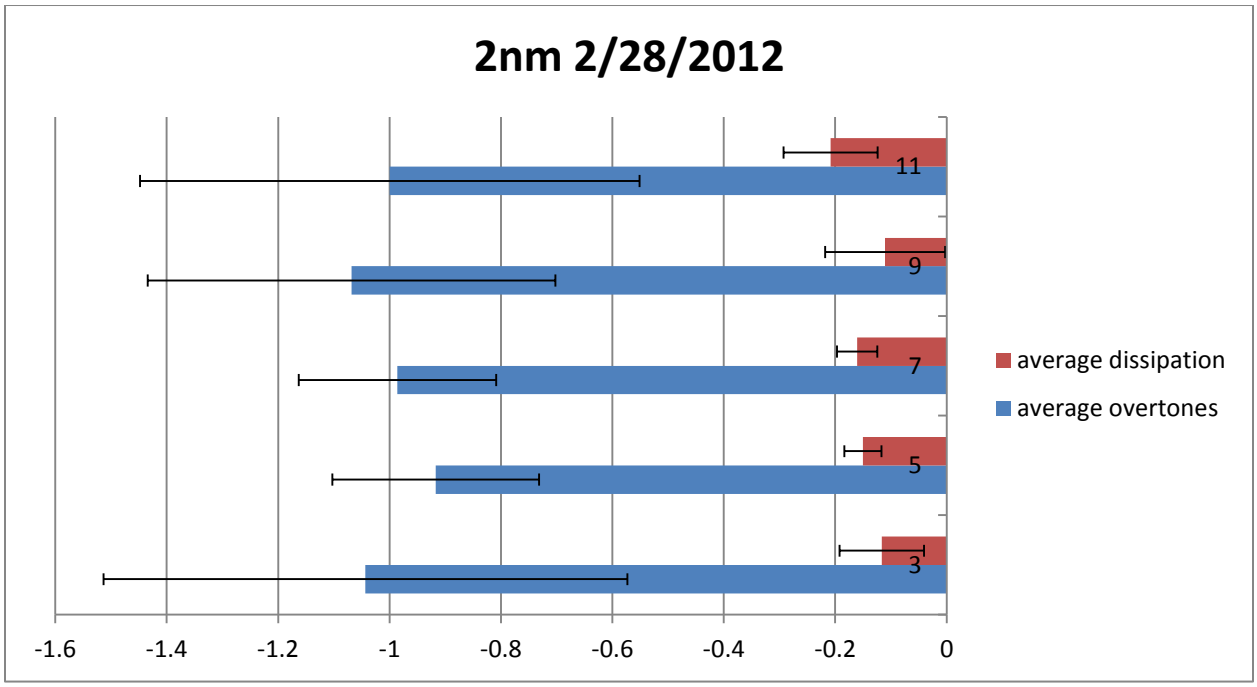
2nm 2/28/2012
11
9
7
5
3
-1.6
-1.4
-1.2
-1
-0.8
-0.6
-0.4
-0.2
0
average dissipation
average overtones

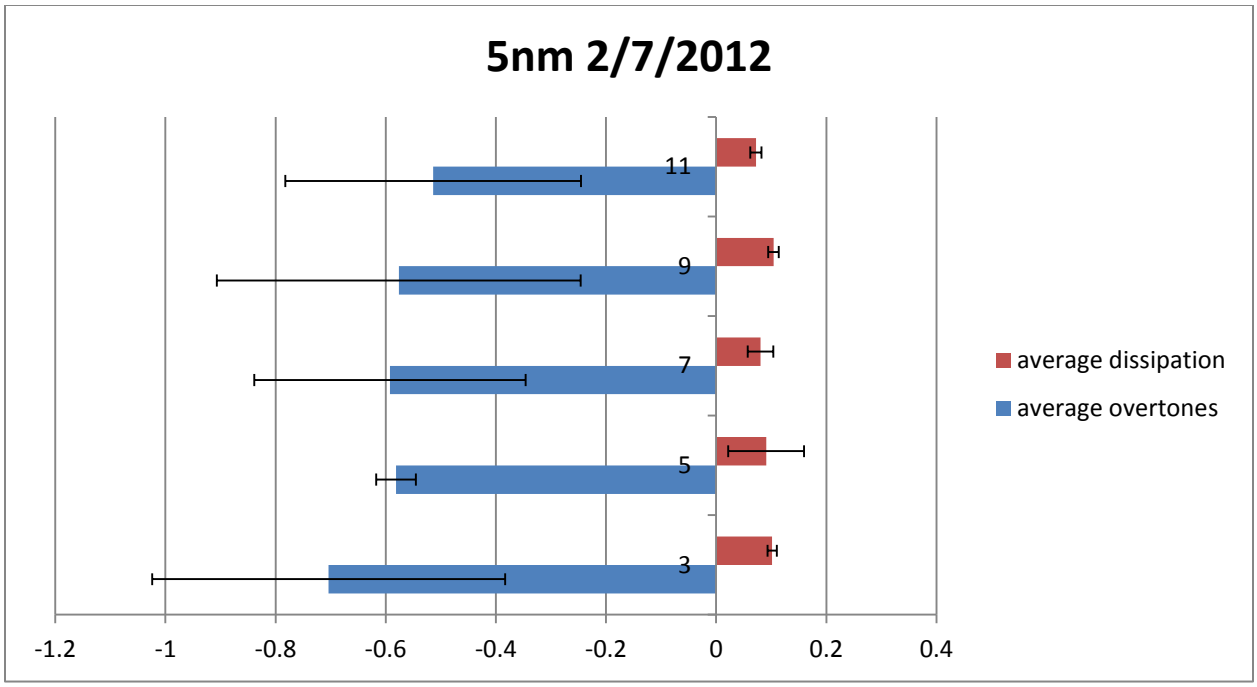
5nm 2/7/2012
11
9
7
5
3
-1.2
-1
-0.8
-0.6
-0.4
-0.2
0
0.2
0.4
average dissipation
average overtones

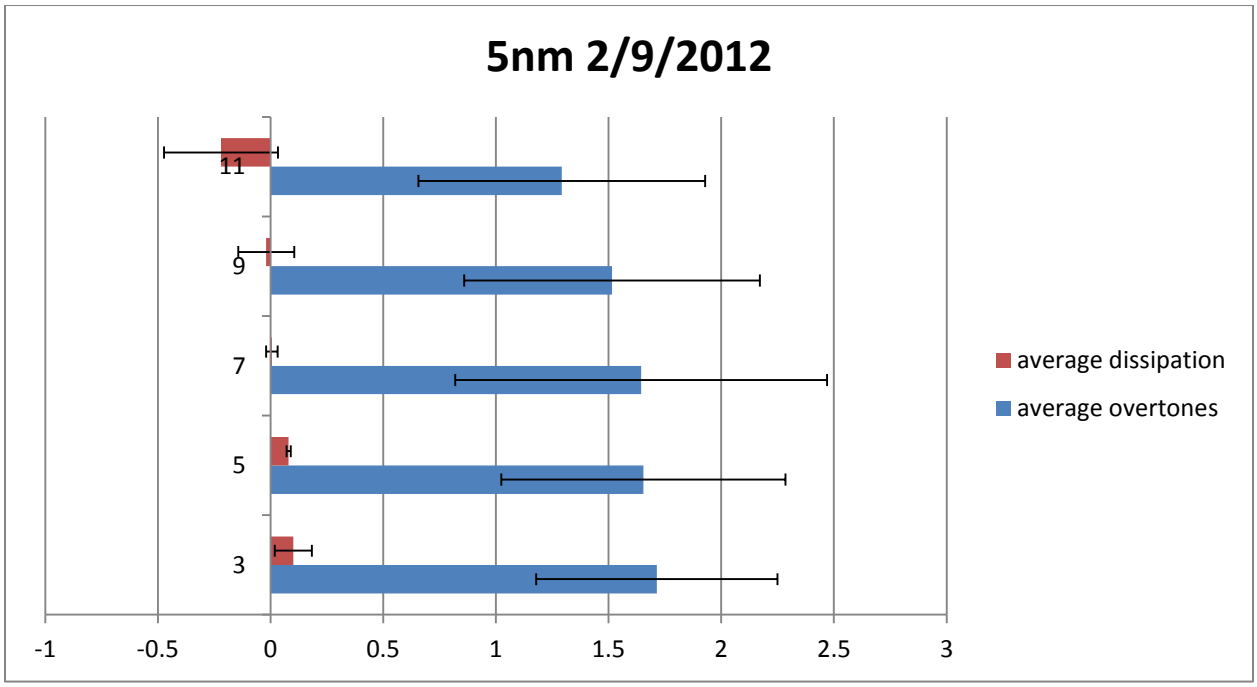
5nm 2/9/2012
11
9
7
5
3
-1
-0.5
0
0.5
1
1.5
2
2.5
3
average dissipation
average overtones

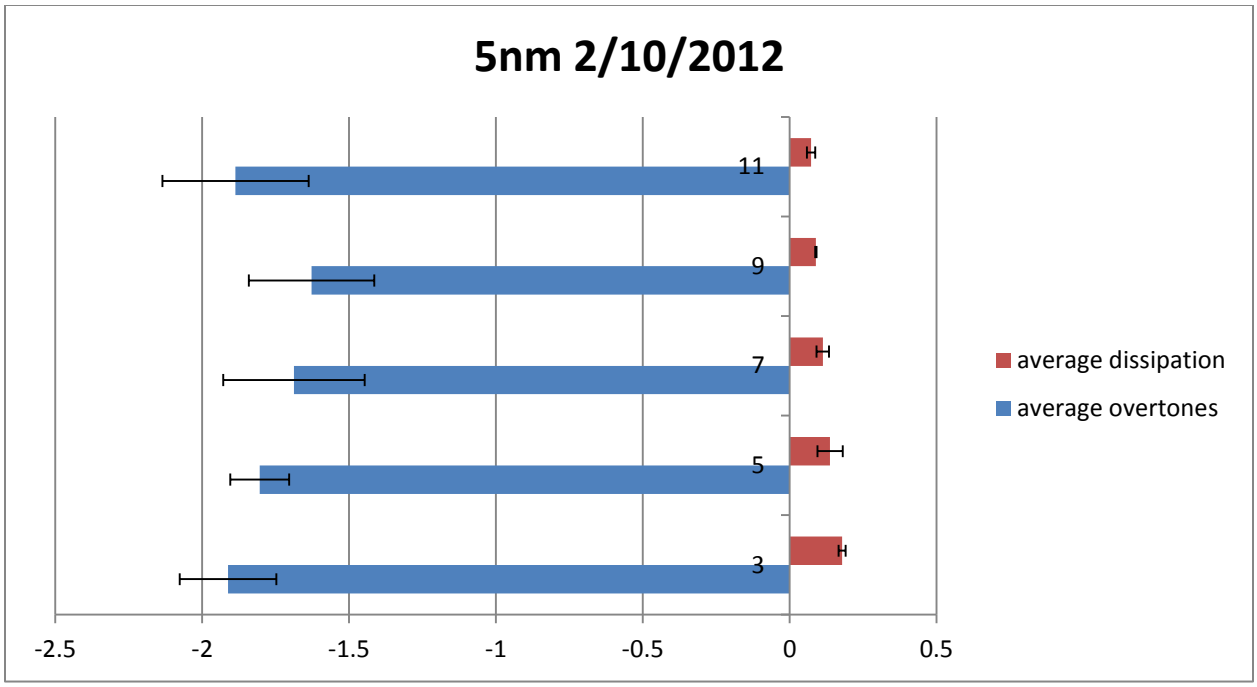
5nm 2/10/2012
11
9
7
5
3
-2.5
-2
-1.5
-1
-0.5
0
0.5
average dissipation
average overtones

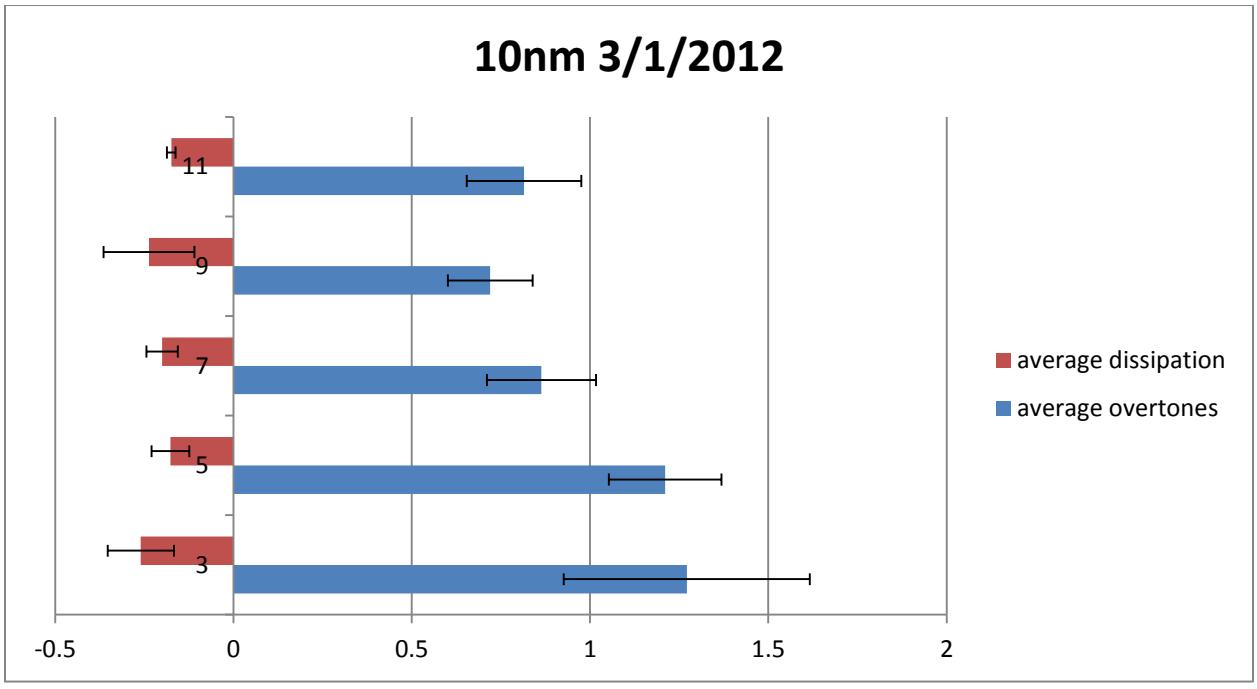
10nm 3/1/2012
11
9
7
5
3
-0.5
0
0.5
1
1.5
2
average dissipation
average overtones

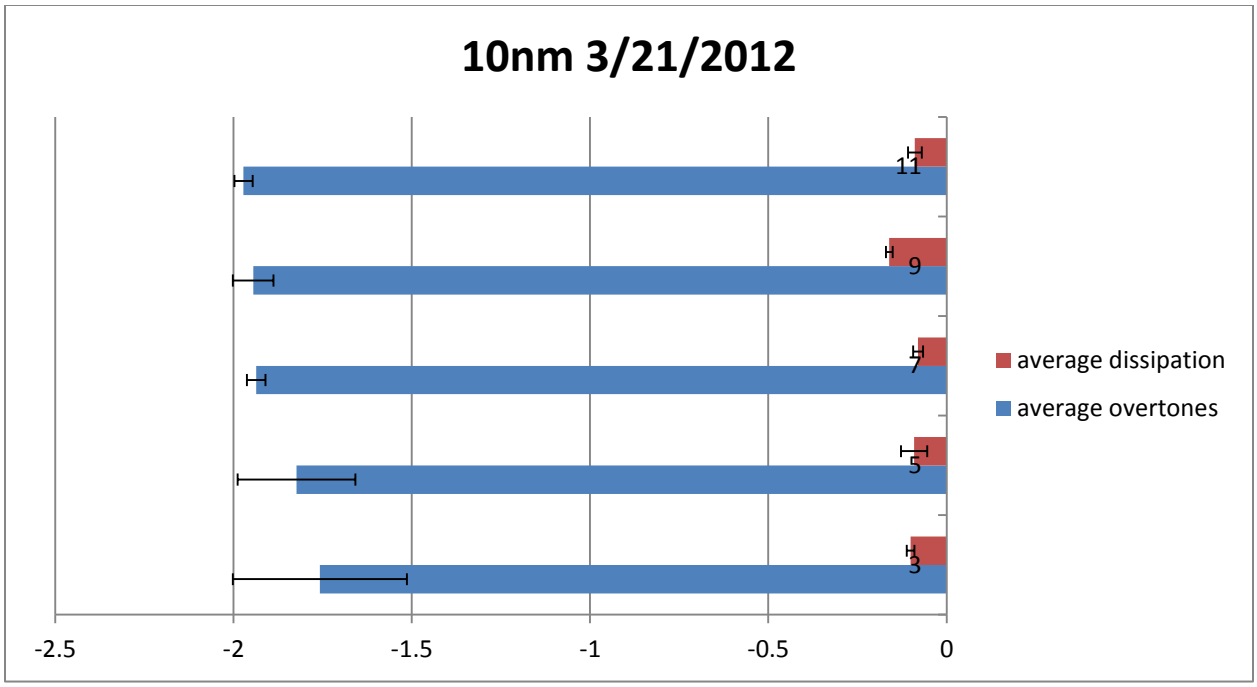
10nm 3/21/2012
11
9
7
5
3
-2.5
-2
-1.5
-1
-0.5
0
average dissipation
average overtones

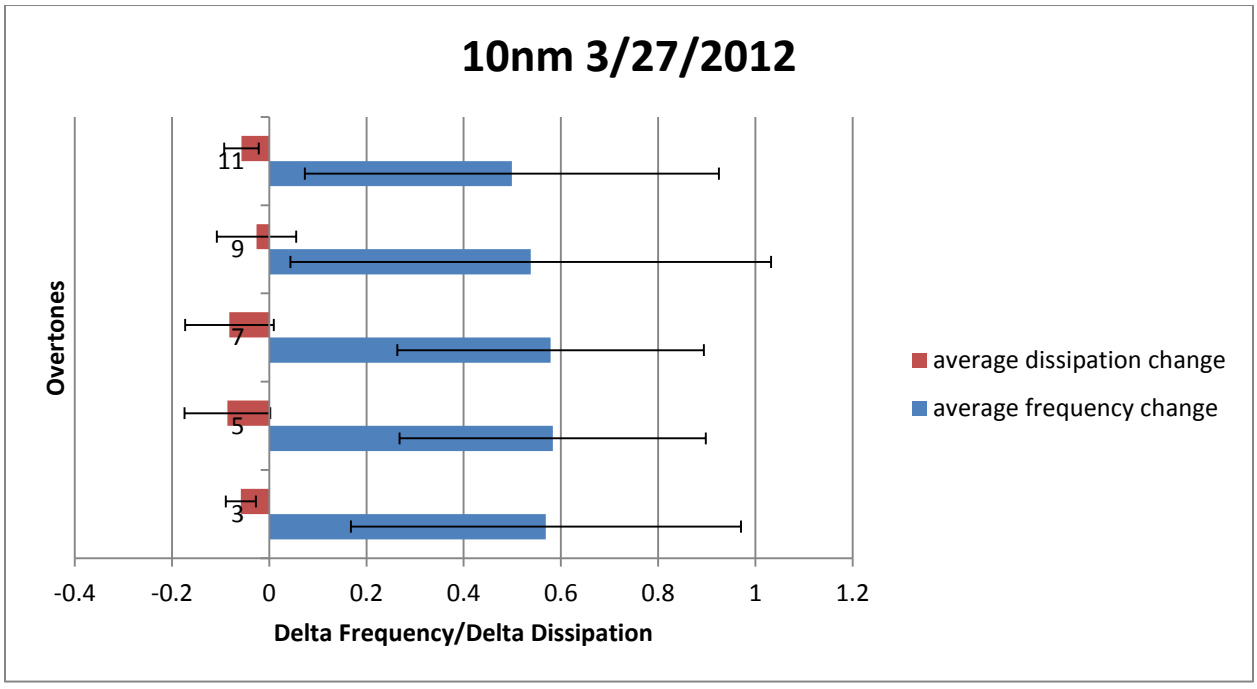
10nm 3/27/2012
Overtones
11
9
7
5
3
-0.4
-0.2
0
0.2
0.4
0.6
0.8
1
1.2
Delta Frequency/Delta Dissipation
average dissipation change
average frequency change

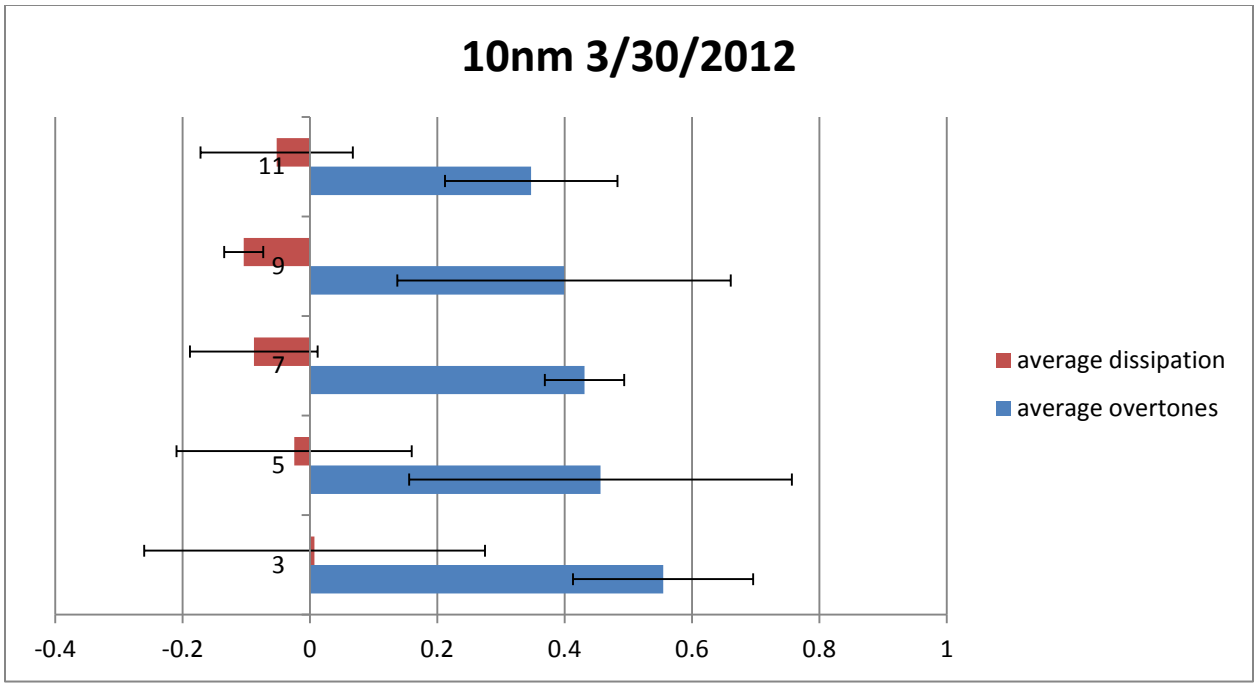
10nm 3/30/2012
11
9
7
5
3
-0.4
-0.2
0
0.2
0.4
0.6
0.8
1
average dissipation
average overtones

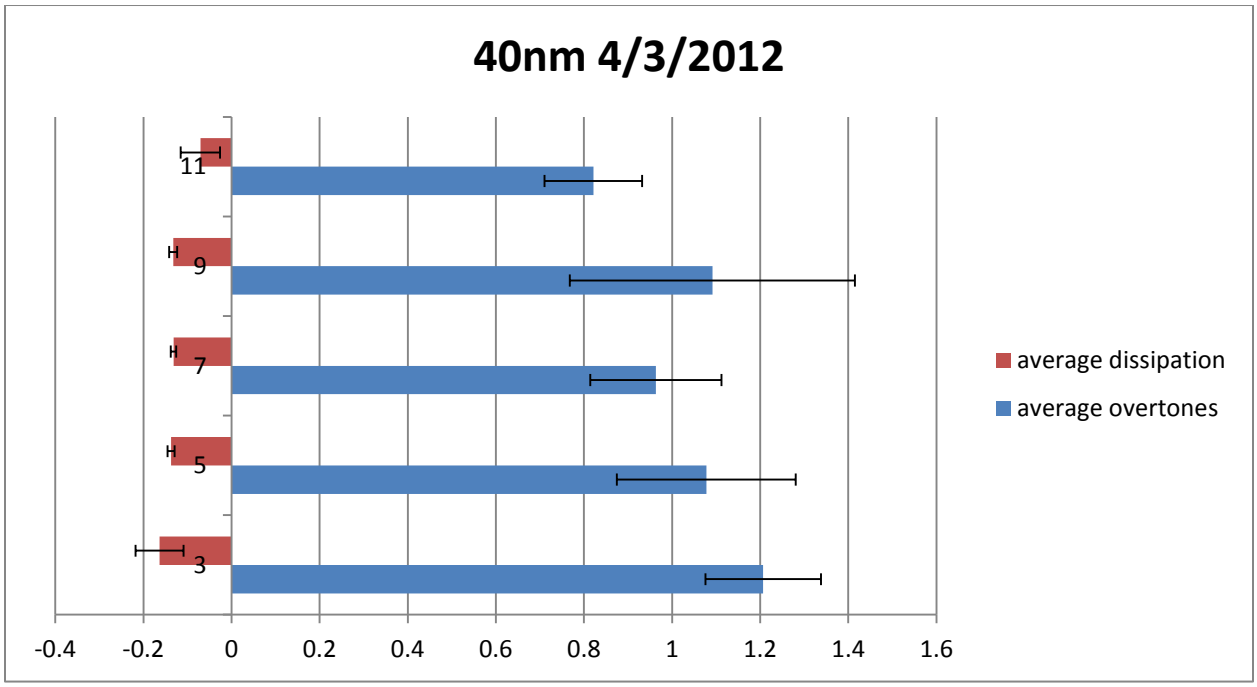
40nm 4/3/2012
11
9
7
5
3
-0.4
-0.2
0
0.2
0.4
0.6
0.8
1
1.2
1.4
1.6
average dissipation
average overtones

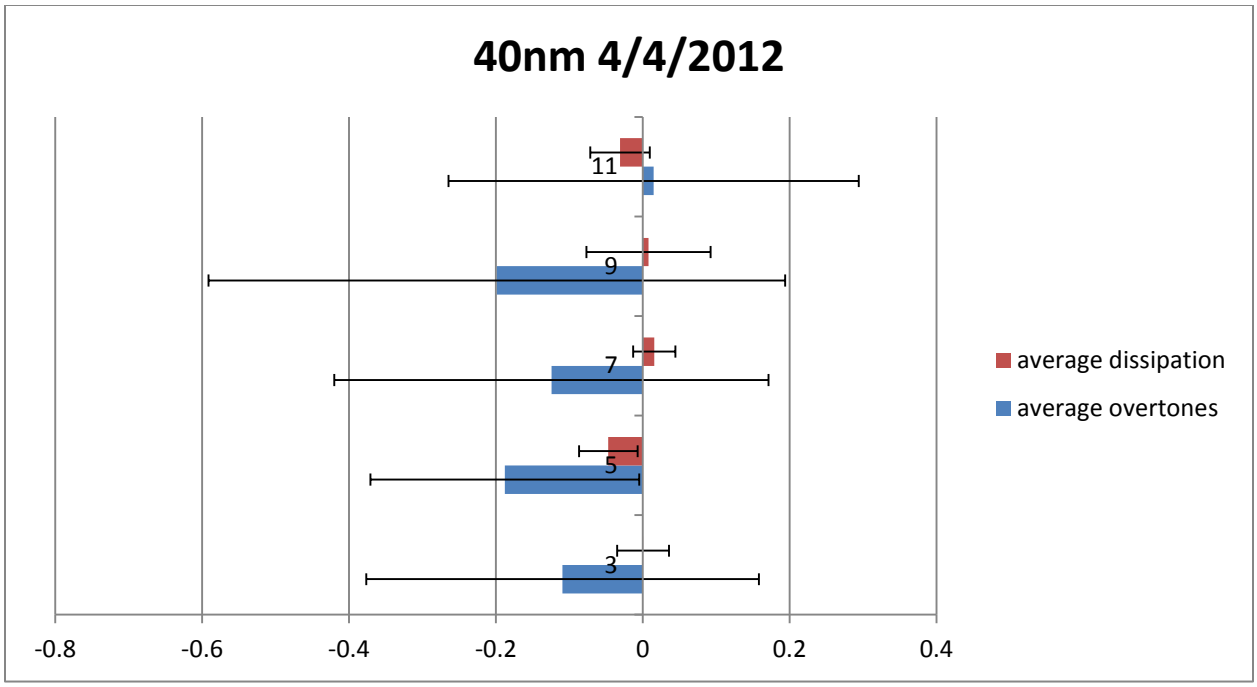
40nm 4/4/2012
11
9
7
5
3
-0.8
-0.6
-0.4
-0.2
0
0.2
0.4
average dissipation
average overtones

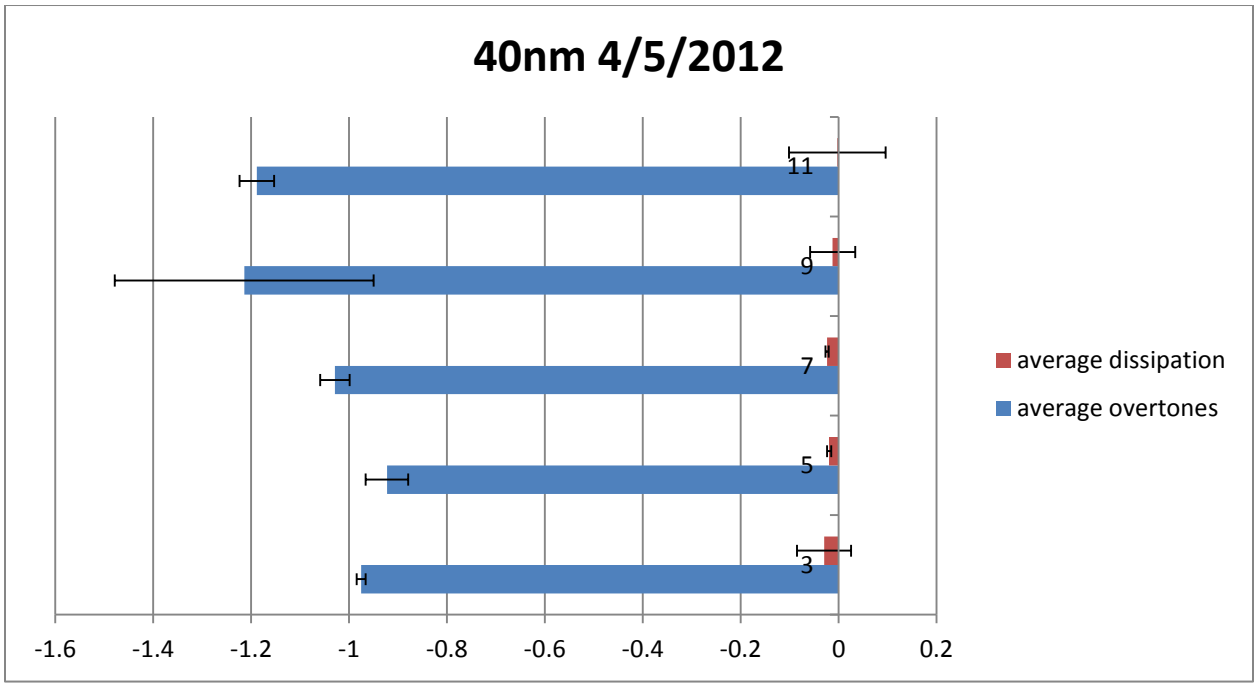
40nm 4/5/2012
11
9
7
5
3
-1.6
-1.4
-1.2
-1
-0.8
-0.6
-0.4
-0.2
0
0.2
average dissipation
average overtones

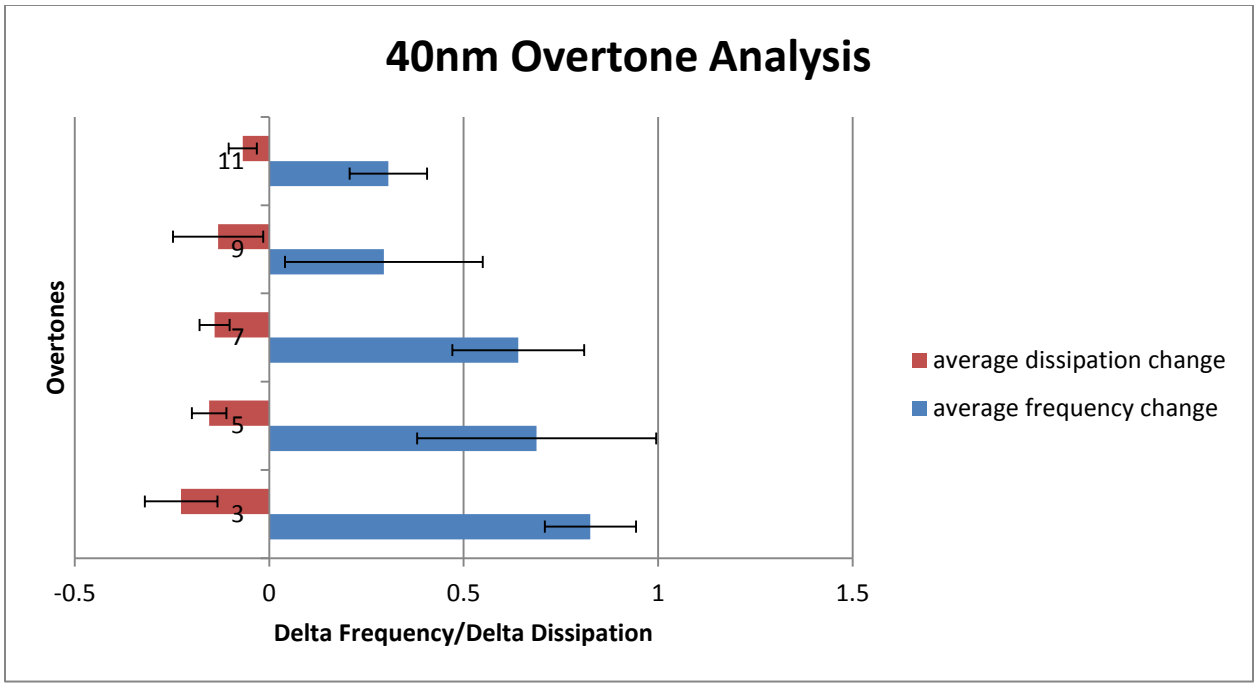
40nm Overtone Analysis
Overtones
11
9
7
5
3
-0.5
0
0.5
1
1.5
Delta Frequency/Delta Dissipation
average dissipation change
average frequency change

References

[1] Lin, Jiaqi, et al. "Penetration of Lipid Membranes by Gold Nanoparticles: Insights into Cellular Uptake, Cytotoxicity, and Their Relationship." ACS Nano (2010): 5421–5429.

[2] ASTM. "Standard Terminology Relating to Nanotechnology." 2006.

[3] Kessler, Rebecca. "Engineered Nanoparticles in Consumer Products: Understanding a New Ingredient." March 2011. *Environmental Health Perspectives.* January 2012

[4] Maynard, A. D. (2006). Nanotechnology: A Research Strategy for Addressing Risk. Washington, DC: Woodrow Wilson International Center for Scholars.

[5] Nanotechnologies, P. o. (2012). Introduction to Nanotechnology. Retrieved April 2012, from Nanotech Project: http://www.nanotechproject.org/topics/nano101/introduction_to_nanotechnolog

[6] Nanotechnologies, T. P. (2012). Consumer Product Inventory. Retrieved April 2012, from Nanotech Project: http://www.nanotechproject.org/inventories/consumer/search/page2/?search=1&keywords=gold

[7] Sandhu, Kulmeet K., et al. "Gold Nanoparticle-Mediated Transfection of Mammalian Cells." Bioconjugate Chemistry (2002): 3-6

[8] Cai, Weibo, et al. "Applications of Gold Nanoparticles in Cancer Nanotechnology." Nanotechnology, Science, and Application (2008): 17-32.

[9] Quick, D. (2012). Gold nanoparticles paint a precise picture of brain tumors before and during surgery. Health and Wellbeing, 1.

[10] Drezek, Rebekah, Vicki Colvin and Nastassja Lewinski. "Cytotoxicity of Nanoparticles." *Small* (2008): 4:26-29

[11] Nature Nanotechnology. (2011). The Dose Makes the Poison. Nature Nanotechnology, 329.

[12] Wise, Kelsey and Murphy Brasuel. "The current state of engineered nanomaterials in consumer good and waste streams." Nanotechnology, Science and Applications Dovepress(2011): 73-86.

[13] Roiter, Y., Ornatska, M., Rammohan, A. R., Balakrishna, J., Heine, D. R., & Minko, S. (2009). Interaction of Lipid Membrane with Nanostructured Surfaces. Langmuir, 6287-6299.

[14] Roiter, Y., Ornatska, M., Rammohan, A. R., Balakrishna, J., Heine, D. R., & Minko, S. (2009). Interaction of Lipid Membrane with Nanostructured Surfaces. Langmuir, 6287-6299.

[15] Camesano, T. (2012, January). Poly(Methacrylic Acid) . (H. lazkani, & A. Carey, Interviewers)

[16] Mikkelsen, R. (2005). Humic Materials for Agriculture. Better Crops, 3

[17] Mechler, A., Praporski, S., Atmuri, K., Boland, M., Separovic, F., & Martin, L. L. (2007). Specific and Selective Peptide-Membrane Interactions Revealed Using Quartz Crystal Microbalance. Biophyscial Jornal.

[18] ASTM. "Standard Terminology Relating to Nanotechnology." 2006.

[19] Schmid, G. (2010). Nanoparticles: From Theory to Application. Wiley-VCH.

[20] Turkevich, J. (1951). A study of the nucleation and growth processes in the synthesis of colloidal gold . *Discussions of the Faraday Society*, 55-75

[21] Daniel, M.-C., & Astruc, D. (2004). Gold Nanoparticles: Assembly, Supramolecular Chemistry, Quantum-Size-Related Properties, and Applications toward Biology, Catalysis, and Nanotechnology. Chemistry Review, 293-246.

[22] Sandhu, K. K., McIntosh, C. M., Simard, J. M., Smith, S. W., & Rotello, V. M. (2002). Gold Nanoparticle-Mediated Transfection of Mammalian Cells. Bioconjugate Chemistry, 3-6.

[23] Leroueil, Pascale R., Stephanie A. Berry and Kristen Duthie. "Wide Varieties of Cationic Nanoparticles Induce Defects in Supported Lipid Bilayers." Nano Letters (2008): 420-424.

[24] Kessler, Rebecca. "Engineered Nanoparticles in Consumer Products: Understanding a New Ingredient." March 2011. Environmental Health Perspectives. January 2012.

[25] Pan, Yu, Sabine Neuss Dr. and Annika Leifert. "Size-Dependent Cytotoxicity of Gold Nanoparticles." Small (2007): 1941-1949.

[26] Hillyer, Julian and Ralph Albrecht. "Gastrointestinal Persorption and Tissue Disstribution of Differently Sized Colloidal Gold Nanoparticles." *Journal of Pharmaceutical Sciences* (2001): 90: 1927-1936.

[27] Connor , Ellen, et al. "Gold Nanoparticles Are Taken Up by Human Cells Do Not Cause Acute Cytotoxicity ." *Small* (2005): 1: 325-327.

[28] Roiter, Y., Ornatska, M., Rammohan, A. R., Balakrishna, J., Heine, D. R., & Minko, S. (2009). Interaction of Lipid Membrane with Nanostructured Surfaces. Langmuir, 6287-6299.

[29] Huang, C.-H. (1969). Phosphatidylcholine vesicles. Formation and physical characteristics. Biochemistry , 344–352.

[30] Yoon, T. H., & Kim, I. H. (2002). Phosphatidylcholine isolation from egg yolk phospholipids by high-performance liquid chromatography. Journal of Chromatography A , 209-216.

[31] Lin, Jiaqi, et al. "Penetration of Lipid Membranes by Gold Nanoparticles: Insights into Cellular Uptake, Cytotoxicity, and Their Relationship." ACS Nano (2010): 5421–5429.

[32] Leroueil, Pascale R., Stephanie A. Berry and Kristen Duthie. "Wide Varieties of Cationic Nanoparticles Induce Defects in Supported Lipid Bilayers." Nano Letters (2008): 420-424.

[33] Noort, D. v., Rani, R., & Mandenius, C.-F. (2001). Improving the Sensitivity of a Quartz Crystal Microbalance. *Mikrochimica Acta*, 49-53.

[34] Manchabi, A., & Cobbold, R. S. (2011). Development and application of piezoelectric materials for. *Ultrasound*, 187-196.

[35] Dixon, M. C. (2008). *Quartz Crystal Microbalance with Dissipation Monitoring: Enabling Real-Time Characterization of Biological Materials and Their Interactions.* The Association of Biomolecular Resource Facilities.

[36] Hook, F., & Rudh, M. (2005). Quartz crystal microbalances (QCM) in biomacromolecular recognition. *BTi*.

[37] Rodahl, M., Hook, F., Fredriksson, C., Keller, C. A., Krozer, A., Brzezinski, P., et al. (1997). Simultaneous frequency and dissipation factor QCM measurements of biomolecular absorption and cell adhesion. *Faraday Discuss*, 229-246.

[38] Pallem, V. L., Stretz, H. A., & Wells, M. J. (2009). Evaluating Aggregation of Gold Nanoparticles and Humic Substances Using Fluorescence Spectroscopy. *Environ. Sci. Technol* , 7531-7535.

[39] Holger Schönherr, *. J., Lenz, P., Frank, C. W., & Boxer, S. G. (2004). Vesicle Adsorption and Lipid Bilayer Formation on Glass Studied by Atomic Force Microscopy. *Langmuir*, 11600-11606.

[40] Mechler, A., Praporski, S., Atmuri, K., Boland, M., Separovic, F., & Martin, L. L. (2007). Specific and Selective Peptide-Membrane Interactions Revealed Using Quartz Crystal Microbalance. Biophyscial Jornal.

[41] Lawaczeck, R., Kainosho, M., & Chan, S. I. (2003). The formation and annealing of structural defects in lipid bilaye rvesicles. BBA Biomembranes.

[42] Richter, R. P., Bérat, R., & Brisson, A. R. (2006). Formation of Solid-Supported Lipid Bilayers: An Integrated View. Langmuir, 3497-3505.

[43] Leroueil, Pascale R., Stephanie A. Berry and Kristen Duthie. "Wide Varieties of Cationic Nanoparticles Induce Defects in Supported Lipid Bilayers." Nano Letters (2008): 420-424.

[44] Lin, Jiaqi, et al. "Penetration of Lipid Membranes by Gold Nanoparticles: Insights into Cellular Uptake, Cytotoxicity, and Their Relationship." ACS Nano (2010): 5421–5429.

[45] Lin, Jiaqi, et al. "Penetration of Lipid Membranes by Gold Nanoparticles: Insights into Cellular Uptake, Cytotoxicity, and Their Relationship." ACS Nano (2010): 5421–5429.